

**NASA TECHNICAL  
MEMORANDUM**



NASA TM X-52127

NASA TM X-52127

FACILITY FORM 602

<u>N65-34000</u> (ACCESSION NUMBER)	_____ (THRU)
<u>121</u> (PAGES)	<u>1</u> (CODE)
_____ (NASA CR OR TMX OR AD NUMBER)	<u>28</u> (CATEGORY)

**AN ANALYSIS OF CHEMICAL UPPER STAGES  
FOR NASA SCIENTIFIC MISSIONS**

by The Advanced Development and Evaluation Division  
Lewis Research Center  
Cleveland, Ohio

GPO PRICE \$ \_\_\_\_\_

CFSTI PRICE(S) \$ \_\_\_\_\_

Hard copy (HC) 4.00

Microfiche (MF) 1.00

ff 653 July 65

**AN ANALYSIS OF CHEMICAL UPPER STAGES FOR NASA SCIENTIFIC MISSIONS**

by The Advanced Development and Evaluation Division

Lewis Research Center  
Cleveland, Ohio

**NATIONAL AERONAUTICS AND SPACE ADMINISTRATION**

AN ANALYSIS OF

CHEMICAL UPPER STAGES

FOR NASA SCIENTIFIC MISSIONS

By The Advanced Development and Evaluation Division  
Lewis Research Center

SUMMARY

34000

An analysis of chemical upper stages for advanced scientific missions has been carried out. Development of a cryogenic upper stage, with a propellant capacity near 7000 pounds, can substantially increase the capability of present NASA launch vehicles for advanced scientific missions. Best performance of the configurations investigated is achieved through use of hydrogen-fluorine propellants in a pump-fed stage requiring the development of a new propulsion system. This performance can be closely matched by a hydrogen-oxygen stage using the RL-10A-3-3 engine which more nearly represents current state-of-the-art in cryogenic propellants. A preliminary design of such a stage, having a propellant capacity of 7000 pounds, was carried out. Several feasible designs were generated that resulted in stage mass fractions of approximately 0.80. Conservative approaches were selected in most system design areas. The major development problems anticipated are associated with the long coast, planetary orbit mission. Here, efficient application of multi-layer insulation and zero "g" venting are required.

The performance capability of the hydrogen-oxygen upper stage in conjunction with the Atlas-Centaur and the Saturn IB-Centaur launch vehicles was evaluated. As an example, for a solar probe mission, the Saturn IB-Centaur can deliver a 500 pound payload to 0.218 AU perihelion distance. Addition of a hydrogen-oxygen upper stage can increase payload to 1840 pounds at this AU distance, or deliver the 500 pound payload to 0.158 AU distance. Similar comparisons are presented for other high energy missions.

INTRODUCTION

Continuing the vigorous pace of the national scientific space program will lead to increasingly difficult launch vehicle requirements as mission energies are increased. The desire for higher mission energy capability is exemplified by increased NASA interest in close solar probe missions, out of the ecliptic plane missions, comet missions, and anti-solar missions including asteroid belt and Jupiter probes. Present medium class NASA launch vehicles cannot provide sufficient mission energy to effectively pursue the foregoing missions. However, the introduction of a small high energy upper

*Handwritten signature*

E-3031-A

stage (or kick stage) into the present NASA launch vehicle family can provide the increased capability for advanced high energy scientific space missions. Furthermore, such a stage would also provide increased payload capability for less energetic missions such as for synchronous orbit and advanced lunar and planetary missions.

The final choice of a kick stage design should be based on a number of considerations including mission performance, program cost, development time and development risk. This report will present information regarding the design and performance of various kick stage concepts. Previous studies (refs. 1 and 2) have examined high energy upper stage design concepts in conjunction with various launch vehicles. The present study enlarges on the previous studies and examines in more detail various kick stage design concepts and missions in conjunction with the present NASA family of launch vehicles.

The results are presented in three sections. In arriving at a final kick stage design several basic decisions regarding kick stage propellant combination, propulsion system and propellant loading will have to be made. The purpose of the first section is to provide design and performance information regarding these choices. The basic kick stage designs investigated are described and the basis for their systems performance and weight is discussed. Comparisons are then made on the basis of mission performance using both the Atlas-Centaur and the Saturn IB-Centaur launch vehicles.

The purpose of the second section is to develop a preliminary design of a representative cryogenic kick stage. The stage discussed is a hydrogen-oxygen kick stage using the RL-10A-3-3 engine. Three broadly different approaches to tankage and primary structure design are presented. System requirements are identified, and various approaches are discussed and evaluated. Launch vehicle structural modifications are reviewed.

In the third section of the report the performance of a specific cryogenic kick stage design is evaluated for a number of future scientific space missions.

#### COMPARISON OF SEVERAL BASIC KICK STAGE CONCEPTS

The purpose of this section is to provide information regarding the choice of kick stage propellant combination, propulsion system and propellant loading. First, the basic kick stage designs investigated will be identified. Next, the basis for their systems performance and weights will be presented. Then, the effect of kick stage propellant combination, propulsion system, and propellant loading will be illustrated by comparing the mission performance of the various kick stage concepts.

### Identification of Designs Investigated

In order to investigate the effect of kick stage propellant combination, propulsion system and propellant loading, a comparative evaluation of several kick stage designs was performed. One storable stage and three cryogenic stages were analyzed. Representative stage layouts and weight tabulations (for typical propellant loadings) for the four designs are presented in figures 1 to 4 and tables I to IV. In the weight tabulations a contingency allowance is included that amounts to about 11 percent of the dry stage weights.

The designs studies were (in the order of increasing performance):

- i) a pressure-fed stage (figure 1 and table I) utilizing storable propellants (monomethylhydrazine (MMH), and nitrogen tetroxide ( $N_2O_4$ )). Propulsion for this stage is the LEM ascent engine, being developed for the lunar excursion module of Apollo program. The engine generates 3500 pounds of thrust at a chamber pressure of 120 psia with a nozzle expansion ratio of 45. This design represents the least complicated, most readily available, lowest cost upper stage development considered in the study.
- 2) A pump-fed hydrogen-oxygen (H-O) stage (figure 2 and table II) utilizing the RL-10A-3-3 engine. This design represents current state of the art in cryogenic propellants. The engine is presently under development for the Centaur stage. It delivers 15,000 pounds of thrust at a chamber pressure of 400 psia with a nozzle expansion ratio of 57.
- 3) A hydrogen-fluorine (H-F) pump-fed stage (figure 3 and table III) again using the RL-10 engine. Although the RL-10 engine is not presently operational with H-F, Pratt and Whitney is under contract to NASA to determine engine compatibility and performance capability utilizing H-F. This design is based on an engine mixture ratio of 9 and represents the quickest approach to an H-F upper stage.
- 4) An H-F pump-fed stage (figure 4 and table IV) designed for a completely new engine. The engine provides 10,000 pounds of thrust at a chamber pressure of 400 psia with a nozzle expansion ratio of 60. The engine would be regeneratively cooled and utilize a topping cycle similar to the RL-10. The stage design is based on an engine mixture ratio of 14 and is the highest performance stage in the study. As such it is also the most complicated and costly stage from the standpoint of development.

The proposed storable propellant kick stage is shown in figure 1. The high bulk density of the propellants permit their containment in four spherical tanks clustered about the LEM ascent engine. The stage structure is composed of a cruciform beam-ring arrangement which provides support for all stage components. Payload support is provided by a space truss attached to the cruciform beam-ring assembly.

The cryogenic kick stages (figs. 2,3, and 4) are similar in configuration, consisting of a single oblate spheroid hydrogen tank mounted forward of a cluster of four spherical oxidant tanks. The stage structure consists of a space truss and cruciform beam-ring

assembly to provide support for all stage components, and payload.

Since, in all missions examined, the kick stage is mated to either the 10 foot diameter Atlas or Centaur vehicles, the kick stage designs were based on this diameter. A stage diameter greater than 10 feet would require a hammerhead Atlas-Centaur launch vehicle resulting in increased vehicle flight loads and locally induced radial loads in the Centaur forward structural ring (Atlas-Centaur station 219). A kick stage diameter of less than 10 feet would lengthen the stage, particularly for the larger propellant loadings, and thus increase vehicle flight bending loads.

Having established the configuration for each of the four basic stages, the next step was to make a preliminary design for each stage at several propellant loadings. The preliminary design included tankage and structural design for purposes of weight estimates. Stage jettison weight curves were developed to be subsequently used for performance and optimum propellant loading studies for the four basic stages. The jettison weight curves versus propellant loading are presented in figures 5 through 8.

### Systems Design

In arriving at the four stage designs presented in figures 1 through 4 and their associated weight summaries presented in tables I through IV and figures 5 through 8, many alternate systems approaches were considered. In the following discussions the systems approaches selected will be identified and significant performance, design, and weight assumptions will be presented. However, the various system areas will be discussed in detail only where they could significantly affect the comparative evaluation of the four basic kick stage designs (for example, selection of engine specific impulse). A detailed discussion of alternate approaches regarding pressurization, insulation, structure, guidance, etc., will be presented in the second section.

A summary of pertinent system design assumptions is given in tables V through VIII for the four basic stage designs.

### Propulsion

Storable engine. - The use of the LEM ascent engine was assumed for the pressure-fed storable stage. This engine produces 3500 pounds of thrust at a chamber pressure of 120 psia. The engine mixture ratio is 1.64 and the nozzle expansion ratio is 45. The engine is fully ablative and has an operating life of over 500 seconds. The existing engine weight is 187 pounds. Reducing some propellant valve redundancy and adding gimbal and actuator systems results in an engine weight of 210 pounds.

A major application for the storable kick stage would be a planetary orbit mission wherein the kick stage provides the braking propulsion at the planet. The effect of storable stage thrust level on payload for a typical Mars orbit mission is shown in figure 9. The curve was calculated assuming engine weights based on 100 psia chamber pressure and a nozzle expansion ratio of 40. As can be seen, thrust level has little effect on payload. The symbol indicates the payload obtained when using the LEM ascent engine and, again, the effect on payload is small.

RL-10 Engine. - Experimental and predicted performance data for the RL-10A-3 engine are presented in figure 10. The solid curves are for H-O and the dashed curves for H-F. The solid curve in the lower left hand corner is the performance curve for the presently existing RL-10A-3-1 which has a nozzle expansion ratio of 40. The upper solid curve is the predicted performance of the A-3-3 version of the engine. The nominal operating point for this engine is at an engine mixture ratio of 5 and at this point, the specific impulse increases from 433 for the standard engine to 444 for the improved engine.

The upper and lower dashed curves are, respectively, the theoretical equilibrium and theoretical frozen performance curves for the RL-10, A-3-3 with fluorine. The center curve with the data points represents experimental performance obtained with fluorine using a modified injector on a chamber with a 40 to 1 nozzle expansion ratio. The curve above it shows the predicted H-F performance in a modified RL-10A-3-3 engine. At an engine mixture ratio of 9, Pratt and Whitney is presently obtaining combustion efficiencies of 99 percent. As can be seen, the theoretical equilibrium performance curve is quite flat, so the specific impulse level of 452 seconds at an engine mixture ratio of 9 seems to be about the ultimate in this engine. Increasing the nozzle expansion ratio to 57 adds an additional 6 seconds to give the predicted value of 458 seconds.

Selection of the RL-10 mixture ratio using H-O or H-F was made from examining data such as that shown on figure 11. For a solar probe mission using the Saturn IB-Centaur boost vehicle plus the kick stage, payload versus mixture ratio is plotted. The H-O curve peaks to the left of the nominal mixture ratio of 5; however, the gain was small and consequently a mixture ratio of 5 was used in all calculations. A mixture ratio of 9 was selected for the H-F kick stage.

The rated thrust level of the RL-10A-3-3 is 15,000 pounds. By incorporating appropriate modifications, the nominal thrust level can be increased or decreased, and if desirable, engine thrust can be traded for specific impulse. In order to demonstrate the impact of mission energy on the selection of kick stage thrust level, two missions were considered. They are: 1) a low energy lunar mission using an Atlas-Centaur and 2) a high energy solar probe mission

with the Saturn IB-Centaur. The results are presented in figure 12. Payload is plotted versus kick stage thrust. The solid curves are based on maintaining the RL-10A-3-3 geometry fixed. Thrust is varied simply by reducing chamber pressure. This curve is presented only to demonstrate the effect of increased gravity losses as thrust level decreases.

The dashed curves show the effect of maintaining both chamber pressure and nozzle exit area fixed, while changing thrust by varying the engine throat area. With engine exit area held constant, any decrease in thrust level produces an increase in specific impulse since the nozzle expansion ratio increases with decreasing thrust. From figure 12(a), it is evident that thrust level has little effect (on a percentage basis) on lunar mission payloads. Over the thrust level range chosen, payload doesn't vary more than three percent. The picture changes substantially for the higher energy mission shown in figure 12(b). The payload level drops markedly (on a percentage basis) with decreasing thrust for the fixed throat area case. This is due to the increased gravity losses associated with the longer burning times that go with low thrust operation. For the variable throat area case, the increase in specific impulse that results from increased nozzle expansion ratio offsets the additional gravity losses, and the payload level remains nearly constant. The conclusion drawn from these curves is that there seems to be no advantage in using the RL-10 at reduced thrust and, therefore, all subsequent data were generated using rated thrust.

New H-F engine. - One of the apparent advantages in using an H-F stage rather than H-O is the fact that higher engine mixture ratios can be utilized, thereby reducing the amount of hydrogen needed. From figure 10, it is evident that the theoretical equilibrium specific impulse of H-F is quite constant over the mixture ratio range of 9 to 14. Experimental data from various engine manufactures indicated that, over this mixture ratio range, combustion efficiencies of 98-99 percent can be expected. It would seem then that with a new H-F engine designed for high mixture ratio operation and having a nozzle contoured to avoid recombination losses, a specific impulse efficiency of 96 percent of theoretical equilibrium should be obtainable. For the purposes of the present study, this was assumed to be the case.

The engine characteristics used in this study are included in table VIII. The engine generates 10,000 pounds of thrust at a chamber pressure of 400 psia with a nozzle expansion ratio of 60. Engine chamber pressure was not optimized in this study. However, over the range of 300 to 500 psia engine weight didn't vary more than 10 or 15 pounds so 400 psia was chosen as being a representative value.

The effects of engine thrust level and nozzle expansion ratio on payload are presented in figure 13 for a solar probe mission with the Saturn IB-Centaur launch vehicle. It is evident from figure 13(b) that a thrust level of 10,000 pounds is about optimum for this type of

high energy mission; however, the selection of nozzle expansion ratio is less straightforward. From figure 13(a) it would appear that a nozzle expansion ratio of 90 to 100 would be desirable for the new engine, however, this curve was generated using a fixed percentage of theoretical shifting specific impulse. In actuality, nozzle friction losses increase with increased expansion ratios. In addition, the bending moments imposed on the boost vehicle increase as the overall length of the kick stage increases. Both of these factors tend to reduce the optimum nozzle expansion ratio; consequently, more detailed calculations are necessary to truly determine the best nozzle expansion ratio. However, it is felt that the 60 to 1 performance will be near optimum.

#### Pressurization

For all of the stages studies, the oxidant tanks were pressurized with helium. Similarly, for the storable stage, the fuel tank was also pressurized with helium. For the pump-fed cases, however, the hydrogen tanks were pressurized during expulsion with hydrogen bleed from the engine and helium was used only for initial pressurization.

In all cases the helium was stored at 520° R and 4000 psia. Helium requirements were calculated by setting up a heat balance for the pressurant, the propellant tank, the propellant vapor in the ullage space, and the liquid surface. The expansion within the pressurant bottle was polytropic with heat transfer from the bottle to the contents. It was assumed that complete mixing occurred between the incoming pressurant and the propellant vapor and that no mass transfer across the liquid-vapor interface took place during propellant expulsion.

#### Insulation and Boiloff

Several insulations, their densities and thermal conductivities are listed in table IX. In reference 3 it was shown that for unvented systems, the payload penalty associated with the propellant thermal protection system is proportional to the product of  $K_p$ , whereas for vented systems the penalty varied as the square root of  $K_p$ . Assuming vented systems and short duration missions, any of the insulations listed could be used on the cryogenic stages (the storable stage requires no insulation for short missions). However, for long storage missions, the penalties become large for any but the multifoil insulations, and since multifoil insulation is good for short missions as well as long, it was used on all insulated stages.

The following ground rules were used in calculating insulation and boiloff weights: 1) Kick stage was oriented with payload toward the sun during all coast periods. 2) Multifoil insulation density was 5.0 pounds per cubic feet. 3) All heat entering propellant tanks resulted in vaporization. 4) To account for insulation thermal shorts

around tank supports, feed and drain lines, etc., values twice the ideal thermal conductivity of the insulation were assumed. This resulted in effective thermal conductivities between  $2 \times 10^{-4}$  and  $5 \times 10^{-4}$  Btu in/hr ft<sup>2</sup>° R depending upon the insulation boundary temperatures.

5) Insulation was assumed to be helium purged during ground hold.

### Structural Materials

Most of the primary structure, including the trusses, rings, cruciform beam, and propellant tanks, was considered to be fabricated from 2219-T81 aluminum alloy. This is a heat treatable alloy with good strength and welding properties and is suitable for use at temperatures as low as 37° R. The material selected for helium and nitrogen storage bottles was Ti-6Al-4V, an intermediate strength, heat treatable and weldable titanium alloy. Material selection for the cryogenic propellant tank support shells depended primarily upon the requirement for low heat conduction into the propellants. Consequently, for missions involving short propellant storage time, Ti-6Al-4V alloy was used; whereas for missions requiring longer space storage time (many days) it was necessary to use glass reinforced plastic construction. In the case of the storable stage, 2219-T81 aluminum propellant tank support shells were used.

### Other Systems

The weight summaries given in tables I through IV include weight assessments for guidance, autopilot, electrical, attitude control, tracking, and telemetry. These systems were not studied in detail for the preliminary comparison of basic kick stage concepts. The weight of these systems should be basically independent of the choice of kick stage propellant combination and be essentially constant over the range of stage sizes considered. Hence, they will not have a major effect on the choice of propellant combination and stage size. The weights presented are based on a review of the weight status of comparable systems on the Centaur stage with modifications reflecting a kick stage application and some allowance for future improvements. The various systems will be discussed in more detail in the second section, when a preliminary design of a specific kick stage is developed.

### Launch Vehicle Performance and Modifications

Integration of the kick stage with the two prime boost vehicles considered in this study is shown in figures 14 and 15. For the Atlas-Centaur configuration (fig. 14), a jettisonable nose shroud covers both the payload and the kick stage and mates with the kick stage interstage at the cruciform beam. The kick stage structure therefore carries only inertial loads while the nose shroud carries the aerodynamic loads during flight through the atmosphere. The interstage structure is required to support both the inertial and aerodynamic flight loads. The overall length of the vehicle shown is 132 feet and it is 10 feet

in diameter.

For the Saturn IB-Centaur configuration (fig. 15), the payload, kick stage, and Centaur are completely enclosed in a jettisonable, split nose shroud which is attached to the Saturn instrument unit. Therefore, neither the Centaur, nor the kick stage, are required to carry the aerodynamic flight loads. Both the kick stage and Centaur interstage structures are designed for inertial loads only. Support structure to prevent lateral motion, along with structure to allow application of Centaur pre-tension loads, have been provided. Overall length of the configuration is 208 feet and it is 260 inches in diameter.

#### Basis for Performance

Trajectories. - All performance and payload data for this study were calculated by fully integrated flight trajectories using the IBM 7094 digital computer. The flight path through the atmosphere was made at zero angle of attack up to booster engine cut off for the Atlas-Centaur launch vehicle and first-stage burnout for the Saturn IB-Centaur launch vehicle.

A parking-orbit ascent trajectory was assumed for all performance presented. All data was generated for a launch azimuth of  $114^\circ$  with the exception of the synchronous orbit mission where a launch azimuth of  $90^\circ$  was chosen. For each launch vehicle combination and mission application, appropriate flight performance reserve (FPR) requirements were determined. As an example, for those cases requiring either sub-orbital or post-orbital kick stage ignition, no FPR was provided in Centaur and a kick stage FPR equivalent to 2.75 percent of the kick stage characteristic velocity ( $\Delta V$ ) was assessed to cover all launch vehicle dispersions. For the special cases where Centaur was required to burnout at specified injection conditions, a Centaur FPR of 1.5 percent of Centaur  $\Delta V$  and a kick stage FPR of 1.8 percent of kick stage  $\Delta V$  were provided. The above FPR requirements were assessed in all cases, except for solar probe missions where it was assumed that no FPR was required.

Atlas-Centaur. - Performance ground rules and weight breakdowns used for payload capability analyses were based on reference 4 except as will be discussed herein and in the discussion describing structural modifications. Centaur Performance: Centaur specific impulse was increased to 444 seconds to reflect eventual capability of the RL-10A-3-3 engine. Atlas Interstage Adapter Heating Limitations: the limiting heating parameter ( $\int qvdt$ ) was decreased to  $0.92 \times 10^8$  lb/ft (nominal) to conform to current planning. Centaur Jettison Weight: the guidance system was removed from Centaur and incorporated in the kick stage, which would then provide required guidance for the entire powered flight. Removal of the guidance system package, as well as associated reductions in the autopilot, electrical, and equipment shelf weights, resulted in a reduction of 357 pounds in Centaur jettison weight. In

addition, 103 pounds of spacecraft adapter and equipment were removed from the basic vehicle. A retro-rocket package was incorporated to provide positive Centaur separation, for an increase of 30 pounds in jettison weight. Therefore, the net result of the above changes was a 430 pound reduction of Centaur jettison weight. In comparison, when a kick stage is not used, Centaur jettison weight was decreased a total of 70 pounds to reflect improvements in guidance, autopilot, and electrical system weights projected for the kick stage time period.

Saturn IB-Centaur. - Performance and weight assumptions for the Saturn IB were based on information contained in an internal MSFC document. Centaur weights and performance were based on, and adjusted, as detailed above for the Atlas-Centaur with the addition of: a) replacement of the 1327 pound jettisonable insulation panels with 150 pounds of fixed insulation, b) an increase of 109 pounds in hydrogen peroxide required during coast to meet the increased weight and time requirements, and c) larger coast ullage motors for a Centaur jettison weight increase of 9 pounds.

#### Shroud and Interstage Requirements

Tabulated below are the values of calculated shroud and interstage weight requirements for incorporation of a representative cryogenic kick stage.

Boost vehicle	Atlas-Centaur	Saturn-IB-Centaur
Nose shroud (lb)	2000	8900
Interstage (kick stage-Centaur)(lb)	700	390
Interstage (Centaur-Saturn)(lb)	--	600

Both the shroud and kick stage interstage weights were made dependent on the type of kick stage as well as propellant capacity in all performance calculations. The shroud and interstage designs are based on the following criteria:

Shroud. - Atlas-Centaur shroud: It was assumed that a semi-monocoque construction barrel section could be added to the Surveyor nose fairing to form a shroud which completely encloses the payload and kick stage. Aluminum alloy 7075-T6 was selected for the barrel section material.

Saturn-Centaur shroud: A 260-inch diameter shroud configuration established by Marshall Space Flight Center was selected for the proposed Saturn-Centaur-Kick Stage vehicle. This shroud completely encloses the payload, kick stage, and Centaur. Semi-monocoque

construction using 7075-T6 aluminum alloy was assumed.

Interstage. - Atlas-Centaur Launch Vehicle--Centaur to Kick Stage: A semi-monocoque construction of 7075-T6 aluminum alloy was assumed for this interstage. The interstage is designed on the basis of stability for aerodynamic and inertial loads using the dynamic load factors listed under design constraints (tables V through VIII).

Saturn Launch Vehicle--Saturn to Centaur and Centaur to Kick Stage: A semi-monocoque construction conical interstage of 7075-T6 aluminum alloy was assumed. The interstage is designed on the basis of stability for inertial loads only using, the dynamic load factors listed under design constraints (tables V through VIII).

#### Structural Modifications

A preliminary analysis was conducted to determine the effect of the additional length and weight represented by the kick stage configuration on launch vehicle flight wind capability.

Atlas-Centaur. - The amount of increase in Atlas and Centaur skin gages and tank pressures was estimated on the basis of providing flight-wind capability equal to the present capability of the Atlas-Centaur vehicle for the Surveyor Mission. For a representative cryogenic kick stage, a structural increase of 260 pounds in Atlas tank weight and 155 pounds in Centaur tank weight was required. In addition, an increase in Atlas-Centaur interstage of 75 pounds was required and an increase in Atlas tank pressure resulted in an increase of 30 pounds in Atlas residuals.

In performance calculations, all of the above weights were varied as required due to changes in overall vehicle length brought about by various types and sizes of kick stages.

Saturn IB-Centaur. - For the purpose of performance evaluation, no change in structural weight was made to the first and second stages of the Saturn IB launch vehicle.

#### Effect of Propellant Combination and Propulsion System

The effect of kick stage propellant combination and propulsion system on mission performance will be examined by presenting mission performance of the Atlas-Centaur and Saturn IB-Centaur launch vehicles using the kick stage designs developed in the preceding discussion. Basic kick stage performance, weight data, and required launch vehicle modifications have already been presented. However, each mission will also give rise to specialized requirements regarding launch azimuth, parking time (and hence propellant boiloff), destruct systems, flight performance reserve, etc. All major mission-oriented requirements and

modifications were assessed but for brevity will not be discussed in further detail. For each mission, consistent mission related assumptions were imposed on the various kick stage designs.

In evaluating the selection of kick stage propellant combination and propulsion system, kick stage propellant loading was varied using the data presented in figures 5 through 8 to arrive at an optimum loading for each application. The desirability of a fixed kick stage propellant capacity is recognized, and the effects of kick stage propellant capacity will be discussed later.

#### Atlas-Centaur-Kick Stage

Lunar mission. - The performance of various kick stages on the Atlas-Centaur launch vehicle is presented in figure 16 for a lunar (Surveyor type) mission. This mission represents a relatively low energy application of the kick stage. Without a kick stage, an injected payload of approximately 2650 pounds is obtained. This is higher than the capability (approximately 2500 pounds via parking orbit) for the Surveyor mission as given in reference 4 due to the projected Centaur stage improvements discussed earlier.

The use of a storable kick stage does not offer a payload improvement for the mission. For the relatively low energy lunar mission, the benefits of additional staging are offset by the lower specific impulse of the storable stage. However, even for the lunar mission substantial payload improvements can be obtained with the use of cryogenic kick stages. Most of this improvement can be obtained through use of the H-O kick stage with smaller, additional improvements to be gained by using H-F in the RL-10 or an H-F kick stage incorporating a new engine.

Synchronous orbit mission. - A similar comparison is presented in figure 17 for a 24-hour synchronous equatorial orbit mission. This mission profile consists of a due east launch from ETR into a 90 nautical mile parking orbit, a relatively short coast to the first equatorial crossing, a second in-plane propulsion phase to raise the apogee to a 24-hour orbit altitude, a long coast phase to apogee, followed by a third propulsion maneuver to accomplish the plane change and circularization into the final equatorial orbit.

For this mission, a small improvement is obtained by use of a storable kick stage. This is partly due to the somewhat higher energy requirements of the synchronous orbit mission compared to the lunar mission. More importantly, without a kick stage, three Centaur propulsion phases are required separated by coast phases of approximately 16 minutes (to reach the equator) and 5.2 hours (to reach apogee). This mission profile introduces, (1) additional sequence of chilldown, start-up, and shut-down losses, (2) substantial boiloff and engine leakage losses, and (3) additional Centaur stage attitude control propellant requirements. Most of these penalties are avoided through

use of the storable stage since in this case the Centaur stage is jettisoned during the second propulsion period prior to the long coast phase to apogee.

As for the lunar mission, the major gains are achieved through use of a cryogenic kick stage. For these cases, the Centaur stage is jettisoned prior to reaching the first parking orbit. The engine associated propellant loss penalties for the cryogenic kick stages are reduced (as compared to Centaur) since only a single engine is used. Furthermore, boiloff penalties during the long coast to apogee are negligible due to the better thermal design and insulation of the kick stage. Most of the improvement is achieved through use of the H-O kick stage with smaller, additional improvements through use of H-F in the RL-10 or using the H-F kick stage with a new engine.

#### Saturn IB-Centaur-Kick Stage

The foregoing missions have indicated a substantial improvement in mission capability through use of a cryogenic kick stage even for missions of moderate energy level. When higher energy missions are considered, the use of a cryogenic kick stage becomes increasingly desirable.

Solar probe mission. - As an example of a high energy mission, figure 18 presents the performance of the various kick stages in conjunction with the Saturn IB-Centaur launch vehicle as applied to a close solar probe mission. Without a kick stage, the Saturn IB-Centaur can deliver a 500 pound payload to about 0.22 AU. Some improvement is obtained with a storable kick stage, but major improvements are achieved only through use of a cryogenic kick stage. The H-O kick stage can deliver a 500 pound payload to 0.155 AU perihelion distance from the sun. The H-F kick stage based on the RL-10 can achieve a 0.142 AU perihelion distance and the H-F kick stage based on a new engine can further improve the perihelion distance to 0.132 AU.

Planetary orbit mission. - The kick stage missions discussed thus far have been missions wherein the kick stage is used to acquire injection energy with respect to the Earth. An additional class of potential kick stage missions are those wherein the kick stage is used to provide a retro maneuver into a planetary orbit. As an example, figure 19 presents the results for a Mars orbit mission similar to the Voyager mission presently being studied by NASA. For the 1971 launch, and a 60 day opportunity, the Saturn IB-Centaur launch vehicle can inject approximately 10,500 pounds onto a Mars transfer trajectory. After coasting approximately 200 days, the kick stage is used to retro into an orbit about Mars. The orbit about Mars was assumed to have a perifocus altitude of 1000 nautical miles, and payload is presented as a function of apofocus altitude. The solid curves represent performance wherein all the payload is braked into an orbit about Mars. The dashed curves present performance for a mission

wherein half the final payload is allocated to a lander which separates from the orbiter prior to retro, and half the payload is braked into an orbit about Mars. For this mission, additional insulation and attitude control propellants were added to the kick stage as a consequence of the long coast phase. On the other hand, kick stage guidance and electrical system weights were reduced since most of these functions were assumed to be provided by the spacecraft (payload). Appropriate boiloff penalties were included for the cryogenic stages.

As can be seen from figure 19, the cryogenic kick stages do not offer (on a percentage basis) as large a payload advantage over the storable kick stage as in the other missions presented. This is due in part to the increased boiloff and insulation penalties for the long coast mission. It is also a consequence of the relatively low kick stage velocity requirement for this mission. The kick stage characteristic velocity ( $\Delta V$ ) required to brake into a Mars orbit ranges from 4500 to 7600 feet per second depending on the apofocus altitude. These relatively low velocity requirements do not fully exploit the high specific impulse of the cryogenic stages.

With the exception of the Mars retro mission, the foregoing mission comparisons have indicated a substantial improvement in mission capability through use of a cryogenic kick stage. This is particularly true for high energy missions such as the solar probe mission presented in figure 18. The results presented in figure 18 also typify the comparisons that would be obtained for other high energy kick stage missions. Comparable results would be obtained for energetic anti-solar missions or out-of-the-ecliptic-plane missions. For high energy missions (fig. 18), as would be expected, best performance is obtained through use of a H-F kick stage based on a new propulsion system. However, the high performance characteristics assumed for this propulsion system combined with the introduction of fluorine into the launch vehicle family represents a substantial advancement in the present state of the art in cryogenic propellants. Much of the improvement to be realized by use of a cryogenic kick stage can be realized through use of a H-O kick stage based on the RL-10A-3-3 engine. Such a stage more nearly represents current state of the art in cryogenic propellants. Also, more than half the additional improvement to be realized through the use of fluorine can be achieved through use of a kick stage based on a H-F version of the RL-10A-3-3. Since the mission performance capability of the three cryogenic kick stages is not markedly different, the final choice cannot be made solely on the basis of performance. Consideration must obviously be given also to cost, development time and development risk. Early development of a cryogenic kick stage would recommend the H-O RL-10 based design. On the other hand, if early availability of a cryogenic kick stage is not a strong requirement, and cost studies are favorable, then serious consideration of an H-F kick stage is warranted.

An alternate possibility is to proceed with the development of an H-O kick stage based on the RL-10, with the provision that the design be compatible with fluorine. With this approach, availability of an H-F version of the RL-10A-3-3 would allow substitution of fluorine for oxygen into the stage at a latter date. With this possibility in mind, the remainder of the present report will be directed toward a more detailed definition of the H-O stage based on the use of the RL-10A-3-3. Because of the similarity between the cryogenic stages, most of this discussion is also pertinent to the design of a H-F kick stage, particularly a stage based on the RL-10 engine. After the design of the H-O kick stage is established, the possibility of substituting fluorine into this stage will be discussed.

### Effect of Kick Stage Propellant Loading

The mission discussion presented thus far has been based on kick stages properly sized for each individual application. Fortunately, for many kick stage applications, approximately the same propellant loading is required. This section will investigate the feasibility of selecting a specific propellant loading for the H-O kick stage to best satisfy a range of scientific missions. Similar trends would also be obtained for an H-F kick stage. The major difference is that the higher performance of the H-F kick stage typically results in optimum propellant loadings about 1000 pounds higher than for the H-O kick stage.

#### Atlas-Centaur

The effect of propellant loading for the H-O kick stage is presented in figure 20 for several missions using the Atlas-Centaur launch vehicle. The three missions presented encompass the mission energy range toward which an Atlas-Centaur-H-O kick stage launch vehicle could be applied. The upper curve is for a lunar mission which represents a relatively low energy application of the Atlas-Centaur-H-O kick stage vehicle. The middle curve is for a 24-hour synchronous equatorial orbit mission. The lower curve is for a 0.33 AU solar probe mission which represents a high energy application of the Atlas-Centaur-H-O kick stage vehicle.

The discontinuities in the curves indicate the kick stage propellant loading for which staging between the Centaur and kick stage occurs in the initial Earth parking orbit.

The mission profile for the lunar and solar probe missions consists of launch into a low Earth parking orbit (90 n.mi.), coast (20 minutes was assumed for development of a launch window), and a second propulsion phase to develop the required mission energy. For these missions, the solid portion of the curves to the right of the discontinuities represents sub-orbital ignition of the kick stage. Hence, one Centaur burn and two kick stage burns (separated by the coast phase) are required. At the discontinuity, staging occurs in Earth parking orbit and (for

the lunar and solar probe missions) only one Centaur burn and one kick stage burn are required. The dashed portion of the curves to the left of the discontinuities represent post orbital staging between the Centaur and kick stage. Here, two Centaur burns and one kick stage burn are required.

Recall that for the synchronous orbit mission, two post orbital propulsion phases are required; one at the first equator crossing to raise the apogee altitude and the second at apogee to perform the plane change and circularization. For the synchronous orbit mission, the solid portion of the curve, again, represents sub-orbital staging of the Centaur. Here, one Centaur burn and three kick stage burns are required. The discontinuity represents staging in orbit and one Centaur burn and two kick stage burns are required. Over the dashed portion of the curve, Centaur-kick stage staging occurs during the first post orbital propulsion phase, and two Centaur and two kick stage burns are required.

For each mission profile appropriate propellant losses associated with engine start-up, shut-down, leakage and cryogenic boiloff have been accounted for. Kick stage jettison weight was varied with propellant loading based on the data presented in figure 6. Also, as kick stage propellant loading was varied, launch vehicle modifications, interstage and shroud weights were varied to reflect changes in kick stage height and weight. Even with the inclusion of all these factors, mission payload capability ( as shown in fig. 20) is relatively insensitive to the selection of a kick stage propellant loading over a fairly broad range. More important, a fixed propellant loading can be selected to give near best performance for all three missions. Because of the flatness of the curves displayed in figure 20, selection of an optimum propellant loading based purely on performance is not realistic. The precise optimum point is sensitive to changes in tankage configuration, choice of minimum gage, selected system approaches, etc. For the Atlas-Centaur launch vehicle, a 7000-pound propellant loading for an H-0 kick stage appears to be a reasonable compromise between stage size and mission performance.

With a 7000-pound propellant load, the hydrogen tank can take full advantage of the stage diameter and still be contained in a  $\sqrt{2}$  oblate spheroid tank. If larger propellant loads are selected, stage length increases (the hydrogen tank becomes more spherical) without a significant improvement in mission payload capability. If smaller propellant loads are selected, mission performance begins to fall off more rapidly. Also, the trade-off between propellant load and stage height is less favorable since (adhering to a  $\sqrt{2}$  oblate spheroid) hydrogen tank diameter as well as height must be decreased. Additionally, a 7000-pound propellant load will allow staging in orbit for the synchronous orbit mission which has the most complex mission profile.

## Saturn IB-Centaur

High energy missions. - The effect of propellant loading for the H-O kick stage is presented in figure 21 for a range of solar probe missions using the Saturn IB-Centaur launch vehicle. Solar probe perihelion distance was varied to illustrate the effect of mission energy on the choice of a kick stage propellant loading. For the Saturn IB-Centaur launch vehicle, the Centaur stage is always used sub-orbitally and staging between the Centaur and kick stage occurs during the second propulsion phase. Thus, all the cases presented in figure 21 require two Centaur burns and one kick stage burn; and the mission profile plays no direct role in the choice of a propellant loading.

Again, particularly for the high energy solar probe missions, payload capability is relatively insensitive to the choice of a propellant loading over a fairly broad range. A 7000-pound propellant load will give near optimum performance over a wide range of mission energy. For the 0.16 AU solar probe mission, a small gain is indicated for the higher propellant loads, but this result is sensitive to the final choice of a stage configuration and design. For the lower energy 0.25 AU solar probe mission, a clearer gain in payload can be observed at the higher propellant loadings. However, this gain is not large in view of the substantial payload that can be delivered with a 7000-pound propellant capacity. Consequently, based on the arguments given previously for the Atlas-Centaur launch vehicle, a 7000-pound propellant load for the H-O kick stage appears to be a reasonable choice.

Planetary orbit mission. - In comparison to the other missions discussed, substantially lower kick stage propellant loadings are desired for a planetary orbit mission. As examples, kick stage propellant requirements for a 1971 Mars orbit mission and a 1973 Venus orbit mission are presented in figures 22 and 23, respectively. Data are presented for 1000 nautical mile circular planetary orbits and for orbits with a 1000 nautical miles perifocus altitude and a 20,000 nautical mile apofocus altitude to display the effect of orbit energy. In addition, results are presented for missions wherein all the payload is braked into orbit and missions where half the final payload is braked into orbit and half the payload is allocated to a landing capsule. The symbols shown in figures 22 and 23 indicate the discrete propellant loads required to accomplish the various missions. The curves present performance for kick stages with a larger propellant capacity, but off-loaded to the required propellant weight.

Over the range of mission parameters presented, the 1971 Mars mission requires a propellant load of 2000 to 4300 pounds and the 1973 Venus orbit mission requires a propellant load of 2700 to 5800 pounds. Clearly, it is not possible to select a propellant loading that best satisfies both the planetary orbit missions and also the kick stage

missions discussed earlier. Selection of a kick stage propellant capacity in the range of 2000 to 6000 pounds to satisfy the planetary orbit missions would significantly compromise kick stage performance in high energy probe missions. It appears more reasonable to size the kick stage near the 7000 propellant load level to obtain best performance for high energy probe missions. The kick stage (Cryogenic) can then be off-loaded for the planetary orbit missions. The curves presented in figures 22 and 23 indicate that this approach will not severely penalize possible future planetary orbit applications.

Concluding briefly, based on the preliminary study thus far, a cryogenic kick stage is required to fully exploit the mission energy capability of the present family of NASA launch vehicles. Best performance is obtained through use of hydrogen-fluorine propellants, but this performance can be closely matched by a hydrogen-oxygen kick stage based on the use of the RL-10A-3-3. A single kick stage with a propellant capacity near 7000 pounds can provide close to maximum performance for both the Atlas-Centaur and Saturn IB-Centaur launch vehicles for a range of potential kick stage missions. Such a stage is oversized for Mars and Venus orbit missions, but could be off-loaded for future planetary orbit applications. The next section of this report will develop a more detailed design of a hydrogen-oxygen kick stage (using the RL-10A-3-3) with a 7000-pound propellant capacity.

#### PRELIMINARY DESIGN OF A HYDROGEN-OXYGEN KICK STAGE

This Section will present a preliminary design of a hydrogen-oxygen kick stage based on the RL-10A-3-3 engine and a 7000 pound impulse propellant load. At the conclusion of this discussion, the possibility of substituting fluorine into the H-O stage will be discussed. Three possible stage configurations are presented. The purpose is to compare the three configurations, establish the feasibility of one or more of the designs, and to identify their associated requirements and problem areas. In each system design area there will be a discussion of the present state-of-the-art, possible choices, selection of an approach, presentation of data supporting the choices, and discussion of potential problem areas.

##### Stage Configurations and Structural Design

The three hydrogen-oxygen kick stage configurations illustrated in figures 24 through 26 will be discussed. Each configuration illustrates a broadly different approach to tankage and primary structure. The tankage, primary structure, interstage, and shroud for each configuration will be described, and the advantages and disadvantages of each configuration will be noted. Comparison of the shrouded configurations adapted to an Atlas-Centaur launch vehicle is presented in figure 27.

Four spheres configuration (config. I). - This stage (fig. 24) is identified by the four spherical oxidant tanks clustered aft of

the single oblate spheroid fuel tank. For a 7000 pound propellant loading, the required fuel volume can be contained in a  $\sqrt{2}$  oblate spheroid tank. This shape utilizes most of the 120 inch stage diameter, minimizing stage length. This is the only proposed configuration which used multiple tanks for one of the propellants. Clearance between the engine and oxidant tanks is obtained by mounting the engine on a truss assembly aft of the cruciform beam. The resulting stage overall length is 180 inches; 15 inches shorter than the nested-tanks configuration (fig. 25), and 20 inches longer than the toroidal oxidant tank configuration (fig. 26). Although the stage is 20 inches longer than the torus configuration, several attractive features are gained. Conventional shaped tanks are used, and the engine thrust loads are carried solely by the space truss. The fuel line would be a direct and short line to the engine pump. The oxidant lines for this configuration are more complicated than for the other configurations and would require manifolding.

The primary structure is a space truss configuration consisting of three 120 inch O.D. rings laced together with diagonal strut members. The diagonal struts can transmit axial and lateral loads. A representative payload adapter structure of similar design is also shown. The rings would be built-up sections and the struts would be round or square tubing. A design feature is the cruciform beam-ring assembly which forms the thrust structure and provides support for the oxidant tanks. This would be a built-up beam of aircraft type construction and would provide reinforcement to minimize radial deflections of the truss. The cruciform beam would also support the helium bottles and engine actuators. Thus, no concentrated loads would be applied to the fuel tank. The conical fuel tank support and the cylindrical oxidant tank supports would be titanium to reduce heat conduction to the tanks. For long coast missions (planetary orbiters) the titanium tank supports would be replaced by fiber-glass plastic tank supports to further reduce the heat conduction to the tanks. Similar tank supports are used for configuration III.

Guidance, telemetry and other electrical equipment would be supported by the payload adapter.

Based upon the use of 2219-T81 aluminum alloy, the structural weight is estimated to be 278 pounds not including the propellant tanks. The tankage weight is estimated to be 212 pounds so the total weight for tankage and structure is 490 pounds. A complete weight summary is shown in table X and it is noted that the four spheres configuration mass fraction is 0.795.

Adapting this stage to the Atlas-Centaur vehicle would require a Centaur-Kick interstage 120 inches in diameter by 142 inches in length (fig. 27). The interstage would be supported by the Atlas-Centaur station 219 ring and would interface the kick stage aft ring. For the purpose of weight estimates, a semi-monocoque interstage similar to the Atlas-Centaur interstage was considered. Its weight is estimated

at 700 pounds. The kick stage would fly out of a hole approximately 82 inches in depth and a clearance angle of about  $23^{\circ}$  would be realized.

The kick stage shroud (fig. 27) would be 120 inches inside diameter by 342 inches in length. Note that the shroud encloses the kick stage and would separate at the stage aft ring. The payload density was assumed equal to the envelope density of Surveyor enclosed by its nose fairing (approximately  $7 \text{ lb/ft}^3$ ). A required payload volume was then calculated using a 3500 pound payload. This procedure was followed for all configurations. For the purposes of weight estimates, it was assumed that a semi-monocoque aluminum barrel section could be added to the Surveyor shroud. The resulting total weight is estimated at 2,000 pounds

Nested tanks configuration (configuration II). - This configuration (fig. 25) is identified by the nested but separate tanks. It is an effort to compact the stage length and reduce stage weight by utilizing the tanks for the thrust load path. The fuel tank is located forward and is designed with a self supporting reversed bulkhead so the oblate spheroid oxidant tank can be nested with the fuel tank. However, the required tank volumes do not lead themselves to full use of the stage diameter and the usual compaction feature of nested tanks is lost. The stage is 195 inches overall; 35 inches longer than the torus configuration and 15 inches longer than the four spheres configuration.

A common bulkhead design similar to the Centaur stage was considered but it was found that hydrogen boiloff would be excessive for long duration missions. Thus, separate tanks that are well insulated from each other are required. For the proposed configuration, the oxidant tank would be supported by a conical shell of glass fiber plastic and the reversed bulkhead would be a sandwich construction using a plastic core. Thus, the cryogenics are effectively insulated from each other.

The fuel line would be an external line from a single sump on the reversed bulkhead tank similar to the Centaur fuel line arrangement. The oxidant line would be a direct and short line from the combination tank sump and engine thrust cone to the engine pump.

The propellant tanks also serve as the stage primary structure. Engine thrust and inertia loads are transmitted by tank membrane stresses. The tank ullage pressure would be maintained sufficiently large so that no compressive stresses would develop. Compressive stresses in the tank membrane would require a stability design criteria and incur a large weight penalty compared with the tensile stress membrane design.

The engine is supported by the combination oxidant tank sump and thrust cone. The thrust cone would distribute the thrust load into the tank as a membrane load and the tank would be strengthened at the thrust cone junction. The engine actuators and helium bottles

would also be supported by the tank. Thus, several concentrated loads would be imposed on the tank. In addition to increasing the tank weight, mounting equipment on the tank substantially complicates the installation of multifoil insulation.

The tank and structural material is 2219-T81 aluminum alloy. Structural weight is estimated to be 163 pounds not including the propellant tanks. The tankage weight is estimated to be 306 pounds so the total weight for tankage and structure is 469 pounds. A complete weight summary is shown in table XI and it is noted that the nested tank configuration mass fraction is 0.799.

Adapting this stage to the Atlas-Centaur vehicle would require a Centaur-kick interstage 120 inches in diameter by 212 inches in length (fig. 27). The interstage would be supported by the Atlas-Centaur station 219 ring and would interface the kick stage forward structural ring. The weight of a semi-monocoque aluminum interstage was estimated at 1040 pounds. This configuration would require flying out of a hole 150 inches in depth, about twice the hole depth for the other configurations. A clearance angle between the stage and interstage of about  $15^{\circ}$  could be realized.

The kick stage shroud (fig. 27) would be 120 inches inside diameter by 287 inches in length. The shroud separates at the stage forward structural ring. For the purposes of weight estimates, it was considered that a semi-monocoque aluminum barrel section could be added to the Surveyor shroud. The resulting total shroud weight was estimated at 1865 pounds.

Toroidal oxidant tank configuration (configuration III). - This stage (fig. 26) is identified by the single toroidal oxidant tank around the engine. Use of a torus permits mounting the engine directly on the oblate spheroid fuel tank so a 160 inch overall stage length is achieved. This is the shortest of the three configurations.

The fuel line would be a direct and short line from the combination tank sump and engine thrust cone to the engine pump. The oxidant line should be relatively short and direct if a suitable sump is provided in the torus. Use of a torus would require a technology development program to study propellant utilization, sloshing, fabrication, and support.

The primary structure is a space truss identical in configuration to that used in the four spheres design except for the thrust structure. The torus design utilizes the fuel tank for transmitting the engine thrust loads to the primary structure. The combination fuel tank sump and engine thrust cone would distribute the thrust load into the tank as a membrane load and the tank would be strengthened at the thrust cone junction. The helium bottles and engine actuators would be supported by the truss. This configuration,

like the nested tanks configuration, would impose concentrated loads on one of the propellant tanks.

A feature of the primary structure design is the torus support. The torus is supported at both the inner and outer meridian in an effort to minimize overturning moments. Overturning moments would produce compressive membrane stresses and hence the torus would be designed by stability criteria rather than be membrane pressure stresses.

The structural and tank material is 2219-T81 aluminum alloy. Structural weight is estimated to be 198 pounds not including the propellant tanks. The tankage weight is estimated to be 215 pounds so the total weight for tankage and structure is 413 pounds. A complete weight summary is shown in table XII and it is noted that the torus configuration mass fraction of 0.803 is the highest value of the three configurations investigated.

Adapting this stage to the Atlas-Centaur vehicle would require a Centaur-Kick interstage 120 inches in diameter by 132 inches in length (fig. 27). The interstage would be supported by the Atlas-Centaur station 219 ring and would interface the kick stage aft ring. The weight of a semi-monocoque aluminum interstage was estimated at 645 pounds. The kick stage would fly out of a hole approximately 71 inches in depth and a clearance angle between the stage and the interstage of about  $20^{\circ}$  could be realized.

The kick stage shroud (fig. 27) would be 120 inches inside diameter by 332 inches in length. The shroud encloses the kick stage and would separate at the stage aft ring. For the purposes of weight estimates, it was considered that a semi-monocoque aluminum barrel section could be added to the Surveyor shroud. The resulting total shroud weight was estimated at 1980 pounds.

The foregoing discussion has compared three broadly different stage configurations. Their respective advantages and disadvantages have been discussed and all three designs appear feasible. Configuration III would appear to be the best choice in view of its better stage mass fraction. Configuration I would probably present the most straightforward development approach but is longer and is approximately 80 pound heavier than configuration III. Configuration II offers a simple propellant feed system but the stage height and weight (particularly in view of its heavy interstage) and the difficult fabrication of a sandwich construction reversed bulkhead indicates that this configuration does not offer an overall advantage over configurations I and III.

## Systems Discussion

Many of the systems design features for the hydrogen-oxygen kick stage have been discussed in the first Section. A summary of the design assumptions were presented in table VI. The following discussion will expand on the data presented in the first Section.

### Engine

The RL-10A-3-3 engine delivers 15,000 pounds of thrust at a chamber pressure of 400 psia with a nozzle expansion ratio of 57. Net positive suction pressure requirements of the engine are 4 psi for the hydrogen pump and 8 psi for the LOX pump. The nominal specific impulse is 444 seconds at an engine mixture ratio of 5.

For multiple firing missions where the total mission time is only a few hours, no major engine problems are foreseen. For long missions, however, several problems arise; namely, engine leakage and thermal and meteoroid protection. The current engine leakage rate is about 3.0 pounds of propellant per hour. For short missions, this is an insignificant loss, but for missions where engine firings may be separated by weeks or months, the loss becomes prohibitive. For example, on a planet orbiter mission, the first midcourse correction may be a week or so after launch with the next one not scheduled for months. The resulting propellant loss would be intolerable even if the RL-10 leakage rate were reduced by a factor of 10. Therefore, for the planet orbiter missions a storable (hydrazine) monopropellant midcourse propulsion system was added to the H-O stage. As on Mariner, parallel feed systems would be utilized. After each midcourse correction, squib valves would be fired to seal off the propellant system. A midcourse propulsion system velocity correction capability of 150 feet per second was used. A specific impulse level of 240 seconds was assumed and the resulting mass fraction of the system was 0.75.

For propellant thermal protection purposes, the kick stage was assumed oriented payload toward the Sun. As a result, the engine will be shielded from the sun and on long missions, unless the engine is fired periodically, its temperature will drop below the minimum starting temperature. Manufacturer's specifications state that the RL-10 will not bootstrap properly if its nozzle temperature is below 300 degrees Rankine. This problem can be circumvented by starting the engine in the idle mode and then accelerating to rated thrust. Of more concern is the possibility of freezing oxygen in the turbopump if its temperature is too low. More than likely, excess electrical power would be available during coast periods so strip heaters could be used to maintain the LOX pump temperature at a safe level. Another possibility would be to reorient the stage to an engine facing the sun attitude several hours prior to engine start and allowing the engine components to warm-up to an acceptable temperature.

The magnitude of the meteoroid penetration problem in space is still highly uncertain. The uncertainties are due to the lack of definitive information regarding the meteoroid mass-frequency relationship and its spatial variation and the lack of understanding as to the proper hypervelocity impact criteria. Based on Whipple's 1963 B flux and Summers' penetration criteria with a factor of 5 to account for bumper effects, a shell around the engine nozzle weighing about 10 pounds would be required to give a probability of 0.99 of not penetrating the engine coolant tubes.

#### Pressurization and Propellant Systems

Pressurization. - There are a variety of pressurization concepts that would fill the requirements of the H-0 kick stage. The ultimate objective, of course, is to select a system that strikes the proper balance between system weight and system reliability. Current state of the art in pump-fed cryogenic stages using regeneratively cooled engines employing a gas generator to drive the turbomachinery is as follows: Initial tank pressurization is accomplished with helium. During propellant expulsion, warm hydrogen is bled off downstream of the cooling jacket and used to pressurize the hydrogen tank. Oxygen is bled off downstream of the oxygen pump, passed through a heat exchanger located in the turbine exhaust duct, and then used to pressurize the oxygen tank.

Hydrogen tap-off is available on the RL-10 and was selected for expulsion pressurization of the hydrogen tank. The engine does not use a gas generator cycle, however, so no built-in heat source is available for vaporizing oxygen. Since it isn't reasonable to add a gas generator merely to vaporize oxygen, the remaining system selection problem becomes principally that of selecting the helium storage conditions and helium inlet temperature to the LOX tanks.

Line drawings of three system concepts are shown in figure 28. For simplicity, only one oxygen tank is shown. System A is the simplest. Helium is stored in an insulated titanium bottle at room temperature and 4000 psia. During expulsion, a polytropic expansion takes place within the storage bottle resulting in a final helium temperature of about 300° R. The system weight is 31 pounds. All weight comparisons here are based on 6000 pounds of propellant at an O/F of 5 and 35 psia propellant tank pressures.

The helium is stored in a titanium bottle located inside the hydrogen tank in system B. This reduces the volume and, hence, the bottle weight. Storage pressure is 1000 psia. The helium passes through a heat exchanger located in the oxygen tank prior to entering the propellant tanks. If an isothermal expansion occurs within the helium bottle, the system weight is about 12 pounds. If, as is more than likely, the expansion is polytropic, then this system could weigh 20 pounds. This is due to the fact that the specific heat ratio for

helium increases rapidly as the temperature drops below 37°R.

The helium is stored within the LOX tank in system C. Because of the uncertainty of using titanium with LOX, either a stainless steel or aluminum bottle is needed. The weight of this system is 26 pounds if we assume an isothermal expansion and use a 301 stainless steel bottle. Use of an aluminum bottle would increase system weight 8 pounds. The optimum storage pressure is 1500 psia. The system weight for a polytropic expansion is estimated at 42 pounds using a stainless steel bottle.

From the above discussion, it is evident that there is nothing to be gained by going from system A to system C, and at best 10 or 20 pounds could be saved by using system B instead of A. Neither B nor C is as simple as A. The additional tank penetrations increase the tank insulation problem, and the pressurant bottle is much less accessible if bottle problems arise prior to launch.

For the above reasons, system A was selected for the H-0 kick stage.

Propellant system. - The net positive suction pressure requirements of the RL-10A-3-3 engine are 4 psi and 8 psi respectively for the hydrogen and oxygen pumps. It was assumed that the propellants would be loaded at 17 psia. Allowing, conservatively, 10 psi pressure drop for lines and valves, results in tank pressures of 31 psi for hydrogen and 35 psi for oxygen. However, in order to guarantee sufficient pressure to overcome the breakaway torque of the turbine, the RL-10A-3-3 specifications call for a hydrogen pump inlet pressure of 30 psia. Therefore, 35 psia nominal tank operating pressure was used for both propellants. Theoretically, once the engine is running, the hydrogen tank pressure could be dropped 4 psi, but this was not done in this study.

The weight of the propellant plumbing system does not vary significantly among the 3 H-0 designs, however, the difference in complexity is significant. Configuration I has the most complicated plumbing. Oxygen is taken out of each tank by lines extending from the bottom of each tank up through the top where they are manifolded together. In addition, the oxidant tanks themselves are manifolded together both at the top and at the bottom to eliminate any pressure differentials that would result in uneven emptying.

The trapped liquids are greatest in configuration I due to the additional line lengths involved. The total trapped liquids (hydrogen and oxygen) are 60 pounds, 45 pounds, and 52 pounds for configurations I, II and III, respectively.

The choice between using an active propellant utilization system or a biased propellant load to minimize propellant outage

in a small cryogenic stage is not an easy one. The problem is complicated by uncertainties in propellant heating, boiloff and stratification.

A rudimentary calculation was performed to determine the probable magnitude of the propellant outage associated with a calibrated propellant system. The method used is described in reference 5. Variations in seven parameters were considered. The parameters and their assumed 3 sigma tolerances are shown in table XIII. Calculating the optimum mixture ratio bias from the RSSed value of the parameter variations results in a maximum propellant outage of 50 pounds. An active propellant utilization system for a stage of this size using capacitance probes would weight in the order of 30 to 50 pounds depending upon the configuration. Therefore, for the purposes of this study, a 50 pound weight allowance was included in the propellant system weights to account for the penalty associated with either an actively controlled or pre-calibrated system.

#### Insulation

Cryogenic stages require some means of thermally protecting the propellant tanks in order to minimize the amount of heat absorbed by the propellant. The methods available to control heat input are many, ranging from a simple insulated tank to the more complex machinery required for refrigeration. The choice of any particular method is usually dictated by weight considerations and the degree of complexity involved, since increased complexity usually has an adverse effect on reliability. In general, thermal protection systems can be classified as passive or active. Passive systems include surface coatings, conventional insulations, multifoil insulations and shadow shields, whereas active systems involve some sort of mechanical refrigeration or reliquifaction device. The tradeoff between active and passive systems is a function of propellant tank surface area-to-volume ratio; the smaller tanks requiring active systems earlier than would large volume tanks. In general, if tank venting is possible, passive systems provide the least weight penalty for mission times up to about a year; however, if tank venting is not permitted or is a major problem in zero g, then active systems become more desirable for shorter duration missions.

In this study only foam and multilayer insulation systems were considered. Lightweight, reliable, active thermal protection systems have yet to be developed. Shadow shields appear attractive; however, at the present time, insufficient design information exists from which to determine the weights and performance associated with a practical shadow shield system.

It was pointed out in the first section that in determining thermal protection requirements for vented systems, the parameter of interest

is the square root of the product of insulation thermal conductivity times insulation density. In figure 29 this parameter is plotted versus insulation weight per unit area for several insulation systems. The thermal properties of foil insulations are expressed in terms of an apparent conductivity that applies only for a given set of boundary conditions. All of the curves and data shown on figure 29 are based on an insulation warm side temperature of  $530^{\circ}\text{R}$  and a cold side temperature of  $37^{\circ}\text{R}$ . The curves marked ideal were generated using the ideal values of thermal conductivity and insulation density and do not include any weight or performance penalty for physical application to a tank. Curves 1 and 2 represent ideal foam and ideal multi-foil insulation respectively. Multifoil insulation, which is really just a series of closely spaced radiation shields separated by low conductivity spacers, depends upon vacuum within the foils for efficient operation. The presence of any gas, liquid, or solid between the foils degrades its performance due to conduction between the foils. This problem of degraded performance is not too serious on the ground because the tanks can be continuously topped off; however, steps must be taken to insure that, once the cryogenic stage has cleared the atmosphere of Earth and the insulation is ready to perform its function, no foreign substance remains within the foil pack. Several techniques are available for accomplishing this.

Curve 3 reflects the addition of a flexible vacuum jacket to encapsulate the insulation. A vacuum of  $10^{-5}$  Torr would be pulled on the system on the ground, compressing the insulation against the tank. Once in space, the compression would be relieved and hopefully the insulation would "fluff" out to its original thickness. Unfortunately, developing a light weight vacuum jacket that will hold such a vacuum when applied to a tank with several penetrations is a formidable task. Preventing permanent sets in the bag or the foils which would prevent the insulation from returning to its original thickness is also a problem.

Curve 3 also depicts the use of a helium purge bag. Gaseous helium is forced through the insulation during ground hold and allowed to escape during ascent and subsequent space flight. This system requires that the helium gas be evacuated rapidly after launch in order to approach the efficient high vacuum performance.

Another solution to the problem is that of attaching another insulation (foam) to the tank wall to provide a relatively warm base surface for the multifoil and purging the foil with dry nitrogen. The characteristics of this system are shown by curve 4. As with the helium purge the mandatory consideration with this system is providing adequate escape paths for the nitrogen so that the foils can be rapidly evacuated once in the vacuum of space.

Two experimental data points are shown on figure 29. The circle in the center represents the results of a test on a 4 foot hydrogen tank at

Lewis (ref. 6) using multifoil insulation with a flexible vacuum jacket. The relatively high level of  $\sqrt{K\rho}$  observed on this test is believed to be primarily the result of incomplete recovery of the vacuum bag. Atmospheric pressure acting on the vacuum bag compresses the insulation against the tank when the foils are evacuated. Theoretically, the insulation should fluff out to its original thickness when atmospheric pressure is removed; however, if permanent sets or creases occur in the vacuum bag then full recovery may not be obtained. Also, on this test, the density of the installed insulation was high (11.7 lbs/ft<sup>3</sup>) compared to the theoretical density (4.7 lb/ft<sup>3</sup>). As more experience is gained in application techniques, the difference between installed and theoretical density should decrease.

The results of a more recent test by Lockheed under NASA contract NAS3-4199 are shown by the square in the lower left of figure 29. The insulation system was helium purged multifoil. The insulation itself was double aluminized Mylar with Dexiglas spacers. Prior to measuring the thermal characteristics of the insulation, the insulated tank was subjected to acoustical, vibration and acceleration tests. Subsequent to these tests the tank was placed in a vacuum facility. After purging the insulation with helium, the facility pressure was rapidly reduced simulating the pressure-time history of a Saturn V launch and the thermal characteristics of the insulation system were determined.

Comparing the test point with the curve for ideal foil, it can be seen that there is less than a factor of two difference between the "laboratory" value of the parameter  $\sqrt{K\rho}$  and that obtained in the test. Therefore, for the purposes of this kick stage study, the use of helium purger multilayer insulation with a density of 5 pounds per ft<sup>3</sup> and an apparent thermal conductivity level of twice ideal was assumed.

Caution is required in interpolating the data of figure 29. The insulation comparison parameter  $\sqrt{K\rho}$  is a measure of the effectiveness of an insulation and it is always desirable to strive for low thermal conductivity and low insulation density; however, in determining the thermal protection system performance, the temperature difference across the insulation is needed. The data on figure 29 are based on insulation boundary temperatures of 530°R and 37°R. In most space flight applications, the temperature difference across a given thickness of foam will be less than that across an equal thickness of multilayer insulation, hence, in determining the thermal protection system weight penalty for a vehicle, it is found to be a function of the parameter  $\sqrt{K\rho}$ , but not necessarily directly proportional to it.

There are three distinct mission types that must be considered when evaluating the kick stage insulation requirements. These are: 1) missions that involve propellant storage through the Earth parking orbit coast phase (less than an hour). 2) missions requiring storage

times of up to six hours (synchronous orbit). 3) missions requiring hundreds of days of propellant storage (planet orbiters).

An Earth orbit parking time of 45 minutes is adequate for all the missions considered in this study. This short time period poses an insulation problem for either foam or foil insulation if tank venting is assumed. If, however, there is a strong incentive to eliminate tank venting then it appears that foam insulation is not adequate for a 45 minute parking orbit period.

The highest heating rates the kick stage will experience, with the exception of that occurring during ground hold, are those encountered in the Earth parking orbit. In addition to solar heating, the vehicle is subjected to Earth thermal heating and albedo heating. Some aerodynamic heating will also occur if the orbit altitude is sufficiently low.

A rigorous determination of the heat input to the kick stage propellant tanks during parking orbit coast is quite complex and was not undertaken for this study. However, taking a worst case example (daylight launch with maximum solar heating) and calculating the pressure rise in a non-vented hydrogen tank, assuming no bulk heating of the hydrogen, gives the following results. With a quarter of an inch of multifoil insulation on the tank, pressure rise during a 45 minute coast in a 100 nautical mile orbit is about 5 psi and tank venting would not be required. With foam insulation, the maximum allowable tank pressure would be exceeded and venting would be required.

The magnitude of the pressure rise would decrease drastically if significant bulk heating occurred rather than purely propellant vaporization; however, until more is known about zero g heat transfer, the conservative approach is to assume pure vaporization.

A comparison of the performance of foam and multilayer insulation for a short mission (6 hour transfer to synchronous orbit) is shown on figure 30. Hydrogen tank pressure at the end of coast is plotted versus insulation weight. The following assumptions were made in making the comparison: (1) The hydrogen tank was one third full during the transfer; (2) all heat entering the tank resulted in vaporization of hydrogen; (3) the stage was oriented payload toward the sun during the transfer; and (4) the initial tank pressure was 17.0 psia (recall that the propellants are loaded at 17.0 psia). During engine firing, the hydrogen tank is pressurized with warm hydrogen gas to 35.0 psia. At engine shutdown, equilibrium vapor pressure is slightly less than 17.0 psia.

The results indicate that venting during transfer will not be needed for this type of mission. The tank pressure rise is less than 2 psi even when using foam insulation. Typical minimum insulation thicknesses are called out on each curve and with these thicknesses, the insulation weights are about equal.

The comparison between foil and foam is less favorable on a long storage time mission such as a planet orbiter. The optimized hydrogen boiloff for the H-O stage on a Mars orbiter mission (assuming a typical 220 day coast time) using multilayer insulation is 300 pounds. Half of this boiloff is due to radiation through the foils and half is due to conduction through the tank supports. The insulation thickness required is 1.5 inches. Comparing this with foam, even with 15 inches of foam on the tank, all of the hydrogen on board would vaporize before Mars encounter. Obviously, foam alone is not suitable for long time cryogenic storage applications.

The effect of multilayer insulation thermal conductivity on thermal protection system weight is shown on figure 31. For the conditions applicable to this example, the ideal thermal conductivity was  $10^{-4}$  Btu in/hr ft<sup>2</sup>°R. The sum of the insulation weight plus hydrogen boiloff weight slightly more than doubles if the thermal conductivity is increased by a factor of 10. The point to be made here is that even though multilayer insulation is necessary for the planetary orbit missions, an insulation performance level substantially less than ideal could be tolerated.

Summarizing the insulation discussion, the use of helium purged multilayer insulation was assumed. A quarter of an inch of insulation was used on all cryogenic tanks for missions involving coast times of up to 6 hours. For the long coast missions, an inch and a half was used on the hydrogen tank and a quarter of an inch on the LOX tanks.

It appears inevitable, based on the present state of the art in thermal protection systems, that zero g venting will be required for cryogenic pump-fed stages when used on missions requiring long propellant storage times. There is presently a great deal of uncertainty regarding the magnitude of the zero g venting problem. Factors that enter into this uncertainty are lack of knowledge in the following areas: (1) propellant settling requirements, (2) degree of thermal stratification of propellants, (3) effectiveness of surface tension devices in locating the ullage bubble. Certainly if surface tension devices prove capable of maintaining the ullage bubble location, then the zero g vent problem largely disappears. If, on the other hand, they don't prove effective, then factors 1 and 2 above become important. The degree of stratification affects how often venting will be required, and the propellant settling requirements determine the propulsion penalty associated with each vent.

#### Shroud Configuration

The kick stage designs considered thus far are based on a space truss primary structure requiring shrouding of the kick stage during flight through the atmosphere. This concept is directly compatible with present NASA plans for shrouding the Saturn IB-Centaur launch vehicle. A 260 inch diameter shroud completely enclosing the

payload and Centaur stage is planned for the Saturn IB-Centaur. For the Saturn IB-Centaur-kick stage launch vehicle (fig. 15), it is assumed that the shroud would be lengthened to also enclose the kick stage. The design details and weights for the shroud and interstage have been given in the first section.

For the Atlas-Centaur-Kick stage launch vehicle it has been assumed, thus far, that the jettisonable nose fairing would be extended to enclose the kick stage. However, several shroud-interstage configurations are possible. To evaluate possible shroud designs, reference configurations have been developed for the three major categories of shroud-interstage designs: short shroud, long shroud, and non-shrouded. The shroud configurations are illustrated in figure 32. The three reference configurations, which illustrate the study approach and show proposed depth of design and weight analysis, are presented during the subsequent discussion.

Short shroud (configuration A). - This is the configuration that has been assumed thus far in the study. It has a jettisonable semi-monocoque nose fairing which enclosed the truss structure of the stage and terminates at the cruciform beam. The primary function of the fairing is the protection of the payload and kick stage from aerodynamic and heating loads which occur during the boost phase of the trajectory. The shroud is jettisoned as soon as the dynamic pressure drops to a permissible value.

The function of the interstage structure for this configuration is to provide structural continuity between the kick stage and Centaur vehicle. The structure must be able to transmit the kick stage-payload inertial loads in addition to the aerodynamic and heating loads which are imposed during the boost phase of flight. A semi-monocoque cylindrical segment was utilized as the primary structure.

Long shroud (configuration B). - The second design was evolved to investigate the possibility of improving the payload capability of the kick stage. This configuration demonstrated the utilization of a fully shrouded payload, kick stage and interstage design. The circumferential separation joint of the shroud is located at the Centaur forward bulkhead joint.

Non-shrouded (configuration C). - The third shroud-interstage configuration utilizes a nose fairing shroud which terminates at the forward location of the kick stage structure. The basic criteria for this design was the use of a portion of the outer fairing for the kick stage structure. The outer shell is designed to transmit inertial, aerodynamic and heating loads which are induced during the boost phase of the flight. Three shell structural configurations were investigated during the study: semi-monocoque, waffle, and honeycomb. The semi-monocoque configuration, which utilized frames and closely spaced hat section stringers, was

optimized from the standpoint of general instability while under the influence of external pressure and axial loads. The semi-monocoque design was determined to be heavier than the sandwich configuration and lighter than the waffle design. However, the semi-monocoque configuration shell may be the best compromise between optimum weight and minimum fabrication problems.

The interstage for this configuration is basically the same structure as that which was described for configuration A.

Configuration selection. - Table XIV summarizes the effect of shroud, interstage, and kick stage jettison weight on the payload weight for the three configurations which are illustrated in figure 32. In reviewing the results of table XIV, the shrouded configuration payloads were larger than those for the non-shrouded cases. The increased payload can be primarily attributed to the lower kick stage jettison weights since there is a direct one to one tradeoff between payload and jettison weight. The truss structure, which was utilized for the shrouded configurations, was the major influencing component that provides the decrease in jettison weight when compared to the cylindrical outer fairing which was employed for the non-shrouded case. (Likewise, since the components would be fully shrouded on the Saturn IB-Centaur launch vehicle, a truss configuration would also be a good choice for the kick stage structure for this application).

The shroud and interstage weights do not trade off directly with the payload weights; consequently, their influence will not be as critical as that of the kick stage jettison weights. Therefore, the weight summary table indicates that for optimum payload weights, the long shroud (config. B) should be preferred. However, for this configuration, jettison dynamic problems are predicated for the large length nose fairing shroud. Also, this design will transmit large local kick loads, which are originated by separation dynamics, into the Centaur vehicle. This loading condition will require local strengthening of the Centaur vehicle. Because of the above mentioned problems which are associated with configuration B, configuration A was established as the basic design throughout the other phases of this study.

#### Guidance

As developed thus far, a single kick stage design concept can be used for a variety of mission types flown on two different launch vehicle configurations. Each of these missions requires a guidance system in the kick stage appropriate to the particular case. In order to minimize development cost and obtain maximum reliability, it is desirable that a single guidance system be used for all of the missions under consideration. The purpose of this section is to identify the guidance and control requirements of the various missions relative to trajectory characteristics, required

accuracy and weight allowance, and to evolve a kick stage guidance system which best satisfies these requirements.

The missions under consideration can be divided into four general categories, as far as guidance requirements are concerned. The following missions will be considered in detail, as typical representatives of these categories:

- (1) solar probe mission (Saturn IB-Centaur)
- (2) lunar mission (Atlas-Centaur)
- (3) synchronous orbit mission (Atlas-Centaur)
- (4) Mars-orbit mission (Saturn IB-Centaur)

The solar probe is a typical high energy mission in which no exact target or orbit is required. Solar escape and out of the ecliptic missions are similar with respect to this classification. Accuracy requirements are generally not severe in these missions, since guidance errors result in degraded mission performance, rather than complete mission failure. For example, guidance errors in the solar probe mission simply result in increased perihelion distance.

The lunar mission falls in the general category of planetary orbiters and probes. Guidance requirements are more severe for these missions, since injection errors must be corrected by the spacecraft in order to achieve the required lunar or planetary arrival conditions. The amount of midcourse propellant required for these corrections is determined by the statistical expected guidance accuracy, and the loss in payload capability is proportional to the weight of this propellant.

Guidance requirements for the synchronous orbit mission are even more severe than for lunar and planetary missions. For this case, the launch vehicle (kick stage) guidance system must guide the synchronizing burn at apogee, as well as the pre-injection phase. Residual errors are again removed by the spacecraft, which in this case detracts from the spacecraft station-keeping capability.

For the Mars orbit mission, the kick stage functions like a spacecraft: that is, it provides midcourse corrections and terminal maneuvers at Mars. Accordingly kick stage guidance will be provided by the spacecraft (i.e., payload) for this case. Since this mission represents a very special case, the guidance system evolved for the first three mission types is not required to be applicable to the Mars mission.

The scope of kick stage guidance is somewhat different for Saturn and Atlas based vehicles. For all Saturn based vehicles, the present inertial guidance system is retained in the SIVB stage, to guide the two Saturn stages. For the solar probe mission, the Centaur guidance system is replaced by a system in the kick stage which guides Centaur and the kick stage into the required heliocentric orbit. For the Mars mission, the Centaur inertial guidance system is retained in

Centaur to guide the injection into the required Mars transfer trajectory.

For Atlas-based vehicles, the Centaur guidance system is again replaced by a kick stage system, which is used to guide the Atlas-Centaur and the kick stage to injection (and to guide the apogee burn for the synchronous orbit mission).

In order to determine the guidance system best suited for the missions under consideration, the guidance system requirements for the solar probe, lunar and synchronous orbit missions will now be considered in detail.

Solar probe. - Figure 33 presents Earth traces of possible boost trajectories for the solar probe mission. These trajectories are approximately great circles which intersect the launch site (Cape Kennedy) at azimuths required for the launch opportunities, limited by range safety (typically,  $90^{\circ}$  to  $114^{\circ}$  from the north). For each trajectory, there is first a powered boost arc of about  $24^{\circ}$  into a parking orbit at 100 nautical miles altitude which used the two Saturn stages and a Centaur first burn. After a coast phase of up to 45 minutes, the Centaur and kick stages burn to propellant depletion over a  $51^{\circ}$  arc. For each launch opportunity, the initial azimuth heading and parking orbit time are set so that the final trajectory has a minimum perihelion.

The enclosed area in figure 33 is the region of possible powered flight trajectories, covering an area almost 14,000 nautical miles long and 1200 nautical miles wide, mostly over open ocean. Regions of radio coverage are shown for two stations, one at the Cape and one downrange. The inner circle is for accurate coverage (elevation  $>20^{\circ}$ ) and the outer circle for maximum coverage (elevation  $>5^{\circ}$ ). Radio coverage of all possible trajectories would require a large number of interconnected ground and ship-borne stations. The required coverage area can be reduced by restricting the launch opportunities, but even allowing only a single trajectory with zero coast time, radio coverage of the total burn arc of  $75^{\circ}$  presents a formidable task.

The accuracy requirements for this mission are presented in table XV. For a rather stringent criteria of losing only about  $4 \times 10^{-4}$  AU in perihelion distance (which is equivalent to an eight pound payload loss) the accuracy requirements are not difficult. For example, along the outgoing asymptote a  $2^{\circ}$  error in direction or a 60 ft/sec decrease in velocity can be tolerated. This is reflected in a tolerance at final injection of velocity direction within  $2^{\circ}$  or velocity within 50 ft/sec.

Although guidance accuracy is not critical at final injection, it is still important along the powered flight to keep the trajectory close to an optimum one and to meet other trajectory constraints. For these

purposes, typically, thrust direction should be within about  $2^\circ$  of the optimum, on the average.

The accuracy requirements for the solar probe mission are the least severe of the three missions considered here and can be met by many current systems.

Lunar missions. - Figure 34 presents a map of Earth traces of possible boost trajectories for lunar missions, typified by Ranger and Surveyor. This map is similar to figure 33, except for the length of powered arcs. The initial boost arc of about  $25^\circ$  uses Atlas, Centaur and the kick stage to attain a parking orbit. After the appropriate coast phase (a maximum of 45 minutes for this mission), the kick stage burns to reach the required energy (over an arc of about  $15^\circ$ ). For each launch opportunity the initial azimuth heading (limited, again, by range safety), the parking orbit time and the final energy are set so that the spacecraft will hit the moon at the desired location, and at the desired time.

The region of possible powered flight trajectories may cover an area 13,000 nautical miles long and 1200 nautical miles wide. The difficulty in radio coverage is self-evident. Again, the required coverage area can be reduced by restricting the launch opportunities, but even covering only the total powered burn arc of  $40^\circ$  would require three tracking ships in the network.

The accuracy requirements for lunar missions are shown in table XVI. The required injection accuracy is based on the midcourse  $\Delta V$  required by the spacecraft to correct for injection errors. A mid-course correction capability of about 30 ft/sec is allowed for this effect, based on statistical expected (or  $1\sigma$ ) values. In addition, a payload loss of no more than 20 pounds due to non-optimum steering is specified.

To satisfy these accuracy requirements, injection velocity should be within 10 ft/sec, and flight path angle within  $0.06^\circ$ . To satisfy mission constraints and payload requirements, altitude should typically be within one mile and thrust direction within  $2^\circ$  of optimum, on the average. Current systems (i.e., the Centaur inertial guidance system) are expected to meet these requirements.

Synchronous orbit mission. - Figure 35 presents an Earth trace of a synchronous orbit boost trajectory. The trajectory shown is based on a due east launch from ETR, and results in a stationary orbit approximately over Singapore. If other stations are desired, the spacecraft is used to move to the desired location.

The initial boost arc of about  $23^\circ$  uses Atlas and Centaur to place the vehicle in a 90 nautical miles parking orbit. The vehicle then coasts to the first crossing of the equator, at which time about 8000 ft/sec is added by the kick stage (over an arc of about  $10^\circ$ ) to attain a transfer orbit which rises from 90 to 19,300 nautical miles

altitude. The path relative to the rotating earth bends as shown, and next crosses the equator about  $180^\circ$  east of the launch site, approximately over Singapore. Final injection requires about 6000 ft/sec added by the kick stage, wherein a plane change is also made, to place the spacecraft in the synchronous equatorial orbit.

Radio coverage is possible for this mission. A station at the launch site and one downrange ship could guide the boost into parking orbit. Another ship near the west coast of Central Africa could guide injection into the transfer orbit. At final injection, Singapore or Canberra (DSIF) could be used.

The accuracy requirements for this mission are presented in table XVII. The accuracy criteria for this mission is the post-injection  $\Delta V$  required for the spacecraft to get on station. The requirements on the final orbit are for the period to be 24 hours and the inclination and eccentricity to be zero. Errors in the period must be corrected, and 100 ft/sec is allowed for this effect. If the inclination is not zero, the major effect would be a daily cyclic change in latitude; if the eccentricity is not zero, there would be a daily cyclic change in longitude. An additional 100 ft/sec is allowed to correct for these two effects. This may or may not be used, depending on the specifications for the final orbit. Also, the total of these corrections may not equal the sum (200 ft/sec) since combined corrections can be made.

The requirements of the spacecraft to stay on station over a long period of time are about 200 ft/sec per year. Thus, the correction  $\Delta V$  allowance here corresponds to using about one year's supply of spacecraft propellant to correct for guidance errors.

In assessing the accuracy required for meeting the above criteria, it is convenient to consider the accuracy required at injection into transfer orbit. This is about 10 ft/sec in velocity and one mile in altitude. At this point, the trajectory history is very similar to a lunar boost trajectory (less about 2000 ft/sec in velocity). The errors that can be tolerated here are about equivalent to those for a lunar trajectory (perhaps a bit more stringent). Thus, a guidance system well suited for the lunar mission will also be suitable for the synchronous equatorial satellite (up to this point).

The coast up to apogee (about 5.2 hours) would help a radio guidance system by allowing long tracking times, but would hurt an inertial system because of the difficulty in maintaining an accurate inertial attitude reference over a long period of time. However, final attitude reference can be off as much as one degree, and still meet the accuracy requirements.

The final velocity (after final injection) should be within 10 ft/sec and the position within 200 miles. These accuracy requirements can be met by current inertial guidance systems and by radio guidance systems

if radio coverage is available and a suitable onboard attitude reference can be provided at final injection.

With all these considerations in mind, the capabilities of various systems can now be examined.

Guidance systems. - Three general types of guidance systems will be considered and evaluated with respect to weight, accuracy and coverage requirements. A comparison of these systems is presented in table XVIII. All radio systems are unacceptable for solar probe and lunar missions because of the large coverage area required. Radio coverage is possible for the synchronous equatorial satellite mission, if a relatively few ground and ship stations are strategically placed. Accuracy is good, but for the synchronous orbit case, the onboard attitude reference required after six hours of flight requires either better gyros than are usual in radio systems or other means such as Earth sensors and/or star trackers. Weight of radio systems is lowest of the three system types considered; guidance systems weighing less than 50 pounds are already in operation.

A second candidate is the radio-inertial system. This system uses radio guidance from the launch site until either a convenient staging point or line-of-sight limit is reached. After that, a simple pre-programmed (open-loop) inertial control is used, possibly aided by a horizon tracker. Coverage for this system is good by definition, but accuracy is questionable and uncertain because it depends not only on small instrument errors but also on small vehicle performance dispersions. For the synchronous orbit mission, accuracy would be very doubtful. The weight of such systems is lower than all-inertia systems.

All-inertial systems have, of course, complete coverage. Even current systems can probably meet the accuracy requirements. The following systems can be considered: (1) the present Centaur inertial guidance system, (2) one of several current ICBM systems, and (3) various proposed new systems. Guidance systems weighing less than 100 pounds have been proposed for development in the next 4 to 5 years.

In the interest of providing one guidance package to be integrated into the kick stage, capable of guiding Atlas, Centaur and itself and to be used for the three classes of missions discussed herein, the choice would be an all-inertial guidance system. Even present inertial systems satisfy all the requirements and can provide the kick stage with adequate guidance over the broad range of missions.

In choosing the particular inertial system to be used, a conservative approach is taken in order to positively demonstrate the feasibility of such a system. The choice is the Minneapolis-Honeywell (M-H) Centaur guidance system. With this system, the following conclusions can be reached:

(1) Performance (payload) is adequate for all missions of interest (all performance data have been presented using weights representing this system).

(2) Accuracy requirements are satisfied for all missions.

(3) Interface requirements are minimized since the M-H system is already compatible with Atlas and Centaur.

(4) Vibration levels on Atlas-based vehicles do not present a problem since the M-H system has been designed for these levels. In addition, recent analyses indicate that Saturn vibration levels are less severe than Atlas specifications so that the M-H system can be flown on Saturn-based vehicles.

Other guidance systems should not be ruled out, however, if more complete analyses demonstrate that significant weight and/or accuracy improvements are possible. In particular, systems have been proposed which offer weight savings on the order of 150 pounds and order of magnitude accuracy improvements.

The solar probe mission represents a somewhat special case because of its low payload weight and lack of sensitivity to guidance accuracy. It is possible that significant payload gains can be realized for this mission by using a radio-inertial, rather than an all inertial guidance system. The overall guidance and related equipment weight of a radio-inertial system would be about 200 pounds lighter than the Centaur inertial system. Further study is indicated in this area to determine the effects of : (1) instrument errors, (2) vehicle performance dispersions, and (3) losses due to non-optimum steering. If these losses do not offset the weight savings achieved, the radio-inertial system could look very attractive for use with the solar probe mission.

Weight Budget. - With the selection of the Minneapolis-Honeywell Centaur guidance system for use in the kick stage, a weight budget can now be established for the kick stage guidance system and other related systems. These weights are not obtained from a detailed design study, but rather from a review of comparable system weights for the Centaur stage (ref. 4), modified to reflect a kick stage application and some anticipated future improvements.

	<u>Solar probe</u>	<u>Lunar</u>	<u>Synchronous orbit</u>
Guidance system	208	208	208
Autopilot	36	36	36
Electrical	165	165	225
Telemetry, tracking and range safety	<u>74</u>	<u>94</u>	<u>74</u>
Total	483	503	553

The guidance system weight shown represents a slight decrease from the present Centaur guidance system, resulting from an assumed computer input-output unit redesign. The decrease in autopilot weight results from both a simpler application and future improvements. Since the kick stage has only one engine, programmer, electronics, and harness requirements are all reduced. In addition, some reduction in kick stage-spacecraft interface requirements is anticipated, and an improved auxiliary electrical box associated with the autopilot gyros is planned. Electrical weights are reduced because of improved, lighter batteries and less electrical cable required for the kick stage. The higher synchronous satellite electrical weight is due to the increased battery requirements for the longer mission time. The kick stage telemetry weights are considerably lower than corresponding Centaur weights because of reduced measurement and telemetry requirements. The additional 20 pounds for the lunar mission represents a spacecraft destruct package, necessary because of the spacecraft propulsive capability in this mission.

Any future modification to the weights shown simply subtracts or adds to payload weight.

#### Attitude Control

The kick stage attitude control system functions to provide initial vehicle acquisition, position stabilization, reorientation, roll control during engine thrusting and may be used to provide propellant settling. In this type of study, only gross estimates of the attitude control total impulse requirements can be made.

A total impulse requirement of 3000 pounds per second was assumed for the planetary orbiter missions and a requirement of 1000 pounds per second was assumed for all other missions.

A cold gas (nitrogen) system was selected for both long and short mission applications. The resulting system weights were 50 pounds for

short missions and 130 pounds for planetary orbiter missions. A weight savings of about 50 pounds could be obtained if a monopropellant (hydrazine) were used for the planetary orbiter missions; however, it was felt that the simplicity and reliability of the cold gas system were worth this penalty.

The nitrogen propellant for the attitude control system is stored in two spherical containers at 520°R and 3000 psia. The tank material is Ti-6Al-4V in the heat treated condition with a design working stress of 80,000 psi.

## Launch Vehicle Structural Modifications

### Atlas-Centaur

Significantly greater loads will be imposed upon the booster structure of the Atlas-Centaur kick stage vehicle than are experienced by the present Surveyor launch vehicle. The increased overall length will cause greater bending moments during the maximum dynamic pressure regime (max  $q\alpha$ ) of flight, and the increased weight on top of Centaur will induce greater inertial force on the booster structure. The new launch vehicle, figure 14, is about 18 feet longer than the present Surveyor booster. The kick stage represents about 15 feet of this increased length with the remainder being allotted for greater payload volume capability. The additional weight on top of Centaur is about 11,000 pounds. Consequently, the booster structure needs to be strengthened, and the effects of added structural weight must be considered in the performance analysis.

When it is decided to strengthen the Atlas and Centaur stages in order to fly the kick stage, consideration may be given to improving the flight wind capability above the current capability. For the purpose of this study, however, the structural analysis is based upon maintaining current wind capability.

In order to estimate the required structural beefup weight, it was first necessary to calculate the distribution of loads along the length of the vehicle for both max  $q\alpha$  and BECO (booster engine cut-off) flight conditions. A rigid body computer program was used to calculate bending moment, shear force, and axial load distribution at max  $q\alpha$ . This program was used to search out the maximum angle of attack,  $\alpha_{max}$ , which is permitted by the strength capability of the present Surveyor launch vehicle. Loads were calculated for specific values of  $\alpha$ , and these were then compared to the allowable structural strength in order to find  $\alpha_{max}$ . In lieu of a detailed wind analysis, it was assumed that this value of  $\alpha_{max}$  should be imposed upon the longer kick stage launch vehicle in order to derive the loads to be used for structural beefup analysis. With this assumption, the new booster structure will have about the same flight wind capability as the present one.

Figure 36 compares the calculated bending moment distribution with the allowable. In this case, the allowable moment distribution reflects the presence of axial compressive forces due to inertial and axial loads. An ultimate factor of safety of 1.25 was applied to the calculated loads. The allowable load carrying capability of the Centaur LH<sub>2</sub> tank structure was based upon minimum ullage pressure of 19.8 psi absolute. The minimum ullage pressures for Atlas were 28.5 psi gage in the LO<sub>2</sub> tank and 57 psi gage in the RP-1 tank. The figure shows that the bending moment exceeds the allowable moment in the Centaur LH<sub>2</sub> tank barrel section ( station location 219-413), the Centaur to Atlas interstage (station location 413-570), and the Atlas LO<sub>2</sub> tank barrel section (station 570-960). Comparison of the current structural capability for the max  $q_x$  condition with that at BECO indicated that the latter condition produces slightly greater structural deficiency in the Atlas LO<sub>2</sub> tank and the interstage.

Strengthening of Centaur and Atlas pressure stabilized tank structure is accomplished most efficiently by raising the allowable pressures and increasing tank skin gages accordingly. Allowable hoop stresses were assumed to be equal to current design values. The nature of the propellant tank design in both of these stages is such that an increased pressure requirement in the upper tank must necessarily be imposed upon the lower tank in order to prevent buckling collapse of the intermediate bulkhead which separates propellants. Strength analysis revealed that the ullage pressure should be increased 6.9 psi in the Centaur tanks and 7.1 psi in the Atlas tanks. As a result, the average increase of skin thickness is about 0.004 inch in Centaur and 0.003 inch in Atlas. Most of the total increased structural weight is due to tank skin thickness requirements, but allowance has been made also for strengthening the rings according to the weight charts of reference 7. As a result of these calculations, the estimated structural beefup weight is 155 pounds for Centaur and 260 pounds for Atlas.

Strengthening of the seminomocoque interstage structure is accomplished by increasing the sizes of stringers and frames. Once again, the structural weight charts of reference 7 were used to obtain the increase in structural weight estimate of 75 pounds.

#### Saturn IB-Centaur

Figure 15 illustrates the Saturn IB-Centaur-kick stage configuration considered in this study. Centaur and the kick stage are enclosed within a 260 inch diameter clam shell shroud, which was chosen to permit the use of large diameter payloads. Since the shroud will carry the airloads, Centaur structure needs to resist only the inertial loads imposed by the kick stage and payload. No major structural beefup of Centaur is required for this purpose. Provision will need to be made for supporting the kick stage from the station 219 ring of Centaur. The shroud structure can also be used to place Centaur in stretch during launch preparations thereby making it possible to preserve structural

integrity in the event depressurization of Centaur tankage is necessary.

A qualitative evaluation was made of the impact upon Saturn IB structure caused by the increased weight and length associated with the added upper stages. The increased weight, length and diameter associated with the shrouded upper stages of this study will induce greater loads into the Saturn IB structure than those developed with the Apollo payload. However, the design loads for the new configuration will not increase in proportion to the applied loads since the ultimate factor of safety can be reduced from the 1.4 used for manned vehicles to 1.25 for unmaned use. Figure 37 compares flight design loads at max  $q\alpha$  for the two booster systems. The total load acting at each station is represented by the ultimate equivalent bending moment, which represents the sum of the true bending moment plus the bending moment calculated to be equivalent to the axial compression load. Data published in an internal MSFC document and an ultimate factor of safety of 1.4 were used to calculate the Apollo launch vehicle moment distribution. The moment distribution for the Centaur launch vehicle was based upon rigid body calculations for the same angle of attack and Mach number as those for the Apollo launch vehicle, and upon other parameters obtained from a Lewis point mass trajectory simulation of the new booster combination. In this case, an ultimate factor of safety of 1.25 was used.

Figure 37 shows that the bending moment for the Centaur launch vehicle exceeds that for the Apollo launch vehicle primarily in the region of the second stage (stations 1663 to 962). The relative amount of the load increase is greatest at the forward end of the second stage and decreases in the aft direction. Consideration of the ultimate design loads as specified by an internal MSFC document indicates that it will be necessary to beef-up the structure of the S-IVE stage and the interstage in order to maintain the existing flight wind capability (95 percent probability of launch in winter months). An alternative solution is to forego making structural changes in the booster and to accept a lesser flight wind capability.

#### Substitution of Fluorine for Oxygen in the Hydrogen-Oxygen Kick Stage--Configuration I

As mentioned earlier in the report, an alternate method of developing an H-F kick stage is to develop the RL-10 H-O kick stage to be compatible with fluorine, and substitute fluorine for oxygen in the stage when the RL-10 engine has proven to be operational with hydrogen-fluorine propellants. This oxidant substitution would require minor strengthening of the cruciform beam and oxidant tank supports of the kick stage, configuration I, figure 24. Total jettison weight for this H-F stage would be about 55 pounds more than the H-O stage because of increased structural, propellant residuals, and contingency weights. The greater density of liquid fluorine compared to liquid oxygen results (for the same tank volume) in an impulse propellant load of about 9000 pounds instead of 7000 pounds, and a mixture ratio (O/F) of 6.72 instead of 5. The specific impulse value for an O/F of 6.72

was estimated to be 457 seconds. A complete weight summary is shown in table XIX and it is noted that the propellant mass fraction of the stage is 0.829.

A performance evaluation of this kick stage was made using both the Atlas-Centaur and Saturn IB-Centaur launch vehicles for solar missions. A comparison of the Atlas - Centaur launch vehicle payload capability for a 0.33 AU. solar probe is illustrated in the bar chart of figure 38 for the H-0 kick stage, the H-0 kick stage using fluorine as the oxidant, and a 9000 pound propellant load H-F kick stage designed specifically for H-F. The RL-10 engine was used on all stages. Using H-F in the H-0 stage increased the payload about 290 pounds. The stage designed specifically for H-F increased the payload only an additional 70 pounds. A similar comparison of these three kick stages is illustrated in figure 39 for the Saturn IB-Centaur launch vehicle and a 0.16 AU solar probe mission. Again, fluorine substitution in the H-0 stage yielded the major portion of the performance improvement afforded by fluorine for a stage using the RL-10. Fluorine substitution in the H-0 stage increased the payload 250 pounds compared to the maximum gain of 305 pounds.

#### MISSION PERFORMANCE

Mission performance data has been presented throughout the report thus far to provide a criterion for evaluation and selection of kick stage parameters. In this section, mission performance will be presented to directly illustrate the advantages of adding a kick stage to the present family of NASA launch vehicles. Also included will be the potential performance improvements afforded by the kick stage when added to the Air Force Titan III vehicles. A representative, but far from inclusive, range of missions is discussed. The mission results presented are based on the hydrogen-oxygen kick stage using the RL-10A-3-3 engine and a 7000 pound propellant capacity. The design details and system performance of this stage (illustrated in fig. 24 and summarized in tables VI and X) have been developed in the previous sections of this report. It should be recognized that each specific mission will give rise to various specialized system requirements (for example, number of engine firing periods, propellant boiloff, etc.). These have been assessed in obtaining mission performance but will not be discussed in detail.

A relatively convenient method of illustrating overall mission performance is through the use of curves of payload versus mission energy. The payload performance of various combinations of NASA launch vehicles is presented in figure 40 as a function of VIS-VIVA energy,  $C_3$ . The vis-viva energy term is equal to the square of hyperbolic excess velocity. Addition of the kick stage, as can be seen, provides a marked increase in payload as the energy increases for the Atlas-Centaur and Saturn IB-Centaur launch vehicles. Another application of the kick stage is as the only upper stage on the Atlas booster. For comparison, the Atlas-Agena D payload performance taken from reference 8 is also included on figure 40. The Atlas-kick stage

vehicle provides mission capability which is nominally between that of the Atlas-Agena and of the Atlas-Centaur. The kick-stage in general can improve the NASA launch vehicle capability at nearly all energy levels.

Since the Air Force launch vehicle family will be largely based on the Titan III vehicle, it is of value to determine the potential benefits of the kick stage on the Titan launch vehicles. Payload as a function of vis-viva energy is presented in figure 41 for the Titan III launch vehicles with and without the kick stage. For completeness, the Centaur stage has also been integrated on the Titan vehicles. As was the case with the NASA launch vehicles, marked performance increases occur for the kick stage to the Titan III C booster (minus the transtage) provides mission capability in the Saturn IB class. Use of the kick stage instead of the transtage on the Titan III A booster also provides a significant improvement in vehicle capability. Although not shown, the 7000 pound propellant capacity of the kick stage is nearly optimum on the Titan III launch vehicles as is the case on the NASA launch vehicles.

A more specific comparison of the added performance benefits attainable by using the 7000 pound propellant loaded H-O kick stage can be made if specific missions are selected. It is then possible to consider mission constraints and thereby provide a more valid comparison between like boosters with and without kick stages.

#### Lunar Mission

The first mission to be discussed will be the lunar mission. Currently, two mission types are planned: (1) The lunar orbiter currently to use the Atlas-Agena launch vehicle and (2) The surveyor soft lander scheduled on the Atlas-Centaur launch vehicle. Both flight profiles require injection energies slightly less than escape energy ( $C_3 - 0.85 \text{ km}^2/\text{sec}^2$ ) and will use a launch azimuth sector from  $90^\circ$  to  $114^\circ$  out of the Eastern Test Range.

The payload for the lunar mission, based on a launch azimuth of  $114^\circ$ , is shown in the bar chart of figure 42 for the Atlas-Agena D (ref. 8), the Atlas-kick, the Atlas-Centaur, and the Atlas-Centaur-kick launch vehicles. A parking orbit mode was assumed in all cases.

The Atlas-Agena D payload capability is approximately 1040 pounds. The Atlas-kick can provide an additional 600 pounds for this mission. Adding the kick stage to the Atlas-Centaur vehicle will increase its capability about 800 pounds for the Surveyor mission. Using the 7000 pound kick stage propellant load, a suborbital ignition of the kick stage is required.

#### Synchronous Equatorial Mission

Another mission of current interest is the 24-hour orbit mission. At present, only small satellites have been placed into synchronous orbits

since the energy level (compared to present missions) and complications of the mission are high. Payloads in excess of 1000 pounds are not presently attainable without resorting to Saturn-Centaur class boosters. The use of a kick stage greatly enhances the payload capability of the Atlas and Titan class boosters. To illustrate the increased capability, a bar chart is shown in figure 43 for this mission for the Atlas-Centaur and Atlas-Centaur-kick stage. In the case of the Atlas-Centaur, it is necessary to provide a three-burn capability in the Centaur stage with approximately a 6 hour coast between the second and third burns. The Atlas-kick launch vehicle is also shown on the chart. The same mission profile requirements for the Centaur stage are also imposed on the kick stage, however, the improved  $H_2$  boiloff situation for the kick stage relative to Centaur (Centaur boils off approximately 100 pounds versus no boiloff for the kick stage) helps offset the lower propellant load of the kick stage resulting in almost comparable payloads for both vehicles. Adding the kick stage to the Atlas-Centaur greatly increases the payload as can be seen on the figure.

Although not displayed on the chart, the Saturn IB-Centaur vehicle could also be used to deliver payloads to synchronous orbit. Again, using a three-burn Centaur, payloads of about 8700 pounds are possible. Addition of a kick stage does not result in dramatic payload increases as with the Atlas-Centaur with only a 12 percent increase possible compared to 150 percent for the Atlas-Centaur. This is, of course, principally a result the Saturn IB-Centaur being a three stage vehicle with the upper two stages using high performance propellants (hydrogen-oxygen) as compared to the Atlas-Centaur with its 2  $\frac{1}{2}$  stages and only one stage using hydrogen-oxygen propellants. However, use of the kick stage allows use of a two-burn Centaur which is jettisoned prior to the long coast to apogee.

#### Solar Probe Mission

As the energy of the mission increases and the energy requirement per stage of a given launch vehicle becomes greater, the benefits afforded by additional staging are more pronounced. The solar probe mission is one in which the maximum energy capability of the launch vehicle is of utmost importance. Since the energy requirement is high and the payload weight will, in general, be low, the burnout weight of the final stage will also have a strong influence on the launch vehicle capability for this mission. The combination of high energy and low burnout weights point toward the use of small high energy propellant upper stages for missions of this type.

The launch window and orbit coast time requirements for the Saturn IB-Centaur using the 7000 pound H-O kick stage is shown in figure 44 as a function of time of the year for a typical solar probe mission. The launch azimuth was restricted between  $90^\circ$  and  $114^\circ$ . Allowing a maximum coast time of about 40 minutes provides for a maximum launch opportunity every day of the year. Similar curves would result for

other launch vehicles. The payload capability of both the Atlas-Centaur and Saturn IB-Centaur launch vehicles is shown in figure 45 as a function of the distance at closest approach to the sun in astronomical units, AU. As is clearly shown, the addition of the kick stage greatly increases the payload capability of both launch vehicles. In calculating the payload, it was assumed that no propellant reserves were needed to account for dispersions in launch vehicle performance. Below nominal performance results in an increased perihelion distance, and above nominal performance results in a decreased distance. If performance reserves were provided, perihelion distance would be equal to that of the below nominal performance where no propellant reserve is provided.

An improvement in payload may result if the solar probe trajectory is allowed to pass close to Venus. With a proper encounter, the gravitational attraction of Venus can be used to deflect the trajectory to a lower perihelion distance. However, the solar probe mission, generally considered a relatively simple mission, then takes on all the complications associated with planetary missions. Midcourse corrections are required along with some form of onboard guidance system. Also, the number of launch opportunities would be restricted to those comparable to a Venus planetary mission, approximately every 19 months. To show the potential payload gain that is afforded by flying close to Venus, payload is presented in figure 46 as a function of perihelion distance for a standard solar probe and two probes passing close to Venus. For the Atlas-Centaur-kick launch vehicle, passing Venus at distances of 1.5 and 1.1 planet radii results in perihelion distances of 0.259 and 0.237 respectively at a payload of 500 pounds compared to a distance of 0.320 for the standard mission. Similarly, the Saturn IB-Centaur-kick vehicle perihelion distances decrease from 0.158 to 0.129 and 0.118 for the 1.5 and 1.1 planet radii swingby's respectively. It appears that large potential benefits can be derived from a close Venus swing-by, but it will be necessary to investigate the mission constraints more thoroughly to determine the exact gain possible.

#### Out of the Ecliptic Plane Mission

Another potential high energy mission of current interest is flight out-of-the-ecliptic plane. The energy requirement for this mission increases as the angle out of the ecliptic increases; and, like the solar probe, no flight performance reserve need be specifically set aside. If the vehicle performs below nominal, the angle out of the ecliptic will be correspondingly reduced.

To illustrate the benefit afforded by the kick stage, payload is presented in figure 47 as a function of the angle out of the ecliptic plane (at one AU) for the Atlas-Centaur and Saturn IB-Centaur launch vehicles. It is evident here, as with the solar probe, that the kick stage extends the launch vehicle capability. For the Atlas-Centaur at 500 pounds payload, the angle is increased from  $12^{\circ}$  to  $17^{\circ}$  and for the

Saturn IB-Centaur from  $23^{\circ}$  to  $27.5^{\circ}$ .

Note that rather than increase the angle out-of-the-ecliptic by using the kick stage, the payload for both vehicles can be more than tripled for the same conditions.

### Planetary Missions

Other missions of current interest are the planetary probes, orbiters, and landers. In view of the current effort on Mars exploration via the Voyager program, it is appropriate to discuss the application of the high energy kick stage for this mission. Earlier in the report, the insulation requirements for such a mission were discussed in some detail and the same assumptions were used here. However, no mention was made of the meteoroid protection requirements. Although the exact meteoroid protection requirements are not as yet defined for a mission such as this, it is best to take a conservative approach to the problem. A meteoroid bumper was designed to shield the propellant tanks and the engine for the high energy kick stage. It was assumed that only propellant tank shielding was required for a storable propellant stage since the ablative thrust chamber engine is not very susceptible to meteoroid damage. The double bumper shield design was based on Whipple's 63B flux estimates, Summers' penetration criteria, and a bumper effectiveness of 5. These assumptions yield a 99 percent probability of no meteoroid impacts on the propellant tanks for a 220 day trip to Mars. The shield weight for the high energy and storable stages was 250 and 147 pounds respectively. In all cases, it was necessary to off-load the high energy stage to meet the propellant requirements for the retro maneuver at Mars whereas the storable stage was specifically sized for the mission. The payload capability of both stages used with the Saturn IB-Centaur launch vehicle is shown in figure 48, for the Mars mission as a function of apofocus altitude. Two mission profiles were considered, one where all the payload is placed in orbit, and one where half the payload is placed in orbit and half is allowed to land on Mars. Notice that for all the payload in the orbit case both stages perform equally despite the off-loading requirement (approximately 3600 lbs. for a 1000 n. mi. circular orbit) with the H-O kick stage. Since the propellant requirement is less when only half the payload is placed in orbit, the properly sized storable stage becomes relatively better than the high energy stage (higher off-loading requirements). A comparable set of payload curves displayed in figure 49 for a Venus mission exhibit similar trends.

As the programs for the exploration of the near planets such as Mars and Venus enter their development phase, attention begins to focus on future missions presently in the study phase. Such a mission would be a probe to the outer planets such as Saturn and Jupiter. To illustrate what could be done on a probe to Jupiter, the payload capability versus trip time is shown in figure 50 for a Jupiter fly-by mission using the Saturn IB-Centaur with and without a H-O kick stage. Using 500 pounds as a lower limit of useful payload, the Saturn IB-Centaur could do a Jupiter fly-by in approximately 480 days, but would

require trip times in excess of 4 years to do a Saturn flyby. If the H-O kick stage is used on this launch vehicle, the Jupiter trip time could be reduced by 80 days or perhaps more significant, the payload could be increased to 1900 pounds. The Saturn flyby mission is more dramatically improved with trip times of 800 days possible with the 500 pound payload.

Also indicated on the figure is the energy required for solar escape. A payload of 1500 pounds is possible at this energy level for the Saturn IB-Centaur vehicle with the kick stage, as compared to zero payload without the kick stage.

#### CONCLUDING REMARKS

Present NASA scientific space missions extend to the Moon and the near planets, Mars and Venus. Under continuing study, however, are future missions designed to explore the entire solar system ranging from close solar missions to missions to the outer planets as well as to the regions outside of the ecliptic plane. These missions, in general, will require a marked increase in launch vehicle injection energy capability. A principal concept for meeting this energy requirement in the near future is to add a small, liquid fueled, high energy upper stage to the present family of NASA launch vehicles. The selection of a final upper stage design will require a careful balance between mission performance capability and development cost, time and risk. This report has presented design and mission performance data regarding several of the foremost high energy upper stage concepts.

Not surprisingly, best mission performance of the stage designs considered herein is obtained through use of hydrogen-fluorine propellants utilizing an optimally sized new engine. On the other hand, the performance of this stage can be closely matched through use of hydrogen oxygen propellants in a stage incorporating the RL-10A-3-3 engine, a concept which more nearly represents current state-of-the-art in cryogenic propellants. Maximum performance difference between the two concepts is noted in the highest energy missions where payload is small and any performance improvements become relatively large. An example of such a case is the application of the Saturn-IB-Centaur plus high energy upper stage vehicle to a close solar probe mission. Here, the H-O stage with the RL-10A-3-3 can deliver a 545 pound payload to a 0.16 AU distance. As discussed in the report, Pratt and Whitney is under contract to NASA to determine RL-10 compatibility and performance capability utilizing fluorine. Consequently, an attractive possibility for introducing fluorine into the high energy upper stage is to design the H-O stage to be compatible with fluorine. With this approach, future substitution of fluorine into the H-O, RL-10 stage increases the payload delivered to 0.16 AU to 795 pounds. Similarly, the 545 pound payload could be delivered to 0.148 AU. In comparison, if the RL-10 stage had been designed specifically for fluorine the payload

at 0.16 AU would be increased to 850 pounds indicating a relatively small penalty for the dual H-O and H-F approach. Best performance, as mentioned, is obtained through use of fluorine in a stage based on a new, optimally sized (about 10,000 pound thrust level) engine. For this case, the payload at 0.16 AU would be increased to 1050 pounds or at 545 pounds payload the AU distance could be decreased to 0.135 AU. However, the requirement for a new engine development and the high performance level assumed for this engine (464 seconds specific impulse at an engine mixture ratio of 14 to one) makes this the most costly and highest risk approach.

To illuminate the design and system requirements for the high energy upper stage, the second section of the report presented a preliminary design discussion of the H-O upper stage based on the use of the RL-10A-3-3 and a propellant capacity of 7000 pounds. As presented in the discussion, the use of hydrogen-oxygen propellants and the RL-10 engine allows the selection of feasible approaches, generally within the present state-of-the-art, in all design areas. The only exceptions are associated with long coast missions such as a planetary retro (Voyager) type mission. Here, there still exist uncertainties regarding propellant insulation, settling and venting and meteoroid protection. However, present NASA plans regarding Voyager envision the use of a special non-cryogenic retro-propulsion module for Voyager. Consequently, there does not appear to be a long coast time requirement for the cryogenic upper stage in the near future. With this in mind, no major technological problems are anticipated in the development of the hydrogen-oxygen upper stage.

The third section of the report discussed the mission performance of the 7000 pound propellant capacity H-O upper stage. The data presented display the advantages of adding a small high energy upper stage to the present family of NASA launch vehicles. To provide a firm basis for these initial performance estimates, the stage performance and jettison weight were based on relatively conservative, current state-of-the-art approaches in the various system design areas. It is expected that ongoing analyses and experimental programs will demonstrate the feasibility of incorporating advanced concepts in some system areas during final stage design and development. Two examples are the possible future substitution of fluorine and or the use of an advanced guidance system. Consequently, it is felt that the performance presented in the third Section provides a lower limit of the ultimate stage performance and that the predicted performance will tend to increase, rather than decrease with time.

## REFERENCES

1. Valentine, H. H., Burley, R. R., and Coleman, R. S.: Analysis of High-Energy Upper Stages for Solar-Probe Missions. NASA TM X 478, March 1962.
2. Dergarabedian, P.: Launch Vehicle Technology Study, Rep. 8496-6008-RC-000, Contract NASw-784, Space Technology Laboratory, March 20, 1964.
3. Knoll, R. H., and Oglebay, J. C.: Lightweight Thermal Protection Systems for Space Vehicle Propellant Tanks. SAE Paper 746C, presented at National Aeronautics and Space Engineering and Manufacturing Meeting, Los Angeles, California, Sept. 23-27, 1963.
4. Hunt, A. E.: Centaur Monthly Configuration, Performance, and Weight Status Report. Rep. GDA63-0495-20, General Dynamics/Astronautics, January 21, 1965.
5. Stechert, D. G.: The Effect of Outage on Missile Performance, Guidance, Navigation, Traching, and Space Physics, Volume III of Ballistic Missile and Space Technology. New York, Academic Press, Inc., 1960.
6. Perkins, P., and Smith L. S.: A Compressed Super Insulation System: Test Results with Liquid Hydrogen Under Approximated Space Conditions. Paper presented at 1963 Cryogenic Engineering Conference, Boulder, Colorado, August 1963.
7. Centaur Capability Handbook, GD/A BTD64-119-1, Rev. A, Oct. 1, 1964.
8. SLV-3 Agena D Performance Workbook, General Dynamics-Astronautics, Report No. GDA/DCG64-004B, June 1, 1964.

TABLE I

Storable Kick Stage Weight Summary; 3,000 Pound  
Propellant Load, LEM Ascent Engine, Short Coast Mission

Pressurization		67
He Tank	60	
Helium	7	
Propulsion		348
Engine	210	
Fuel Tank	29	
Oxidant Tank	29	
Prop. System	80	
Structure		145
Guidance and Autopilot		244
Electrical		165
Attitude Control		50
Tracking (C-Band)		29
Telemetry		45
Residuals		35
Contingency		124
Burnout Weight		1252
Impulse Propellant		3000
Stage Total Weight		4252
Stage Mass Fraction		0.706

TABLE II

Hydrogen-Oxygen Kick Stage Weight Summary; 7,000 Pound  
Propellant Load, RL-10A-3-3 Engine, Short Coast Mission

Pressurization		40
He Tank	31	
Helium	4	
Hydrogen	5	
Propulsion		712
Engine	350	
Fuel Tank	125	
Oxidant Tank	87	
Insulation	40	
Prop. System	110	
Structure		278
Guidance and Autopilot		244
Electrical		165
Attitude Control		50
Tracking (C-Band)		29
Telemetry		45
Residuals		60
Contingency		179
Burnout Weight		1802
Impulse Propellant		7000
Stage Total Weight		8802
Stage Mass Fraction		0.795

TABLE III

Hydrogen-Fluorine Kick Stage Weight Summary; 7,000 Pound Propellant Load, Modified RL-10A-3-3 Engine, Short Coast Mission

Pressurization		31
He Tank	25	
Helium	3	
Hydrogen	3	
Propulsion		655
Engine	350	
Fuel Tank	89	
Oxidant Tank	77	
Insulation	29	
Prop. System	110	
Structure		230
Guidance and Autopolot		244
Electrical		165
Attitude Control		50
Tracking (C-Band)		29
Telemetry		45
Residuals		70
Contingency		167
Burnout Weight		1686
Impulse Propellant		7000
Stage Total Weight		8686
Stage Mass Fraction		0.806

TABLE IV - II

Hydrogen-Fluorine Kick Stage Weight Summary; 7,000 Pound  
Propellant Load, New Engine, Short Coast Mission

Pressurization		30
He Tank	25	
Helium	3	
Hydrogen	2	
Propulsion		513
Engine	250	
Fuel Tank	68	
Oxidant Tank	78	
Insulation	27	
Prop. System	90	
Structure		209
Guidance and Autopilot		244
Electrical		165
Attitude Control		50
Tracking (C-Band)		29
Telemetry		45
Residuals		70
Contingency		149
Burnout Weight		1504
Impulse Propellant		7000
Stage Total Weight		8504
Stage Mass Fraction		0.823

TABLE V

## Design Constraints for the Storable Kick Stage

Pressurization System

Fuel Tank Pressurant	Helium
Initial Supply Pressure	4000 psia
Initial Supply Temperature	520°R
Final Supply Pressure	275 psia
Final Supply Temperature	290°R
Oxidant Tank Pressurant	Helium
Supply conditions as above	
Helium Supply Tank	
No. Req. - 1	Shape - Sphere
Desing Temp. - 520°R	Design Working Pres- ure = 4000 psia
Mat'l. Ti-6Al-4V	Factor of Safety = 2 (U.T.S.)
Design Working Stress = 80,000 psi	

Propulsion System

Engine - LEM Ascent	Nom. $I_{sp}$ = 305 sec.
Thrust = 3500 lb.	$\epsilon$ = 45.6
$P_c$ = 120 psia	O/F = 1.64
Fuel Tank	
Ullage Vol. - 1 percent	
No. Req. - 2	Shape - Sphere
Design Temp. = 520°R	Design Working Pres. = 170 psia
Mat'l. - 2219-T81-Al	Factor of Safety = 1.10 (Y.S.)
Design Working Stress = 40,000 psi (Membrane Only)	
Tank Wall Min. Gage (Nom.) = .040 in.	Gage Tolerance = $\pm 0.005$ in.
Oxidant Tank	
Ullage Vol. = 1 percent	
No. Req. - 2	Shape - Sphere
Design Temp. = 520°R	Design Working Pres. = 170 psia
Mat'l - 2219-T81-Al	Factor of Safety = 1.10 (Y.S.)
Design Working Stress = 40,000 psi (Membrane Only)	
Tank Wall Min. Gage (Nom.) = .040 in.	Gage Tolerance = $\pm 0.005$ in.

Structure

Stage Diam = 10 ft.		
Desing Conditions	Dynamic Load Factor	
Boost	Axial	Lateral
Rebound	2.0	---
Max qa	2.2	0.5
Max g	6.0	---

Factor of Safety

- 1.25 Applied to Ultimate Loads
- 1.10 Applied to Yield Loads

TABLE VI

## Design Constraints for the Hydrogen-Oxygen Kick Stage

Pressurization System

Fuel Tank Pressurant	Helium	Hydrogen
Initial Supply Pressure	4000 psia	300 psia
Initial Supply Temperature	520°R	290°R
Final Supply Pressure	135 psia	300 psia
Final Supply Temperature	300°R	290°R
Minimum NPSP	4 psi	
Oxidant Tank Pressurant	Helium	
Supply Conditions as Above		
Minimum NPSP	8 psi	
Helium Supply Tank		
No. Req. - 2	Shape - Sphere	
Design Temp. - 520°R	Design Working Pressure - 4000 psia	
Mat'l. - Ti-6Al-4V	Factor of Safety - 2 (U.T.S.)	
Design Working Stress - 80,000 psi	(Membrane Only)	

Propulsion System

Engine - RL-10A-3-3	
Thrust - 15,000 Lb.	Nom. $I_{sp} = 444$ sec.
$P_c = 400$ psia	$\epsilon = 57$
	$O/F = 5$

Fuel Tank

Ullage Vol. - 5 percent	
No. Req. - 1	Shape - Oblate Spheriod ( $a/b = \sqrt{2}$ )
Design Temp. = 300°R	Design Working Pres. = 35 psia
Mat'l. - 2219-T81-Al	
Tank Wall Min. Gage (Nom.) = .040 in.	Gage Tolerance = $\pm 0.005$ in.

Oxidant Tank

Ullage Vol. - 3 percent	
No. Req. - 4	Shape - Sphere
Design Temp. = 300°R	Design Working Pres. = 35 psia
Mat'l. - 2219-T81-Al	
Tank Wall Min. Gage (Nom.) = .040 in.	Gage Tolerance = $\pm 0.005$ in.

Structure

Stage Dia. = 10 ft.		
Design Conditions	Dynamic Load Factor	
Boost	Axial	Lateral
Rebound	2.0	---
Max $q_a$	2.2	0.5
Max g	6.0	---

Factor of Safety

- 1.25 Applied to Ultimate Loads
- 1.10 Applied to Yield Loads

TABLE VII

## Design Constraints for the Hydrogen-Fluorine Kick Stage

Pressurization System

Fuel Tank Pressurant	Helium	Hydrogen
Initial Supply Pressure	4000 psia	300 psia
Initial Supply Temperature	520°R	290°R
Final Supply Pressure	135 psia	300 psia
Final Supply Temperature	300°R	290°R
Minimum NPSP		4 psi
Oxidant Tank Pressurant	Helium	
Supply Conditions as Above		
Minimum NPSP		8 psi
Helium Supply Tank		
No. Req. - 2	Shape - Sphere	
Design Temp. - 520°R	Design Working Pressure = 4000 psia	
Mat'l. - Ti-6Al-4V	Factor of Safety = 2 (U.T.S.)	
Design Working Stress = 80,000 psi (Membrane Only)		

Propulsion System

Engine - RL-10A-3-3 Modified for Fluorine Service

Thrust = 15,000 lb.	Nom. $I_{sp}$ = 458 sec.
$P_c$ = 400 psia	$\epsilon$ = 57
	$O/F$ = 9

## Fuel Tank

Ullage Vol. = 5 percent	
No. Req. - 1	Shape - Oblate Spheriod (a/b = $\sqrt{2}$ )
Design Temp. = 300°R	Design Working Pres. = 35 psia
Mat'l. - 2219-T81-Al	
Tank Wall Min. Gage (nom.) = .040 in.	Gage Tolerance = $\pm 0.005$ in.

## Oxidant Tank

Ullage Vol. = 5 percent	
No. Req. - 4	Shape - Sphere
Design Temp. = 300°R	Design Working Pressure = 35 psia
Mat'l. - 2219-T81-Al	
Tank Wall Min. Gage (Nom.) = .040 in.	Gage Tolerance = $\pm 0.005$ in.

Structure

Stage Dia. = 10 ft.

Design Conditions

	Dynamic Load Factor	
Boost	Axial	Lateral
Rebound	2.0	---
Max $q\alpha$	2.2	0.5
Max $g$	6.0	---

Factor of Safety

1.25 Applied to Ultimate Loads

1.10 Applied to Yield Loads

TABLE VIII

## Design Constraints for the Hydrogen-Fluorine Kick Stage

Pressurization System

Fuel Tank Pressurant	Helium	Hydrogen
Initial Supply Pressure	4000 psia	300 psia
Initial Supply Temperature	520°R	290°R
Final Supply Pressure	135 psia	300 psia
Final Supply Temperature	300°R	290°R
Minimum NPSP		4 psi
Oxidant Tank Pressurant	Helium	
Supply Conditions as Above		8 psi
Helium Supply Tank		
No. Req. - 2	Shape - Sphere	
Design Temp. - 520°R	Design Working Pressure = 4000 psia	
Mat'l. - Ti-6Al-4V	Factor of Safety = 2 (U.T.S.)	
Design Working Stress = 80,000 psi (Membrane Only)		

Propulsion System

Engine - New H-F Engine		
Thrust = 10,000 lbs.	Nom. $I_{sp}$ = 464 sec.	
$P_c$ = 400 psia	$\epsilon$ = 60	
	O/F = 14	
Fuel Tank		
Ullage Vol. = 5 percent		
No. Req. - 1	Shape - Oblate Spheroid ( $a/b = \sqrt{2}$ )	
Design Temp. = 300°R		
Mat'l. - 2219-T81-Al		
Tank Wall Min. Gage (Nom.) = .040 in.	Gage Tolerance = $\pm 0.005$ in.	
Oxidant Tank		
Ullage Vol. = 5 percent		
No. Req. - 4	Shape - Sphere	
Design Temp. = 300°R	Design Working Pres. = 35 psia	
Mat'l. - 2219-T81-Al		
Tank Wall Min. Gage (Nom.) = .040 in.	Gage Tolerance = $\pm 0.005$ in.	

Structure

Stage Diam = 10 ft.

Design Conditions	Dynamic Load Factor	
	Axial	Lateral
Boost		
Rebound	2.0	---
Max $q\alpha$	2.2	0.5
Max g	6.0	---

Factor of Safety

- 1.25 Applied to Ultimate Loads
- 1.10 Applied to Yield Loads

TABLE IX

## Comparison of Various Insulations

<u>Insulation</u>	Thermal Conductivity between 520 R and 37 R, k, $\times 10^5$	Density $\rho$ ,	$k\rho$ <u>Btu in. lb</u>	$\left( \frac{\sqrt{k\rho}}{\text{hr-ft}^2 \text{ } ^\circ\text{R ft}^3} \right)^{1/2}$
	<u>Btu in./hr-ft<sup>2</sup> °R</u>	<u>lb/ft<sup>3</sup></u>	<u>hr-ft<sup>2</sup> °R ft<sup>3</sup></u>	<u>hr-ft<sup>2</sup> °R ft<sup>3</sup></u>
Corkboard	30,000	20	6.0	2.45
Fiberglass	21,000	4	0.84	0.92
Foam	14,800	2	0.296	0.54
Evacuated Perlite	864	8	0.069	0.262
Evacuated Fiberglass	1,000	4	0.040	0.20
Evacuated Foil	24	4.7	0.001125	0.0338

TABLE X

Weight Summary for a 7000 Pound Hydrogen-  
Oxygen Kick Stage Configuration I

Pressurization		40
He Tank	31	
Helium	4	
Hydrogen	5	
Propulsion		712
Engine	350	
Fuel Tank	125	
Oxidant Tank	87	
Insulation	40	
Prop. System	110	
Structure		278
Guidance and Autopilot		244
Electrical		165
Attitude Control		50
Tracking (C-Band)		29
Telemetry		45
Residuals		60
Contingency		179
Burnout Weight		1802
Impulse Propellant		7000
Stage Total Weight		8802
Stage Mass Fraction		0.795

TABLE XI

Weight Summary for a 7000 Lb. Hydrogen-Oxygen Kick Stage  
Configuration II

Pressurization		40
He Tank	31	
Helium	4	
Hydrogen	5	
Propulsion		801
Engine	350	
Fuel Tank	225	
Oxidant Tank	81	
Insulation	35	
Prop. System	110	
Structure		163
Guidance and Autopilot		244
Electrical		165
Attitude Control		50
Tracking (C-Band)		29
Telemetry		45
Residuals		45
Contingency		174
Burnout Weight		1756
Impulse Propellant		7000
Stage Total Weight		8756
Stage Mass Fraction		0.799

TABLE XII

Weight Summary for a 7000 Lb. Hydrogen-Oxygen Kick Stage  
Configuration III

Pressurization		40
He Tank	31	
Helium	4	
Hydrogen	5	
Propulsion		730
Engine	350	
Fuel Tank	125	
Oxidant Tank	90	
Insulation	55	
Prop. System	110	
Structure		198
Guidance and Autopilot		244
Electrical		165
Attitude Control		50
Traching (C-Band)		29
Telemetry		45
Residuals		52
Contingency		171
Burnout Weight		1724
Impulse Propellant		7000
Stage Total Weight		8724
Stage Mass Fraction		0.803

TABLE XIII

Propellant System Parameters Used in  
Determining Propellant Outage

<u>Parameter</u>	<u>3 Sigma Variation</u>
Engine Mixture Ratio	±2.0 percent
Oxidizer Volume	±0.5 percent
Fuel Volume	±0.5 percent
Oxidizer Tank Pressure	±3.0 psi
Fuel Tank Pressure	±3.0 psi
Oxidizer Temperature	±1.0°R
Fuel Temperature	±1.0°R

TABLE XIV

Comparison of Kick Stage Shroud Concepts  
Atlas-Centaur Launch Vehicle

<u>Item</u>	<u>Configuration C - Non-Shrouded</u>				
	<u>Configuration A Short Shroud</u>	<u>Configuration B Long Shroud</u>	<u>Semi- Monocoque</u>	<u>Waffle</u>	<u>Honeycomb</u>
Shroud Wt. lb.	2000	2480	1830	1830	1830
Interstage Wt. lb.	700	415	700	700	700
Kick Stage Jettison Wt. lb.	1802	1802	1923	1975	1900
Payload Weight					
Lunar Mission	3490	3554	3382	3330	3405
Synchronous Orbit	2040	2109	1931	1879	1954
Solar Probe lb.	580	614	465	413	488

TABLE XV

## Guidance Requirements for Solar Probe Mission

Criteria:  $4 \times 10^{-4}$  AU Increase in Perihelion (Equivalent  
to 8 Lb. Payload Loss)

Accuracy Required:

At the Outgoing Asymptote:

Velocity Within	60 ft/sec
Velocity Direction Within	2 Deg.

At Final Injection:

Velocity Within	50 ft/sec
Velocity Direction Within	2 Deg.

Along Powered Flight:

Thrust Direction Within 2 Deg. of Optimum,  
on the Average.

TABLE XVI

## Guidance Requirements for Lunar Mission

Criteria: Midcourse  $\Delta V$  Required to Correct for Injection Errors - 30 ft/sec ( $1 \sigma$ ). Payload Loss Due to Guidance (Non-optimum Steering) - 20 lb. (Maximum)

Accuracy Required:

## At Injection:

Velocity Within	10 ft/sec
Velocity Direction Within	.06 Deg.
Altitude Within	1 Mile

## Along Powered Flight:

Thrust Direction Within 2 Deg. of Optimum,  
on the average.

TABLE XVII

## Guidance Requirements for Synchronous Orbit Mission

Criteria:

Post-Injection $\Delta V$ to Correct Period	- 100 ft/sec ( $1\sigma$ )
Post-Injection $\Delta V$ to Correct Cyclic Latitude and Longitude	- 100 ft/sec ( $1\sigma$ )
Payload Loss Due to Guidance (Non-Optimum Steering)	- 20 lb. (Maximum)

Accuracy Required:

## At Injection into Transfer Orbit:

Velocity Within	10 ft/sec
Altitude Within	1 mile

## At Final Injection:

Velocity Within	100 ft/sec
Attitude Reference Within	1 Deg.
Position Within	200 Miles

## Along Powered Flight:

Thrust Direction Within 2 Deg. of Optimum, on the average.

TABLE XVIII

## Comparison of Kick Stage Guidance Systems

Guidance Systems	Coverage	Accuracy	Weight
All-Radio	Unacceptable for solar probe and lunar; possible for synchronous orbit	Good Requires long term attitude for synchronous satellite	Excellent (e.g., systems weighing < 50 lb. already in operation)
Radio-Inertial (e.g., Agena)	Complete	Runs open loop beyond Cape; depends on small vehicle and instrument errors	Good
All-Inertial	Complete	Current Systems: Adequate to good. Proposed Systems: Good to excellent	Current Systems: Adequate. Proposed Systems: very good. ( e.g., < 100 lb. Guidance System Weight)

TABLE XIX

Hydrogen-Fluorine Kick Stage Weight Summary  
 9000 Pound Propellant Modified RL-10 Engine  
 Based on Substitution of  $F_2$  for  $O_2$   
 in the 7K H-0 Stage

Pressurization		40
He Tank	31	
Helium	4	
Hydrogen	5	
Propulsion		712
Engine	350	
Fuel Tank	125	
Oxidant Tank	87	
Insulation	40	
Prop. System	110	
Structure		308
Guidance and Autopilot		244
Electrical		165
Attitude Control		50
Tracking (C-Band)		29
Telemetry		45
Residuals		80
Contingency		184
Burnout Weight		1857
Impulse Propellant		9000
Stage Total Weight		10857
Stage Mass Fraction		.829

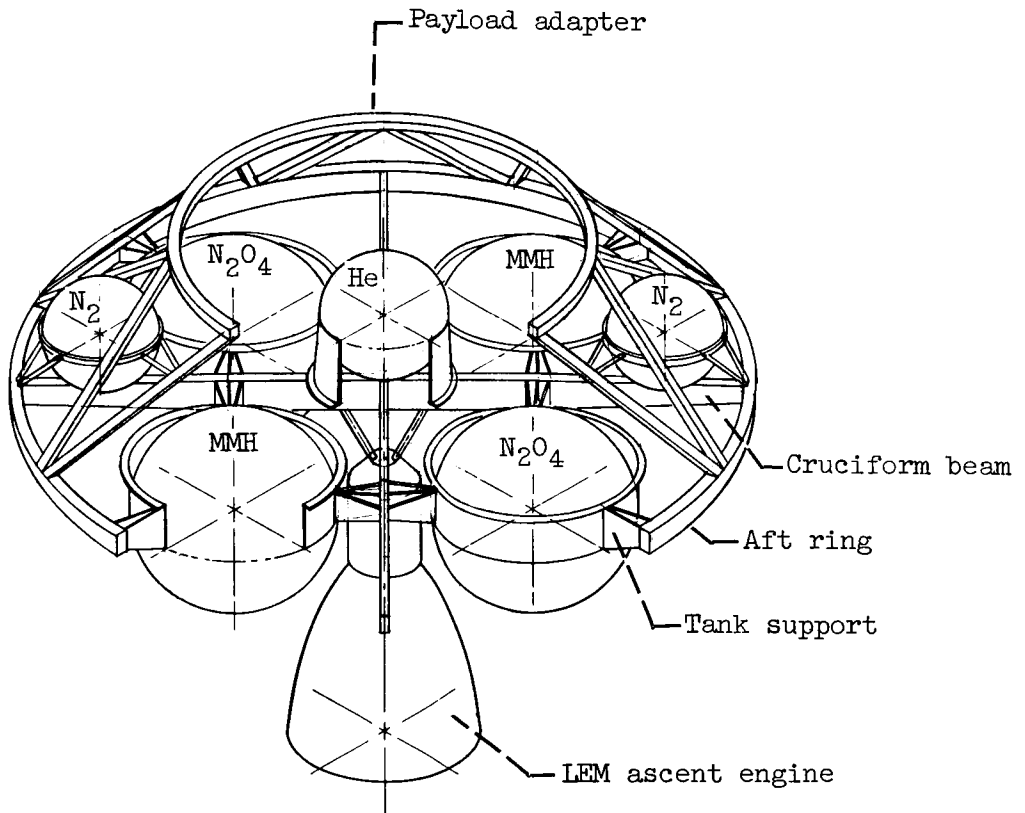


Figure 1. - Storable propellant kick stage.

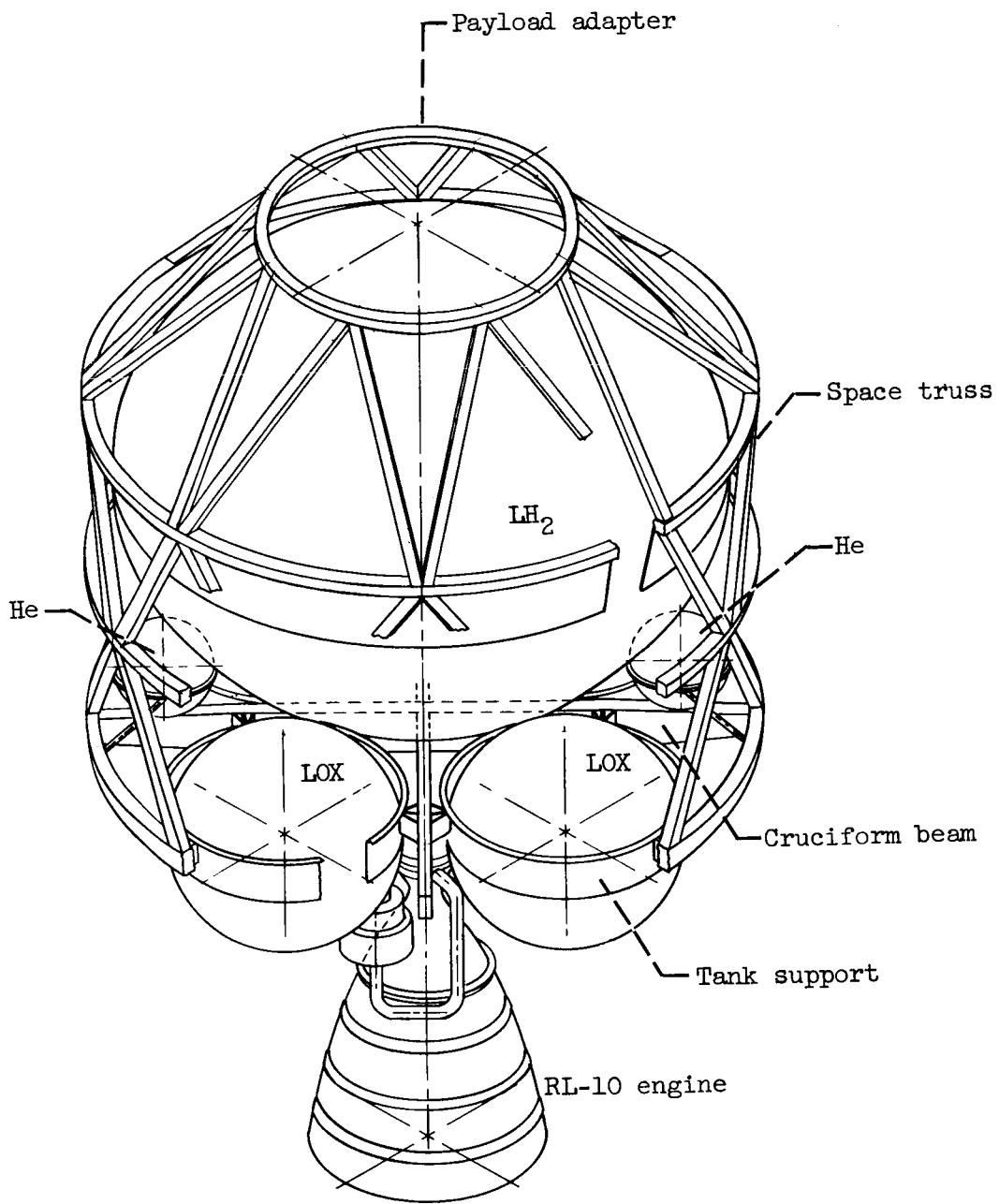


Figure 2. - Hydrogen-oxygen kick stage.

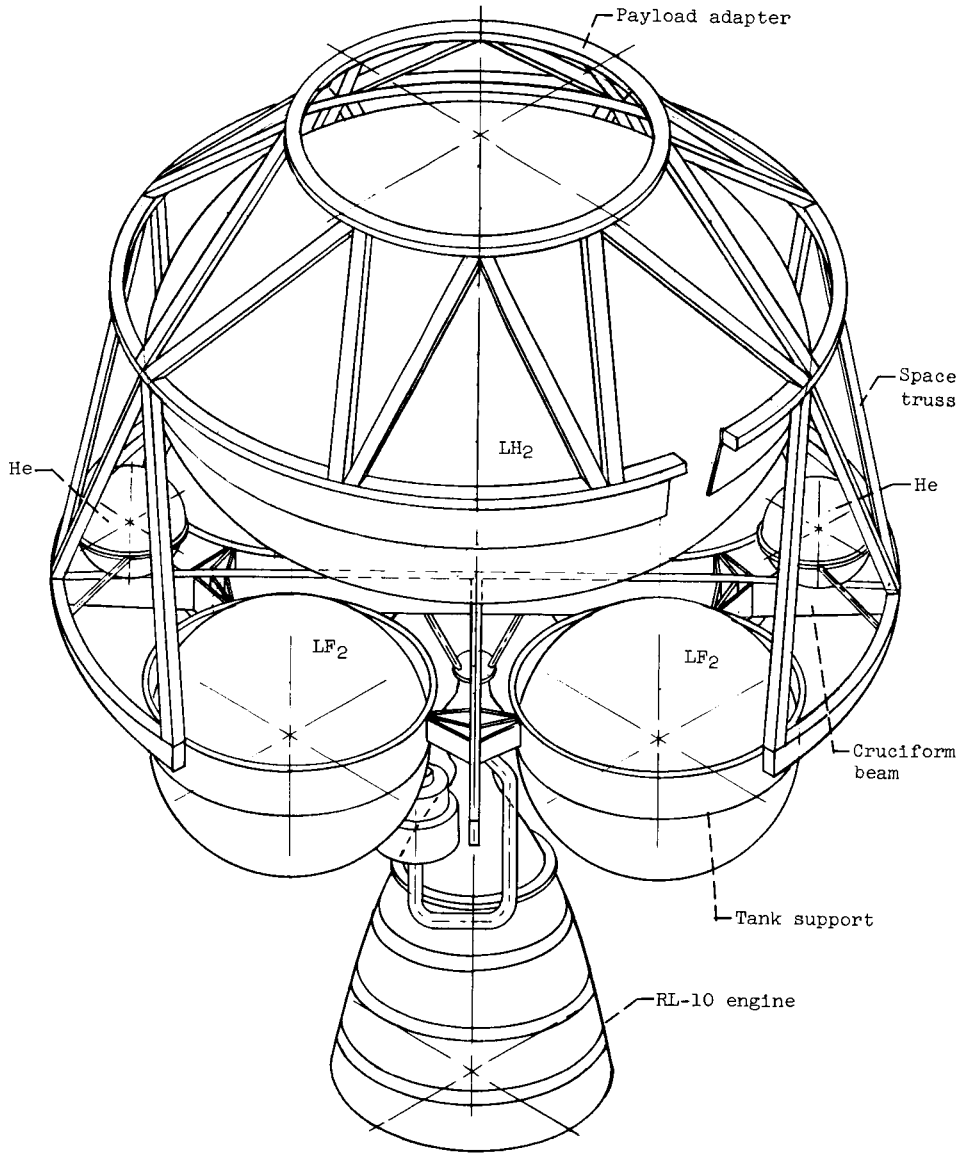


Figure 3. - Hydrogen-fluorine kick stage.

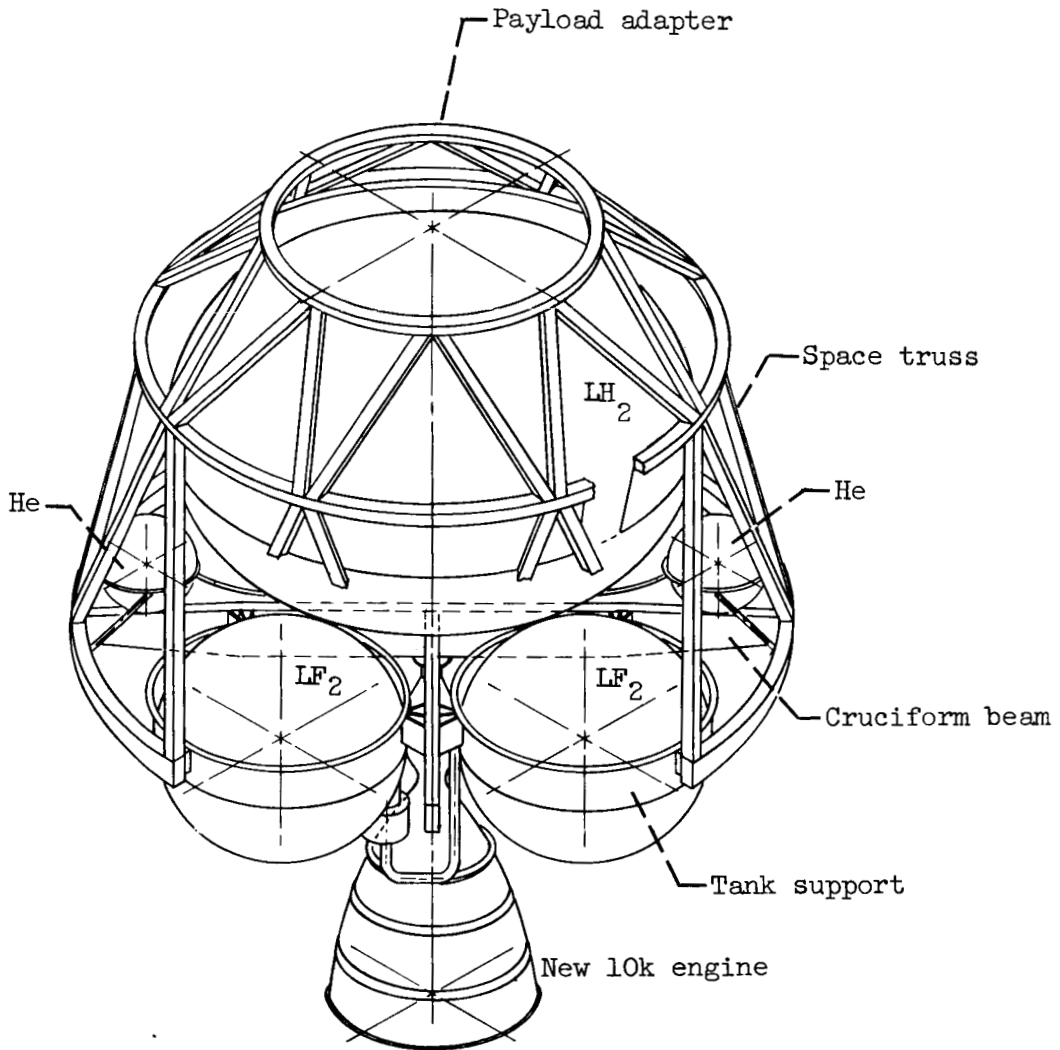


Figure 4. - Hydrogen-fluorine kick stage with new engine.

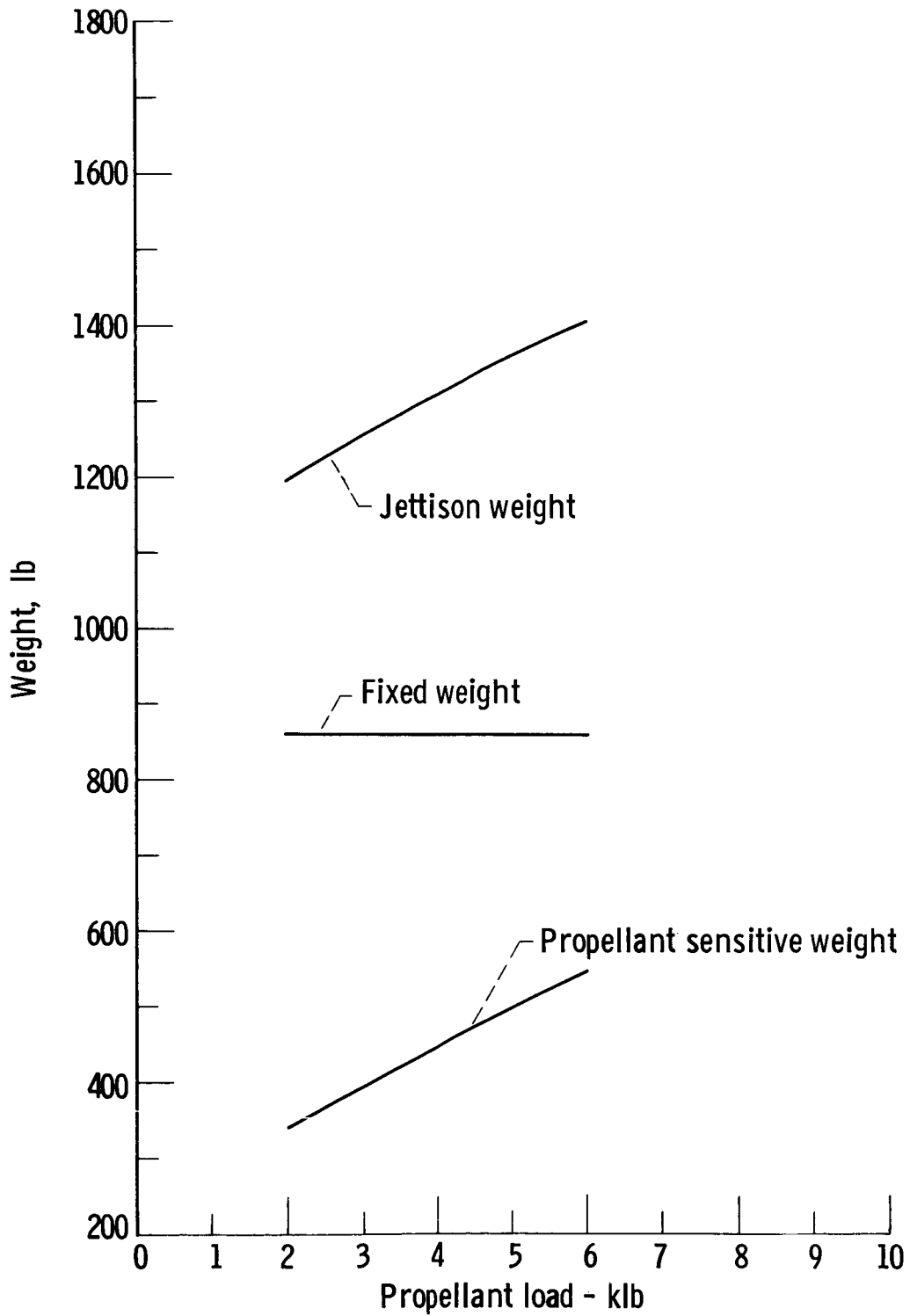


Figure 5. - Jettison weight breakdown for storable kick stage. LEM ascent engine.

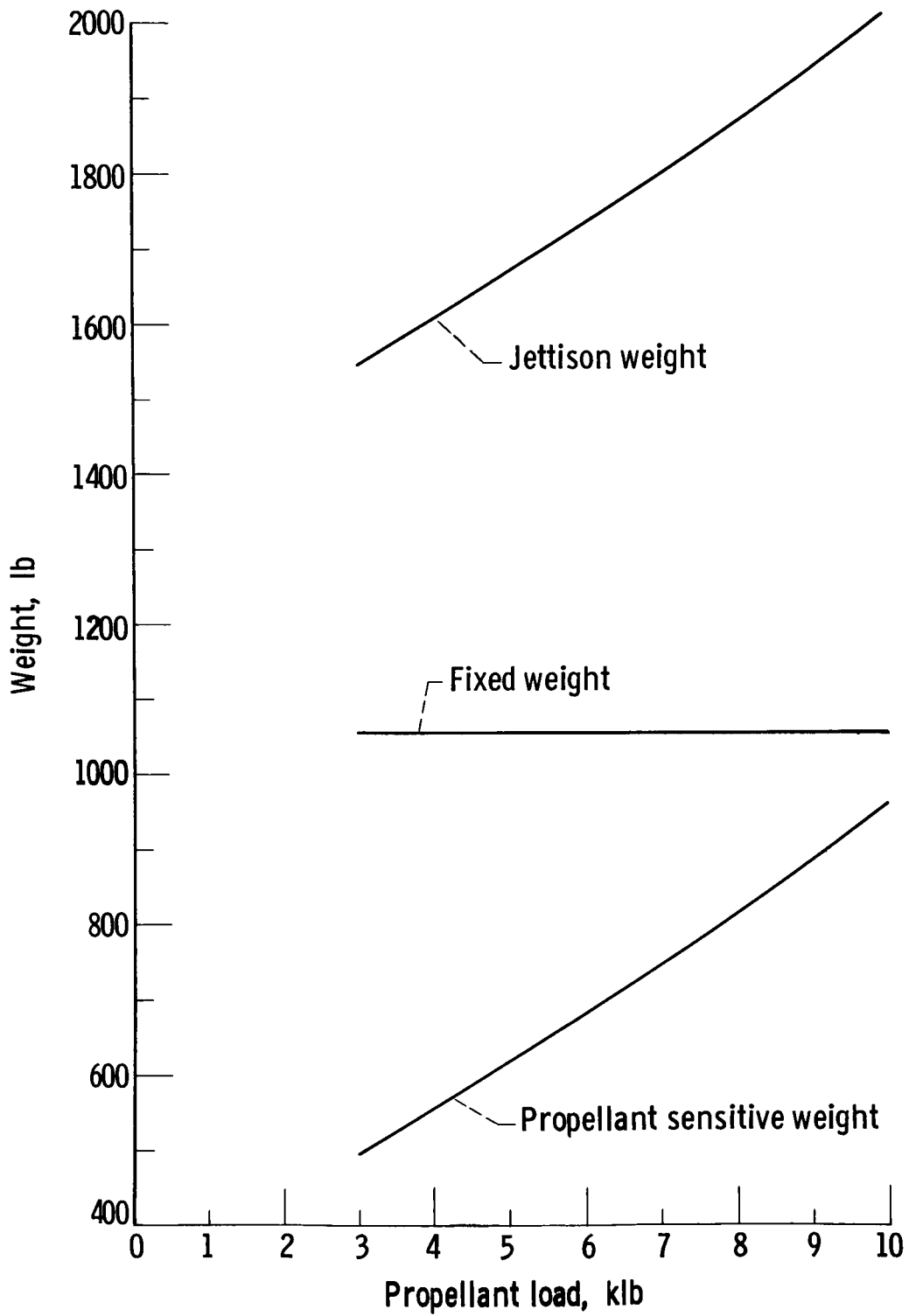


Figure 6. - Jettison weight breakdown for H-O kick stage.  
RL-10A-3-3 engine.

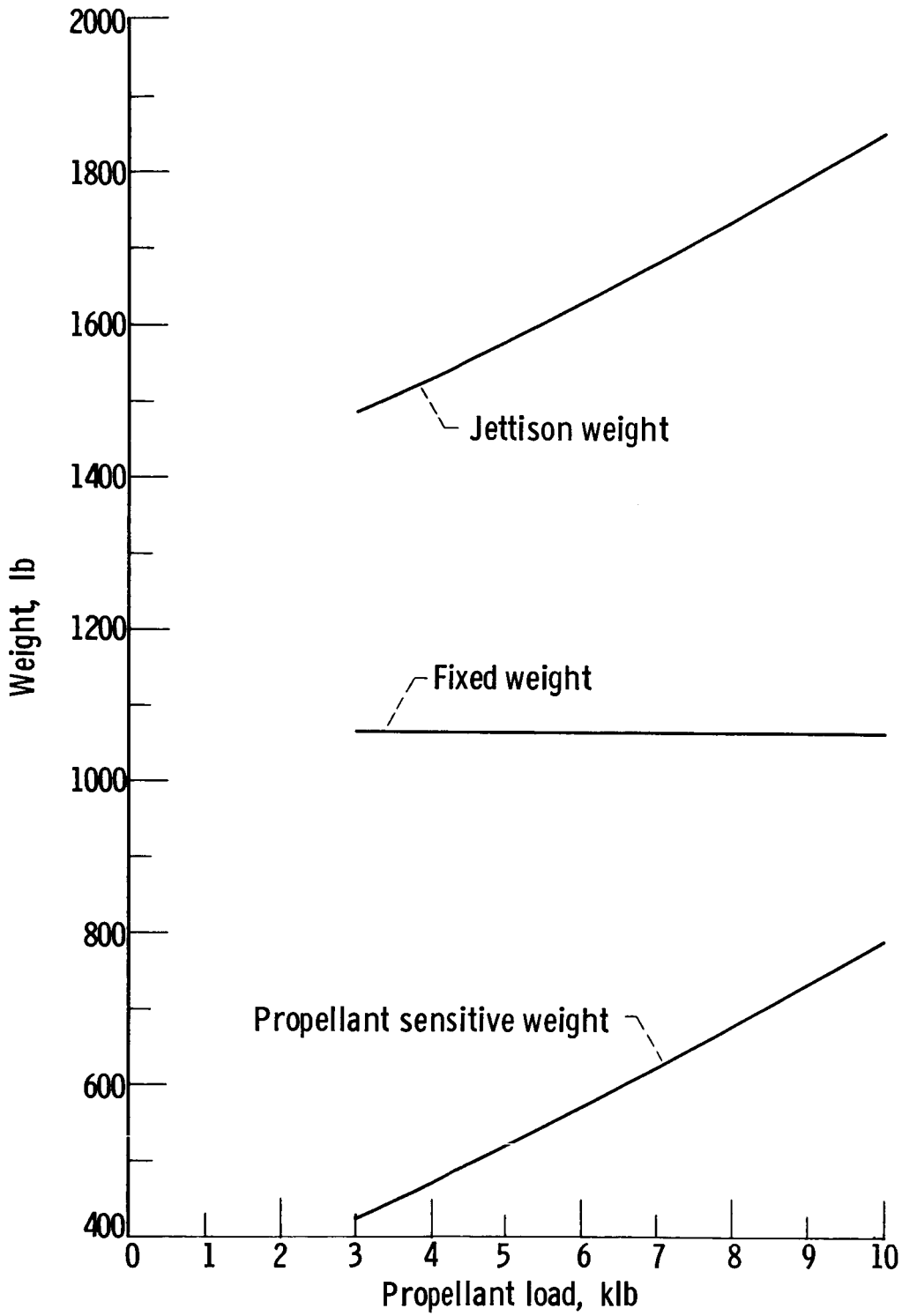


Figure 7. - Jettison weight breakdown for H-F kick stage Modified RL-10A-3-3 engine.

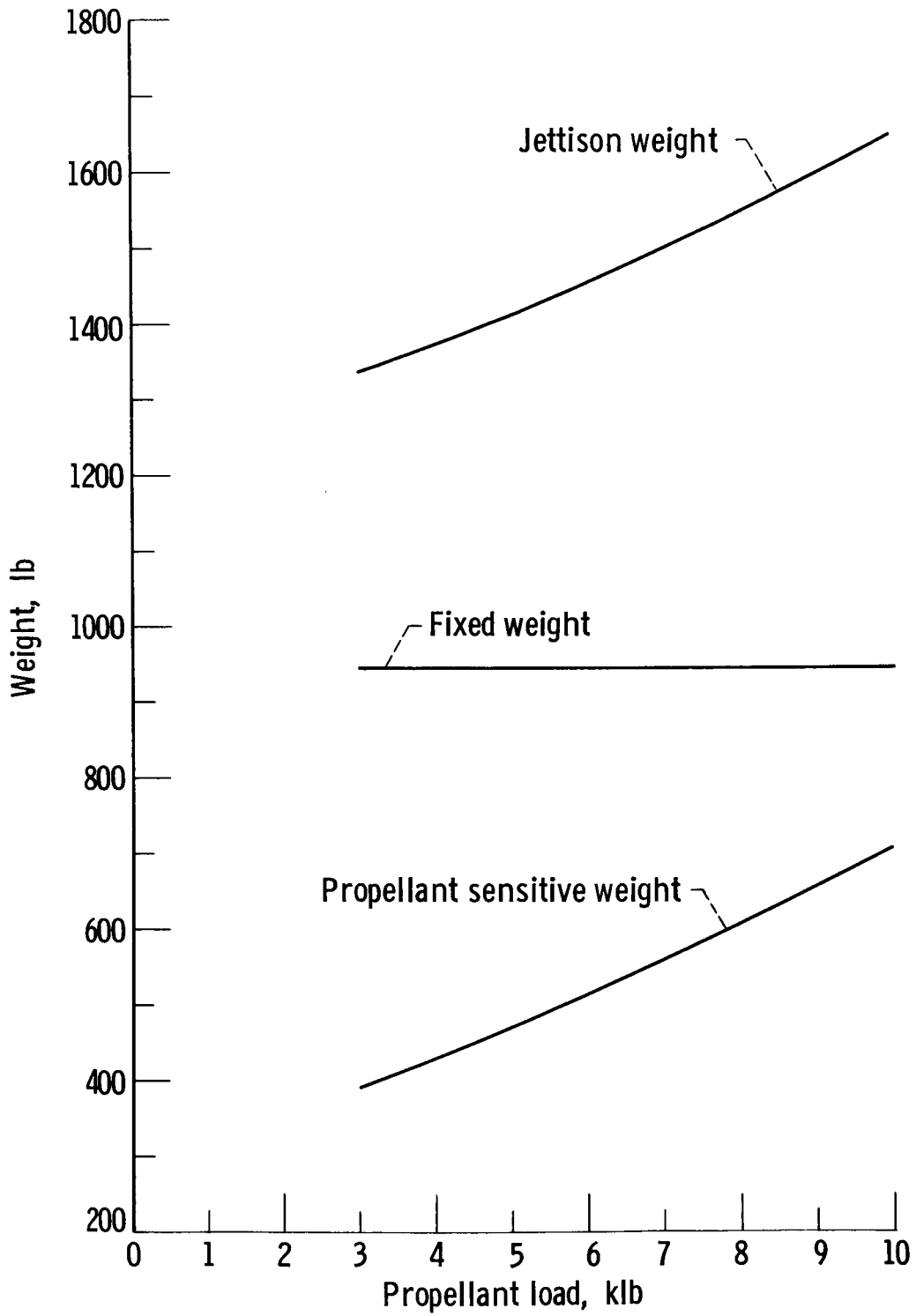


Figure 8. - Jettison weight breakdown for H-F kick stage.  
New 10K engine.

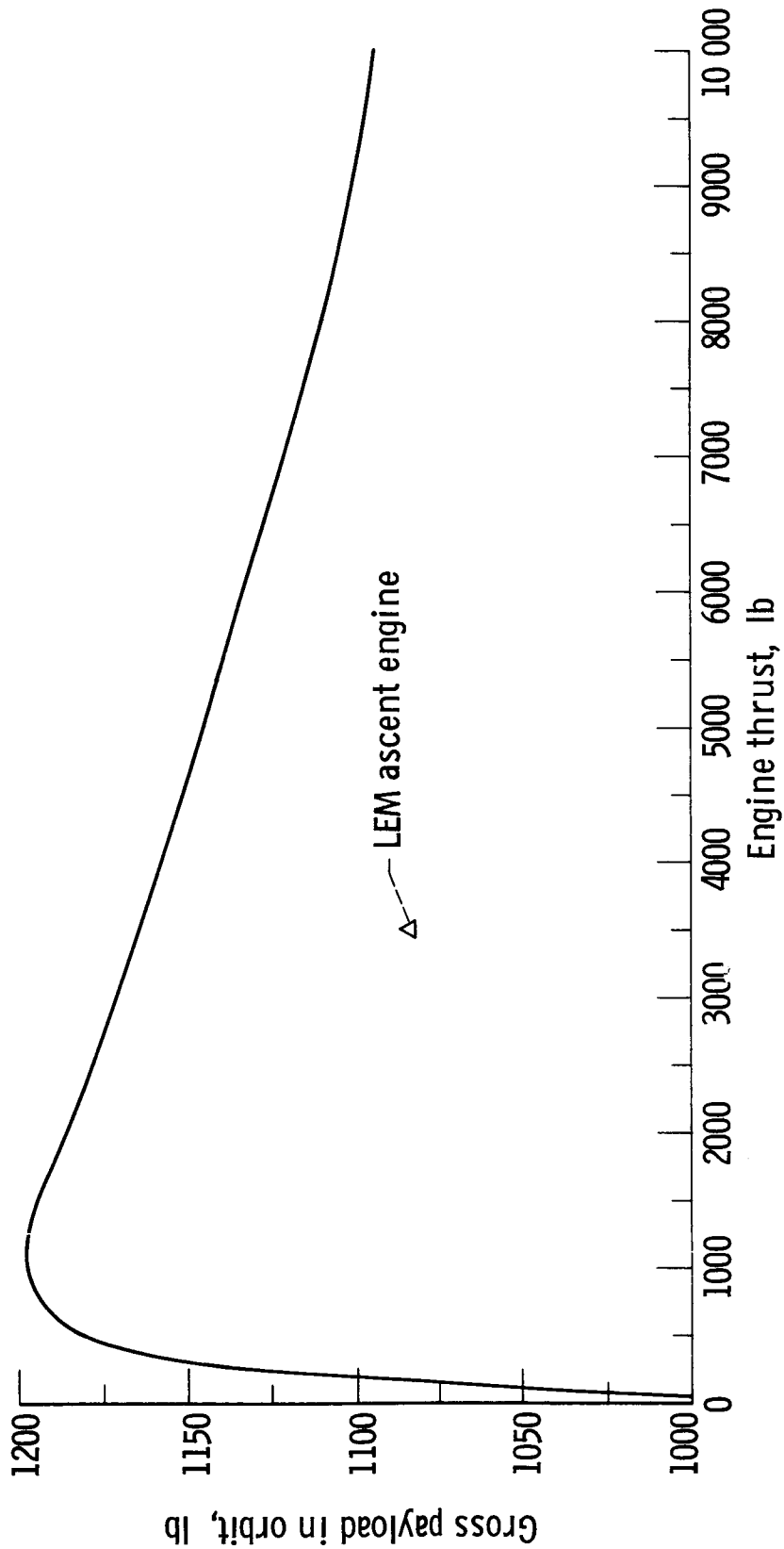


Figure 9. - 1971 Mars orbit mission. Saturn 1B-Centaur launch vehicle. 1000 nautical miles circular orbit. Lander capsule weight, 5000 pounds.

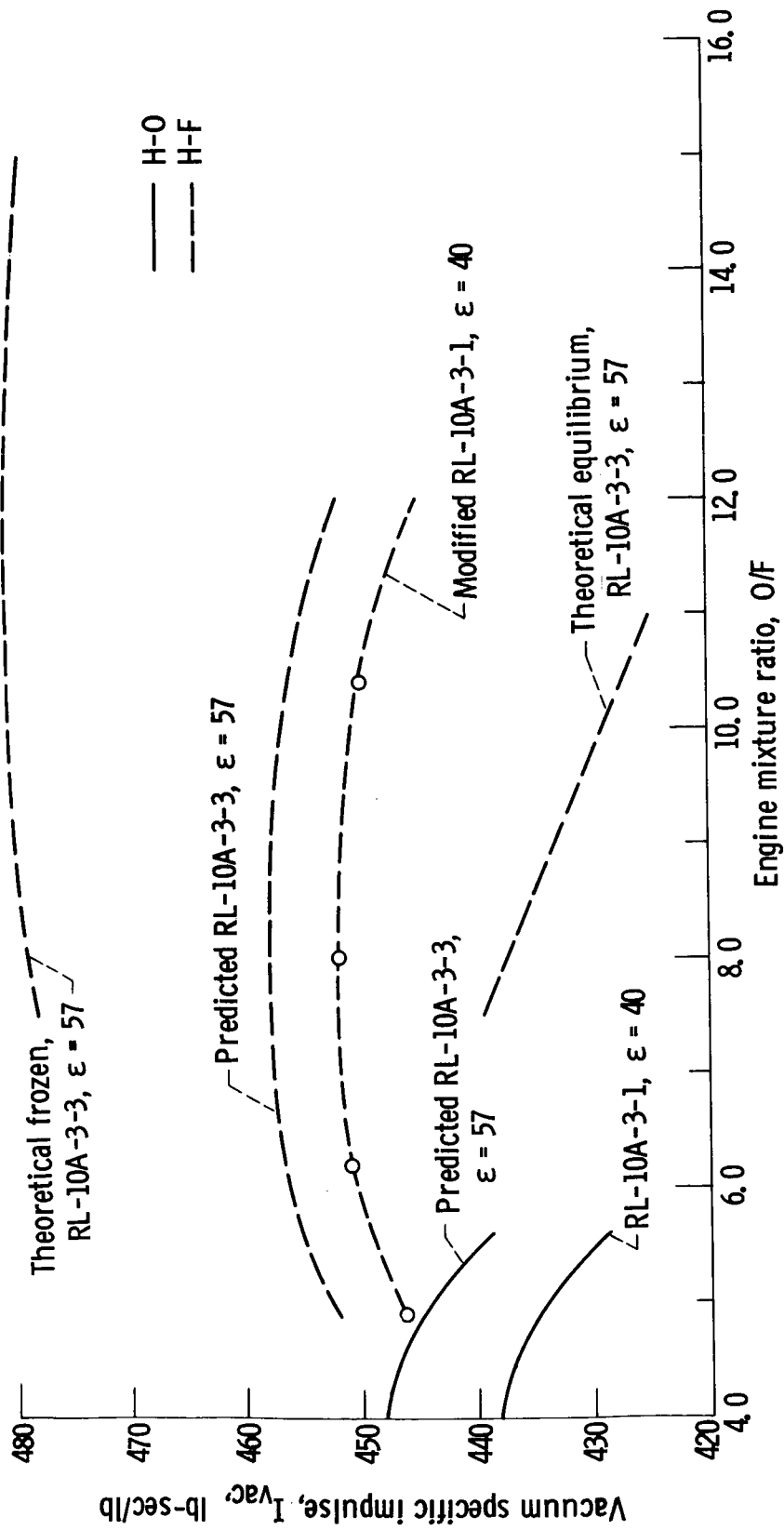


Figure 10.- Experimental and predicted performance of H-O and H-F in the RL-10 engine.

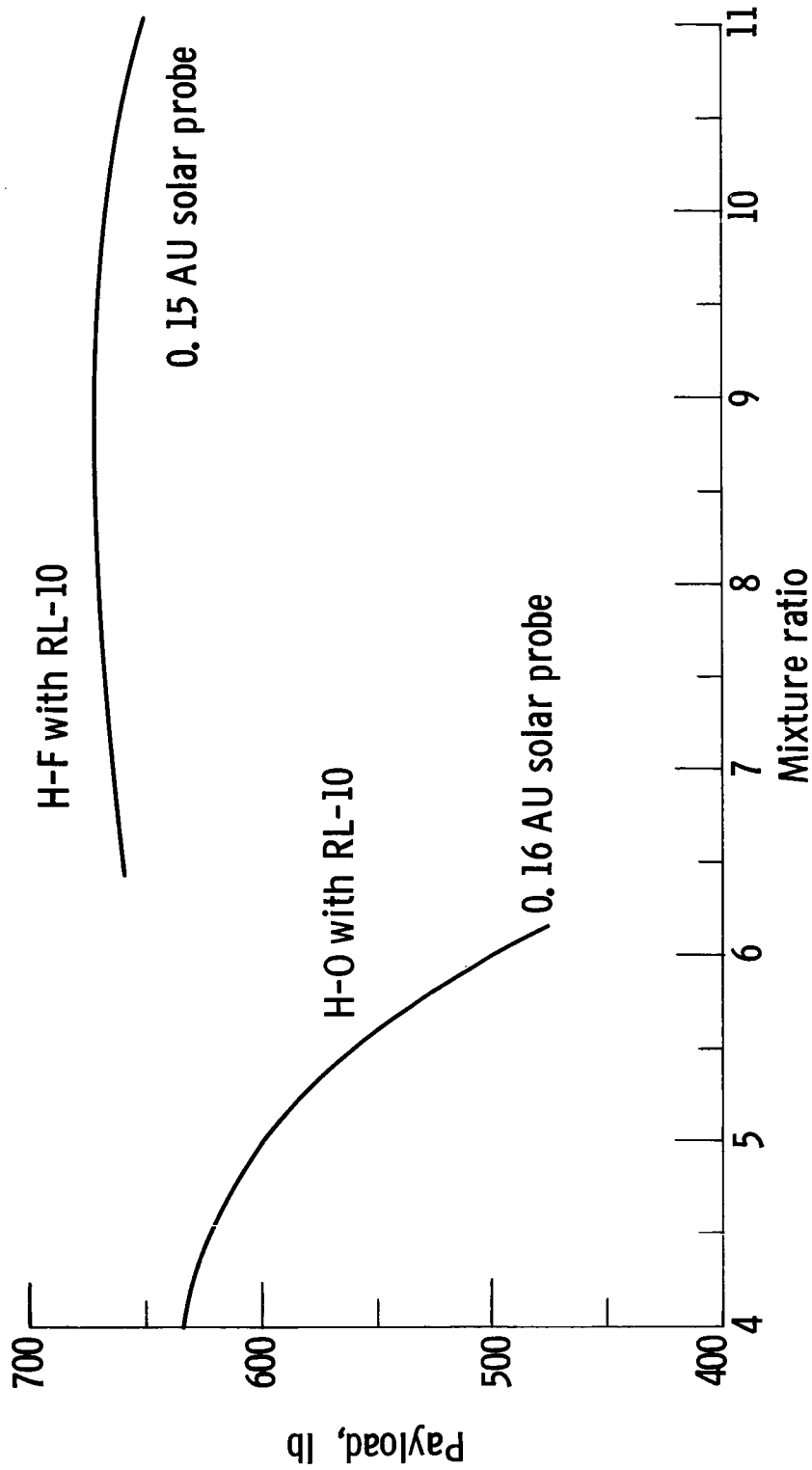
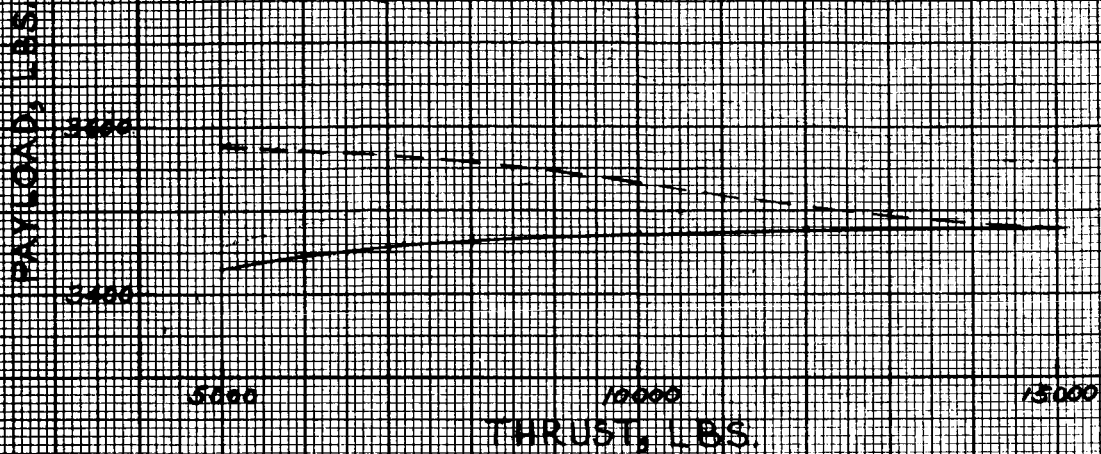
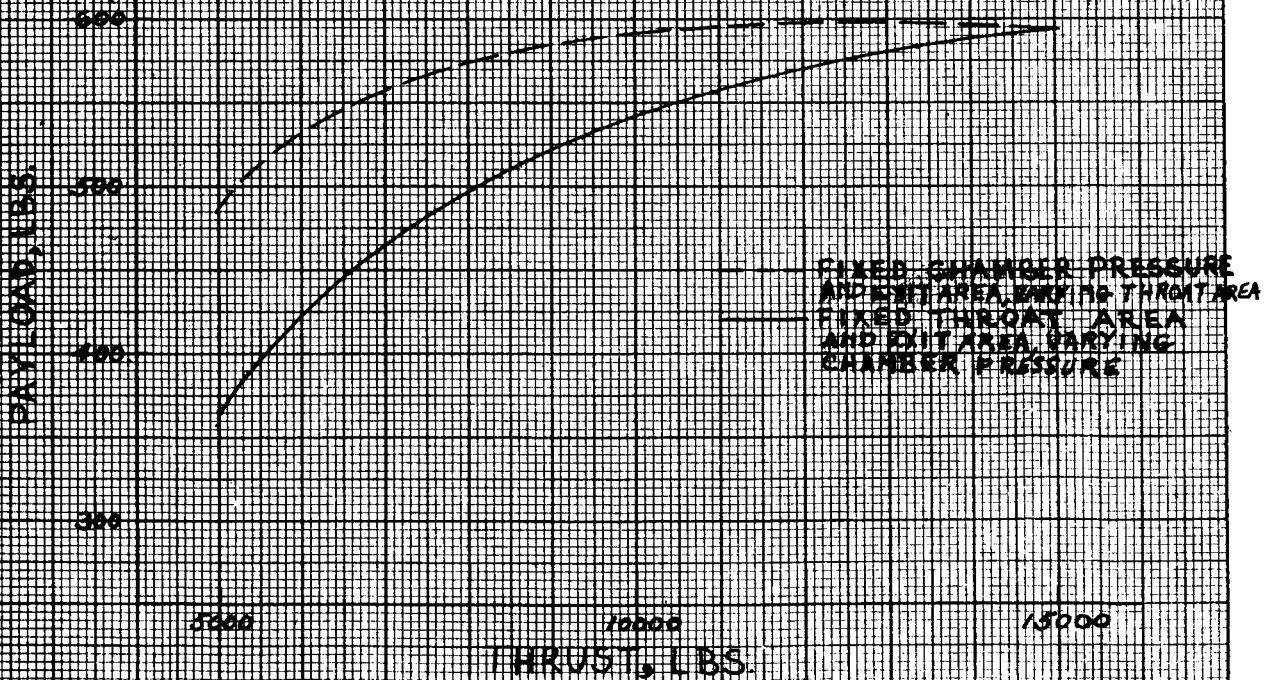


Figure 11.- Effect of kick stage mixture ratio on solar probe payload for H-O and H-F propellants using the RL-10 engine. Saturn 1B-Centaur launch vehicle.



2) LUNAR MISSION, ATLAS-CENTAUR LAUNCH VEHICLE



3) SOLAR PROBE MISSION, SATURN-CENTAUR LAUNCH VEHICLE

FIGURE 12-PAYLOAD VARIATION WITH THRUST FOR THE H-O RICK STAGE WITH THE RL-10 ENGINE

PAYLOAD WEIGHT, LBS.

500

700

600

500

40

60

80

100

NOZZLE EXPANSION RATIO

THRUST = 10,000 LBS.

a) EFFECT OF NOZZLE EXPANSION RATIO

PAYLOAD WEIGHT, LBS.

700

600

500

400

4000

8000

12000

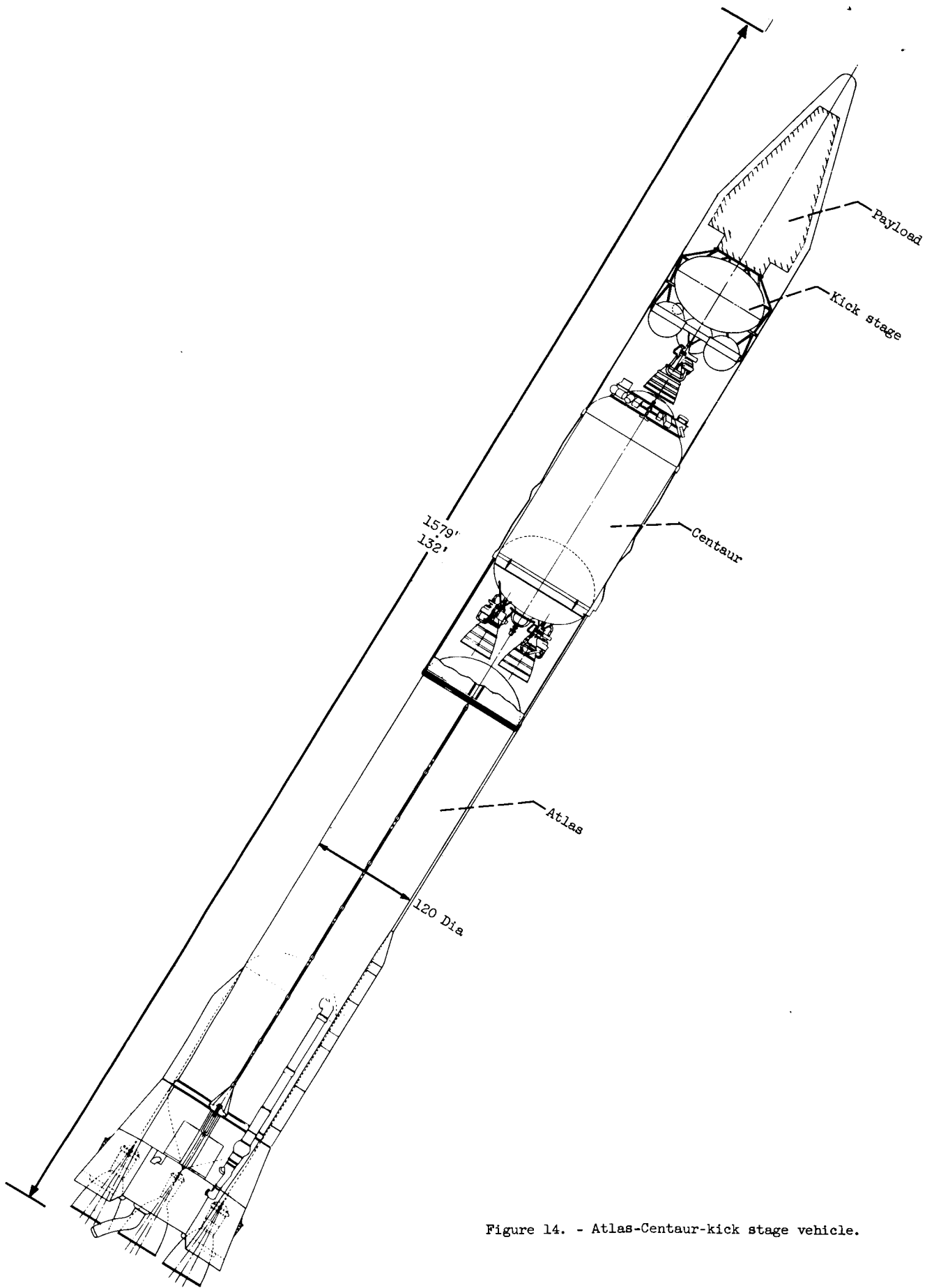
16000

NOZZLE EXPANSION RATIO = 60

ENGINE THRUST, LBS.

b) EFFECT OF ENGINE THRUST

FIGURE 12.- PAYLOAD VARIATION WITH ENGINE PERFORMANCE PARAMETERS FOR THE H-F KICK STAGE 0.15 AU SOLAR PROBE ; SATURN 1B-CENTAUR LAUNCH VEHICLE



E-3031a

Figure 14. - Atlas-Centaur-kick stage vehicle.

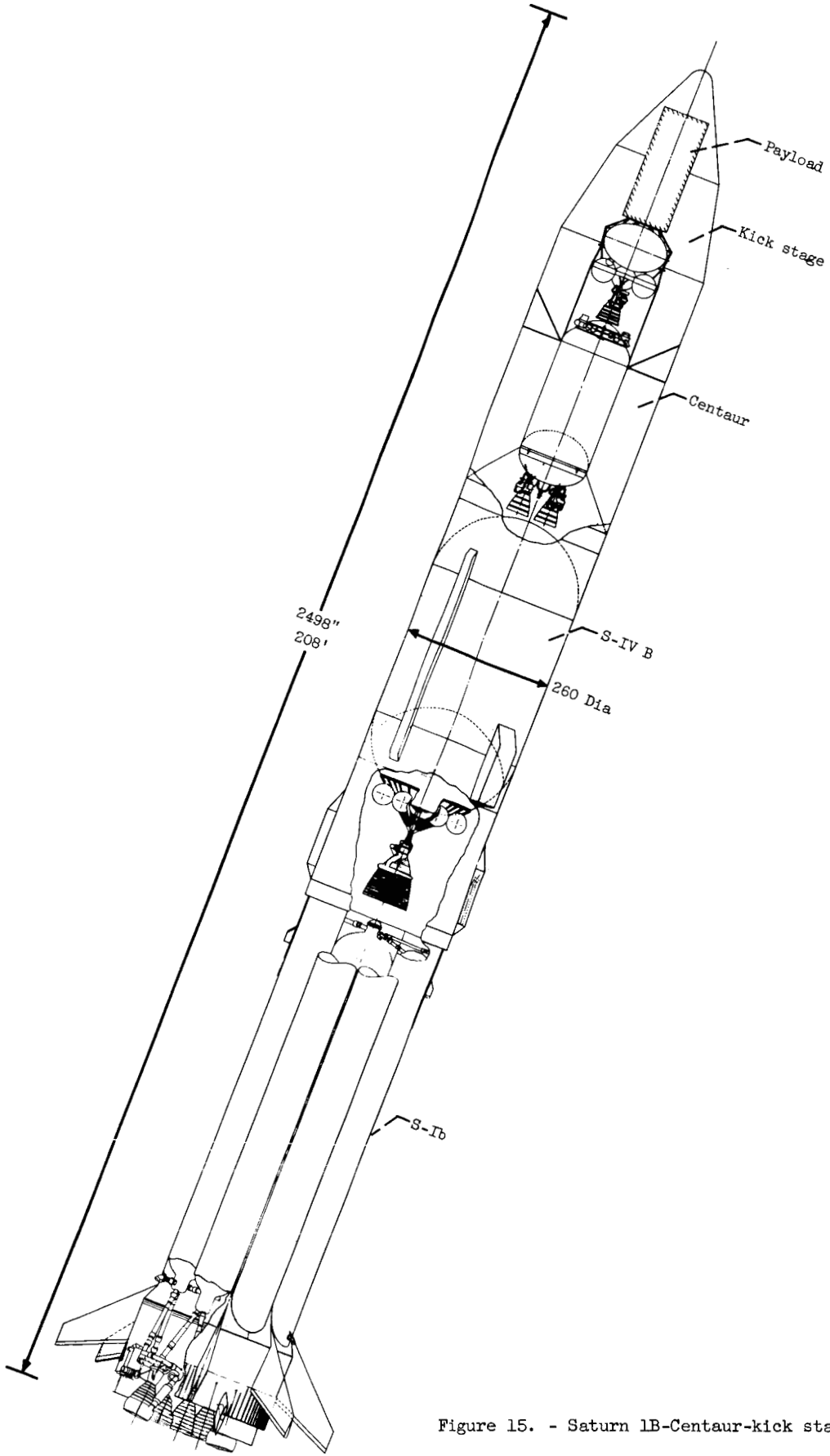


Figure 15. - Saturn 1B-Centaur-kick stage vehicle.

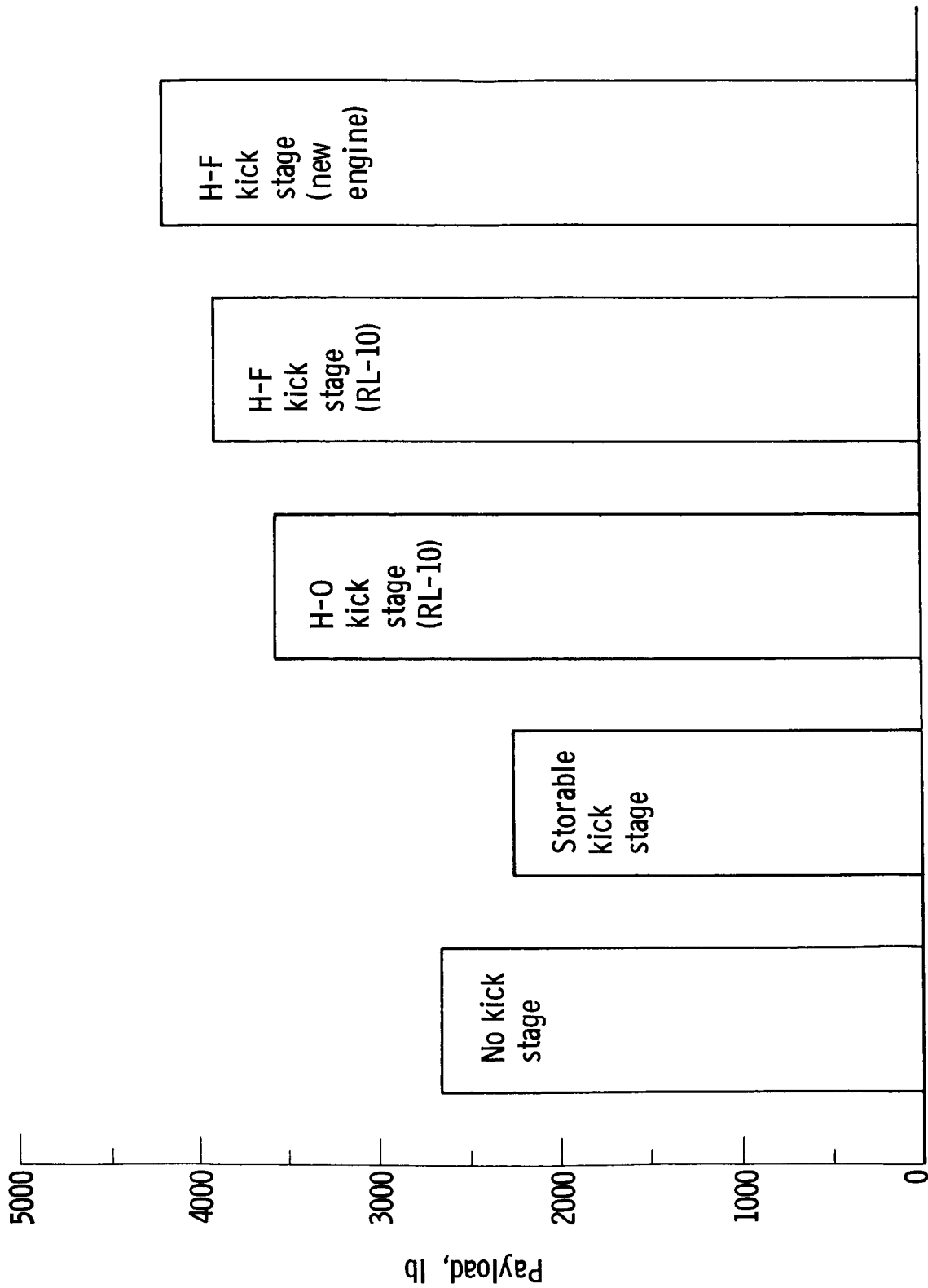


Figure 16. - Comparison of payload capabilities of various kick stages for lunar mission. Atlas-Centaur launch vehicle; optimum kick stage propellant weight.

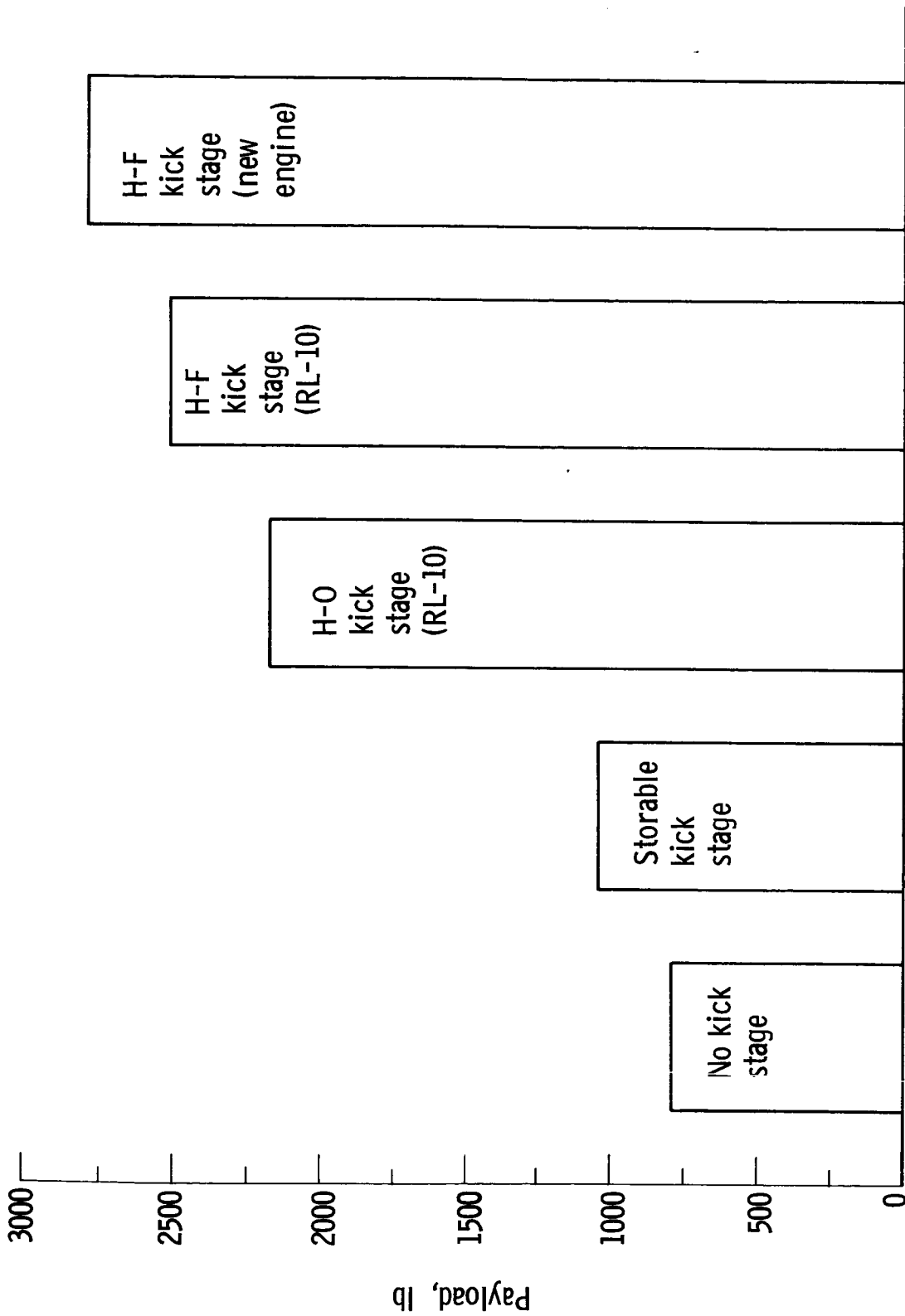


Figure 17. - Comparison of payload capabilities of various kick stages for 24-hour synchronous-equatorial orbit mission. Atlas-Centaur launch vehicle; optimum kick stage propellant weight.

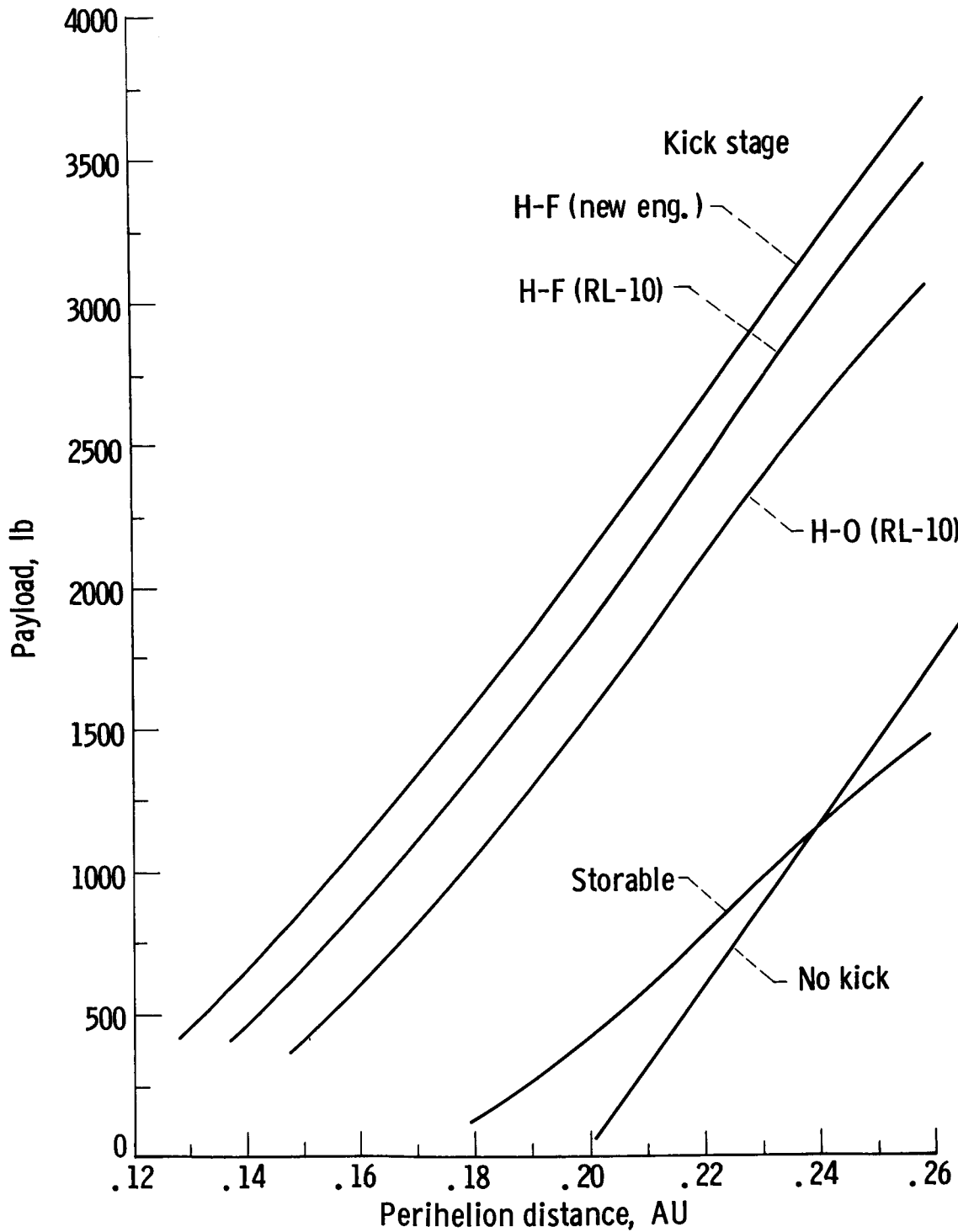


Figure 18. - Comparison of payload capabilities of various kick stages for solar probe missions. Saturn 1B-Centaur launch vehicle; optimum kick stage propellant weight.

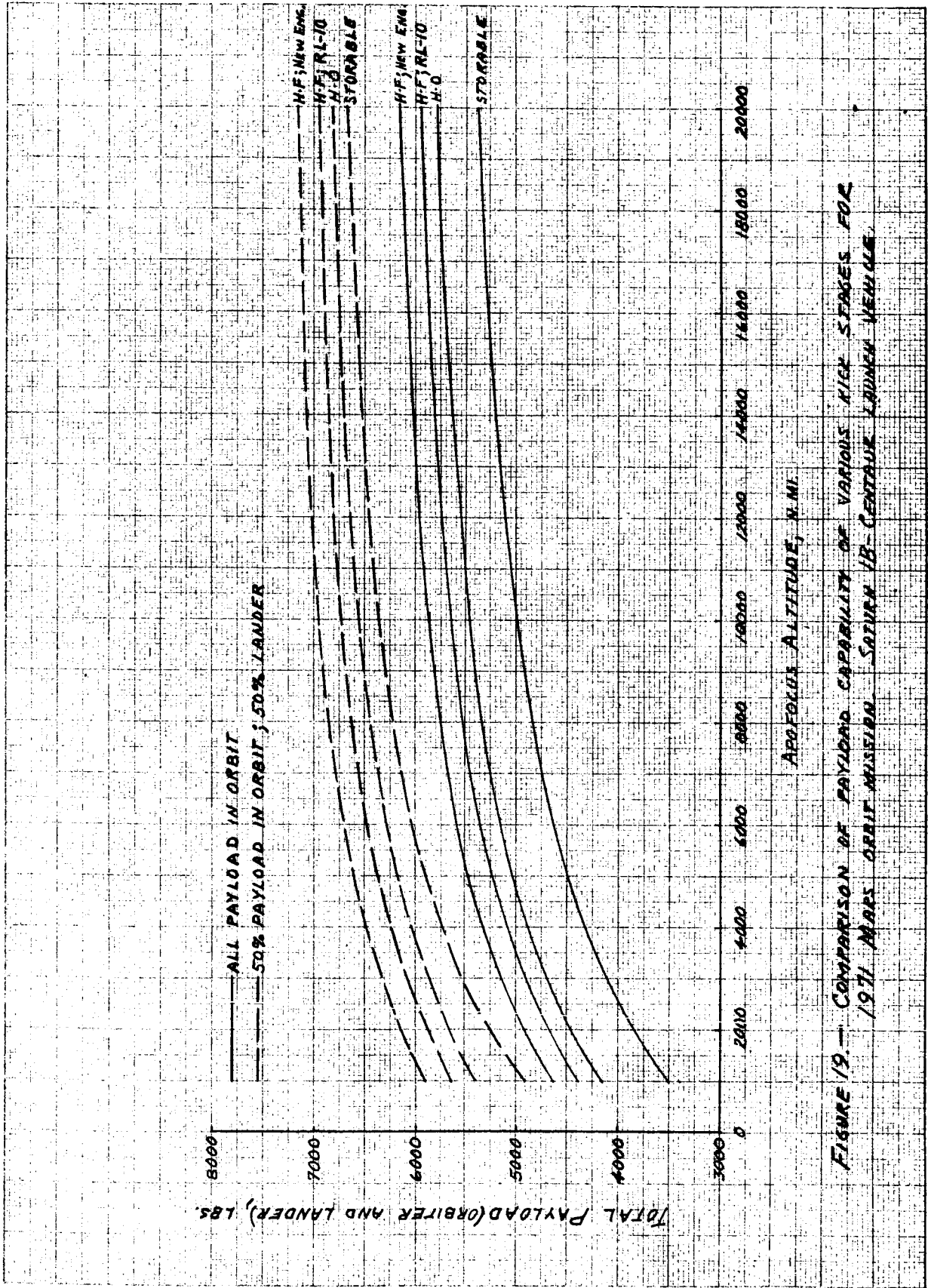


FIGURE 19. — COMPARISON OF PAYLOAD CAPABILITY OF VARIOUS RIER STAGES FOR 1971 MARS ORBIT MISSION SATURN IB-CENTAUER LAUNCH VEHICLE.

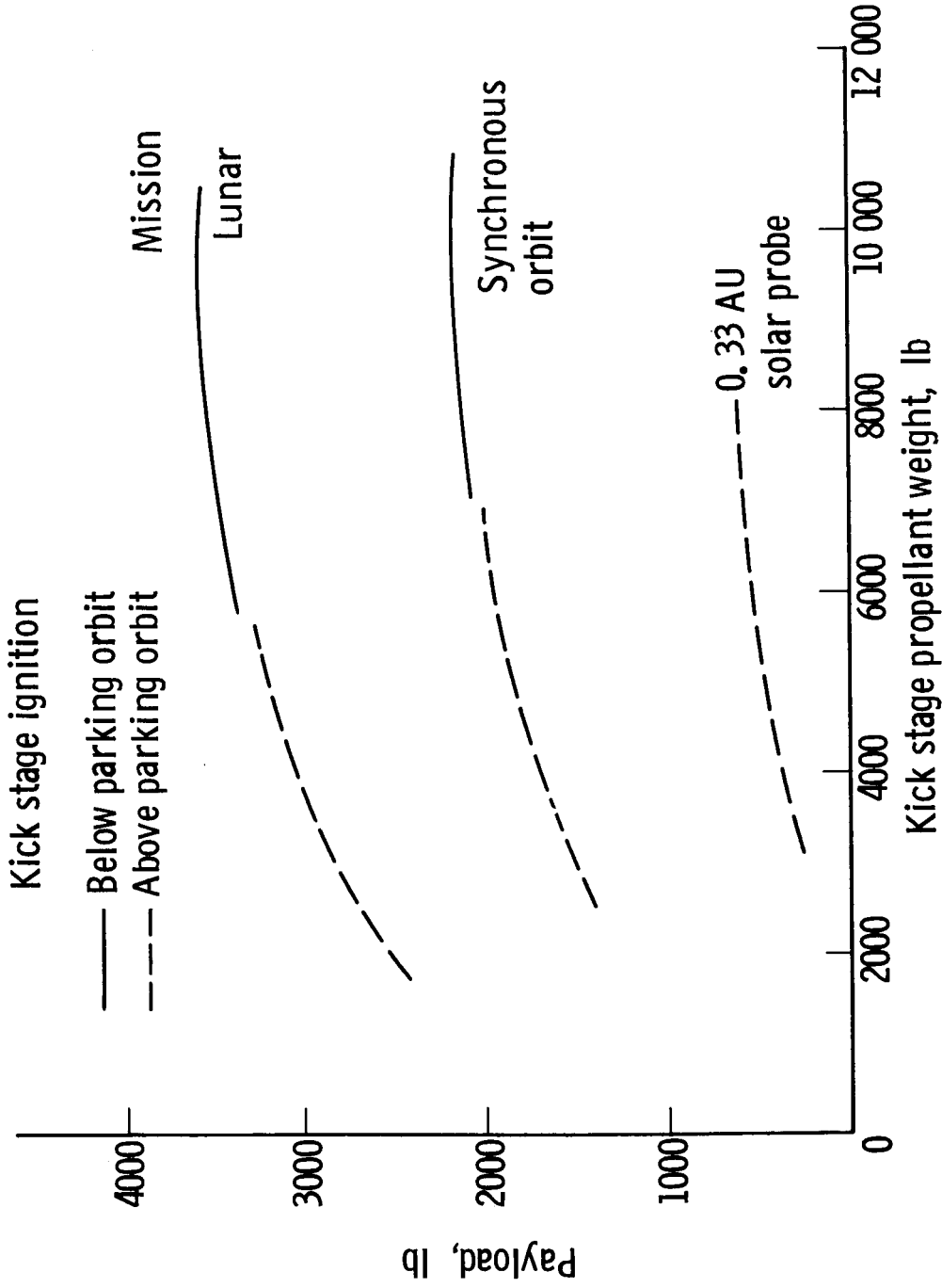


Figure 20. - Variation of payload capability with propellant weight for H-O kick stage. Atlas-Centaur launch vehicle.

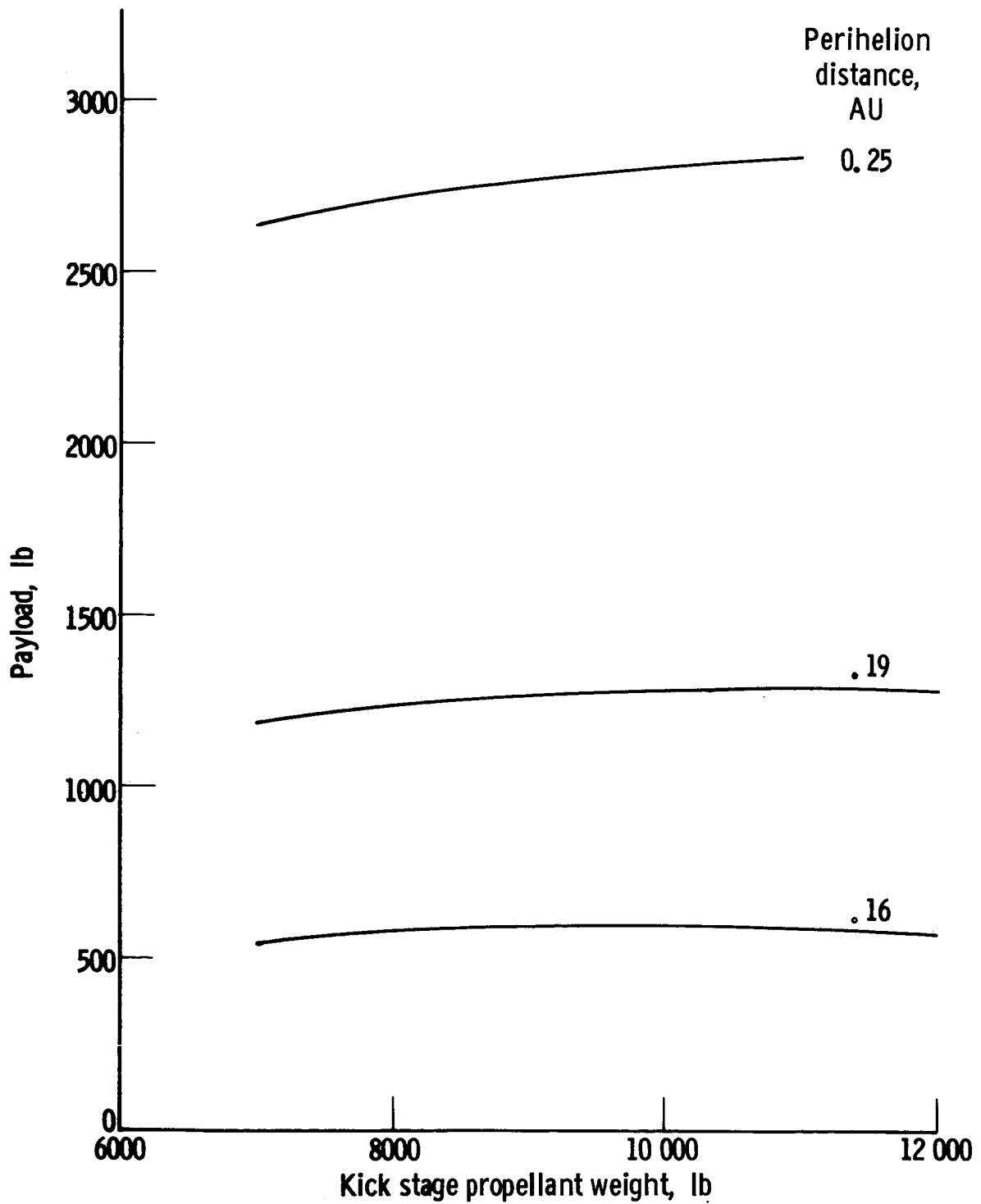


Figure 21. - Variation of payload capability with propellant weight for H-O kick stage. Solar probe missions; Saturn 1B-Centaur launch vehicle.

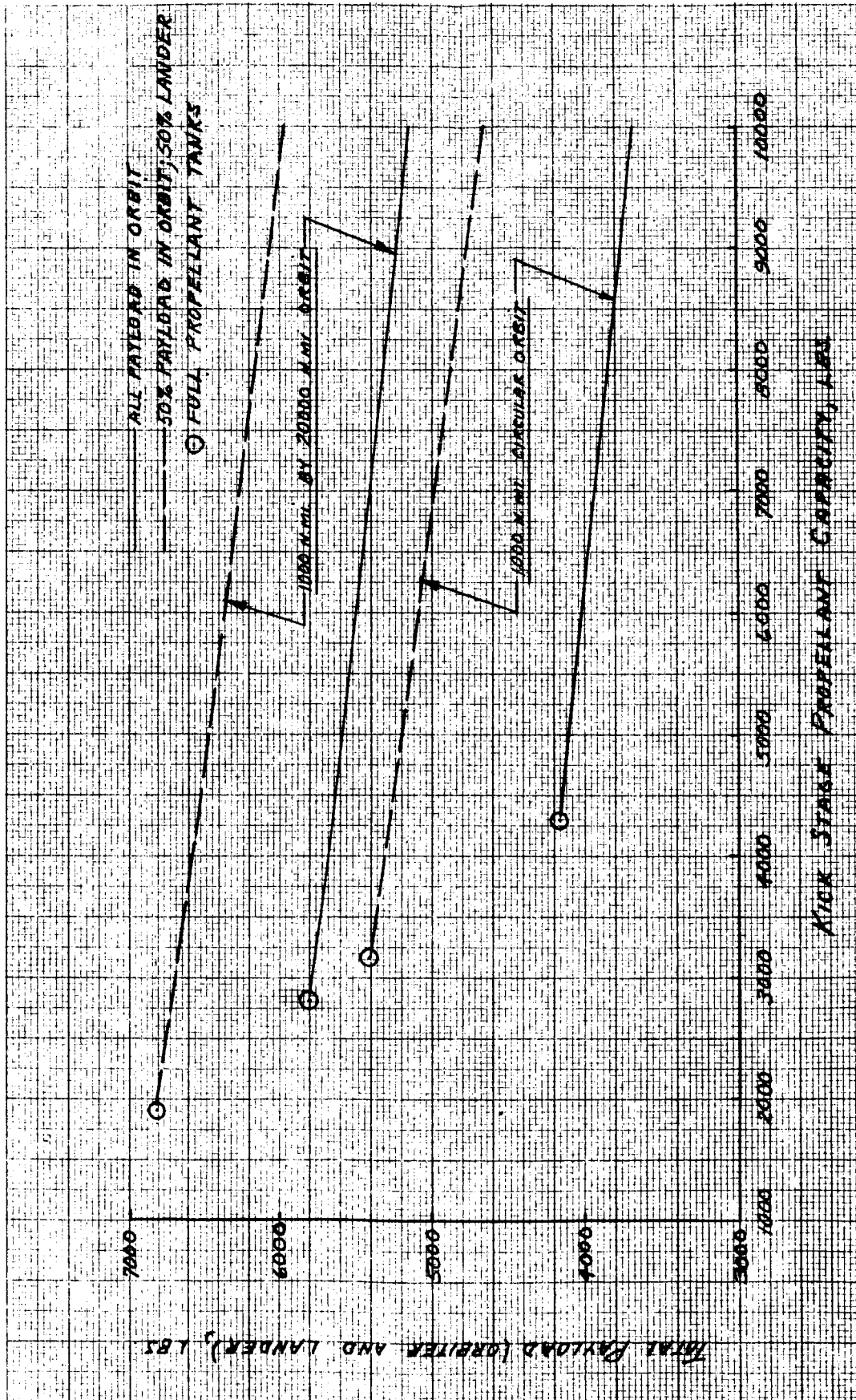


FIGURE 22 - VARIATION OF PAYLOAD CAPABILITY OF THE H-0 KICK STAGE WITH PROPELLANT CAPACITY, AGENS ORBIT MISSION, SATURN 1B-CENTRAIR LANTERN VEHICLE

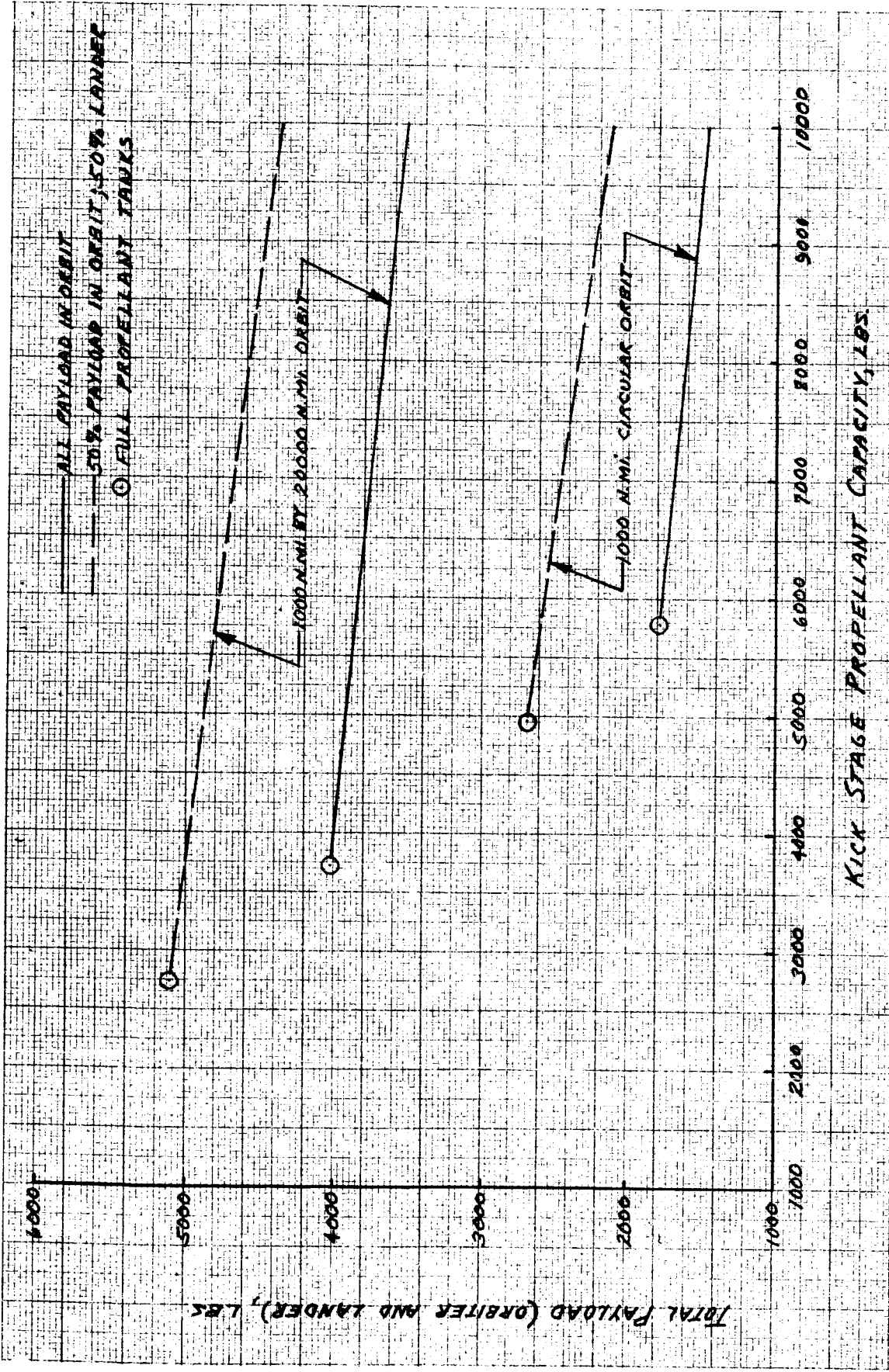


FIGURE 23. - VARIATION OF PAYLOAD CAPABILITY OF THE H-0 KICK STAGE WITH PROPELLANT CAPACITY. VENUS ORBIT MISSION; SATURN IB-CENTAUR LAUNCH VEHICLE.

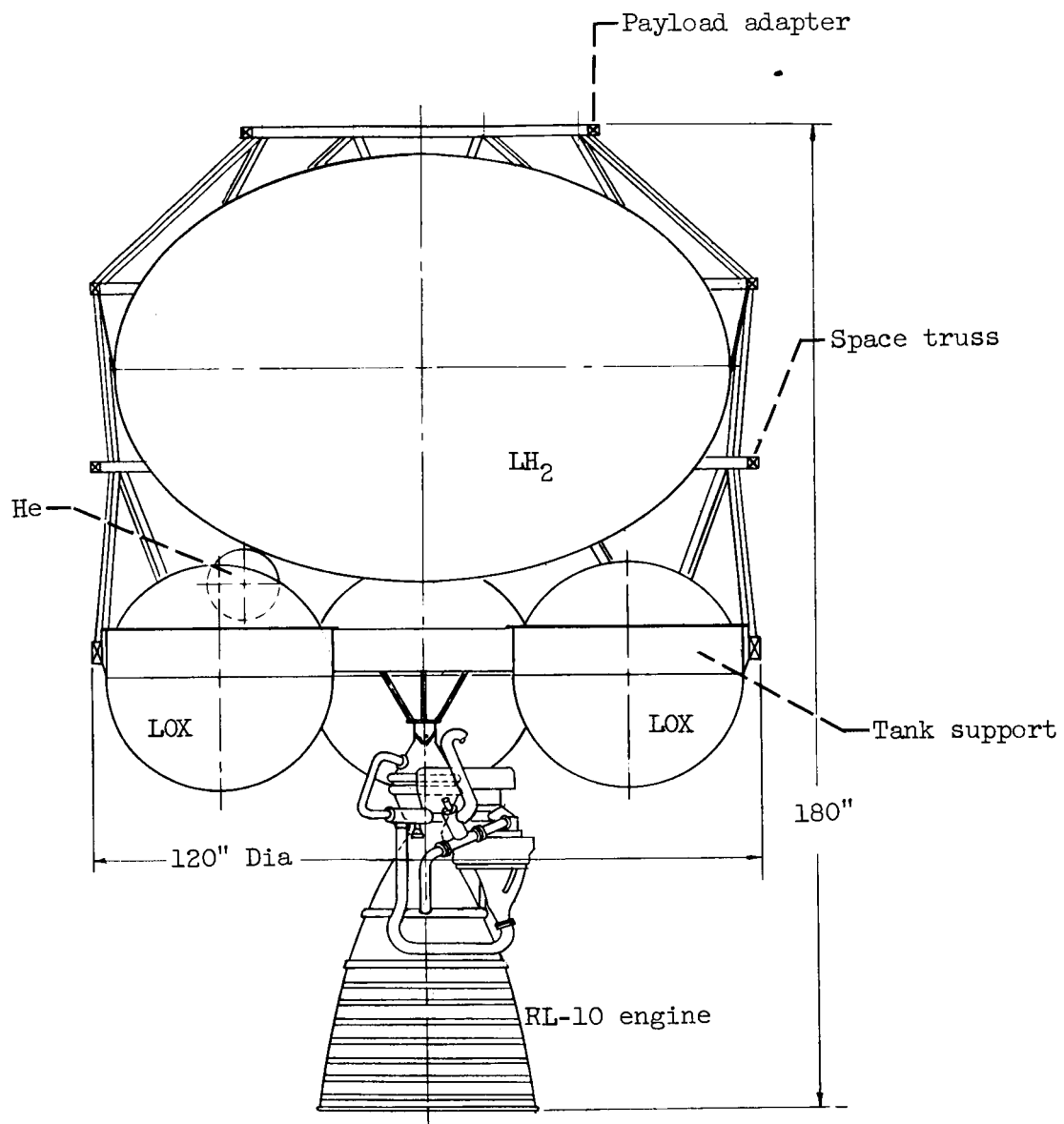


Figure 24. - Hydrogen-oxygen kick stage. Configuration I.

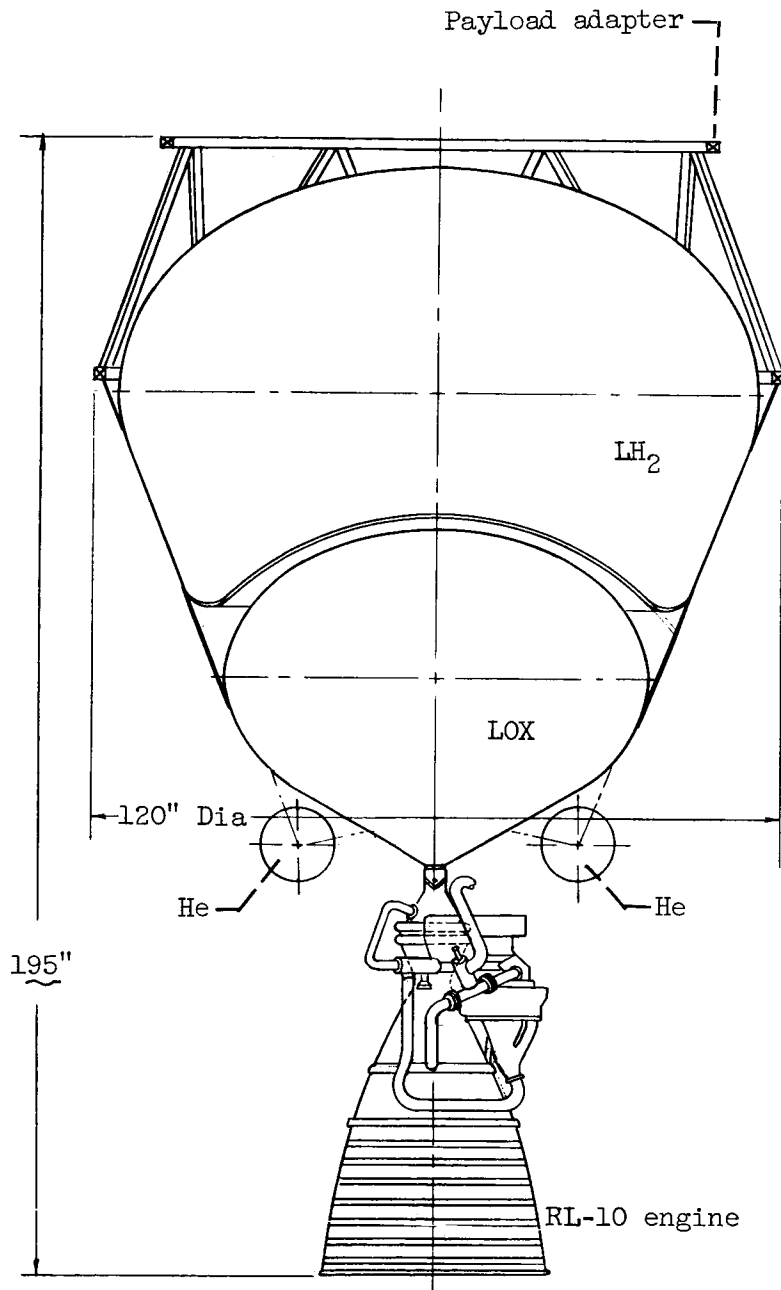
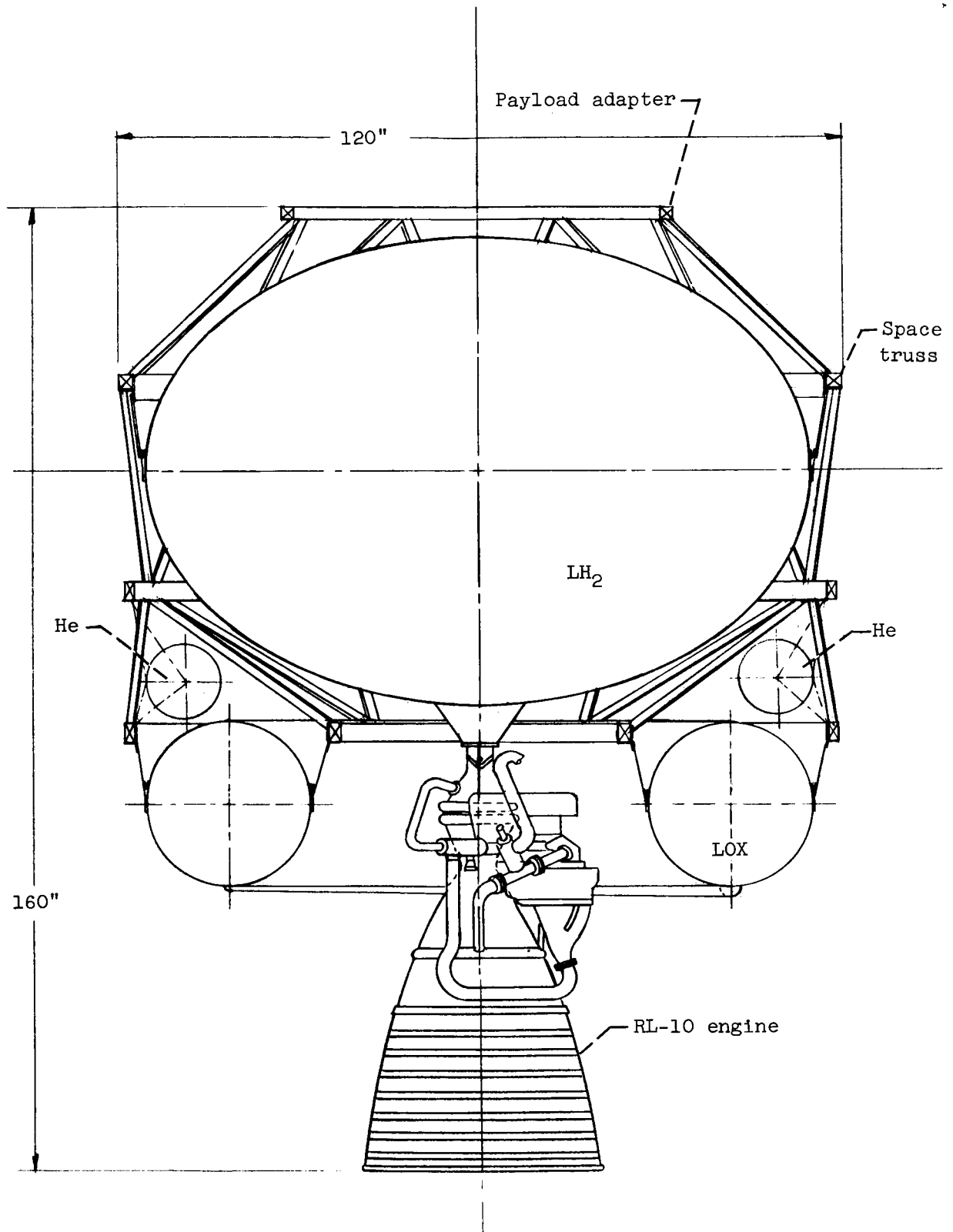


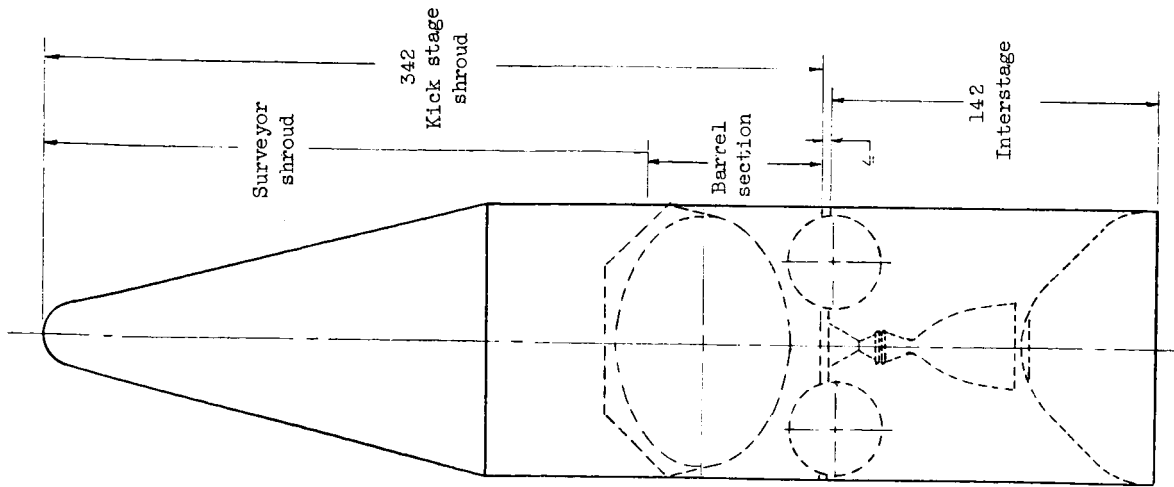
Figure 25. - Hydrogen-oxygen kick stage. Configuration II.



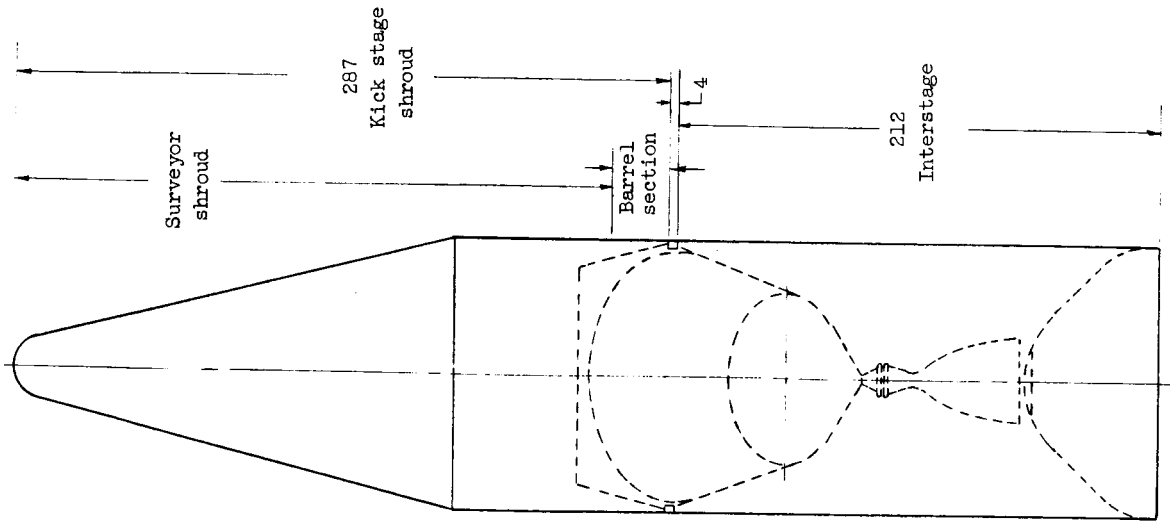
E-3031a

Figure 26. - Hydrogen-oxygen kick stage. Configuration III.

Configuration I



Configuration II



Configuration III

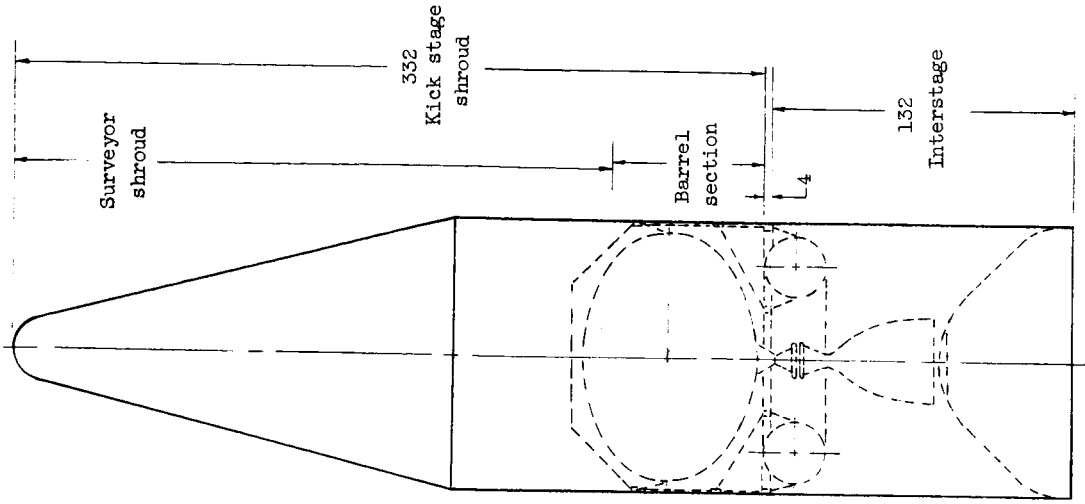


Figure 27. - Comparison of H-O kick stage configurations. Atlas-Centaur launch vehicle.

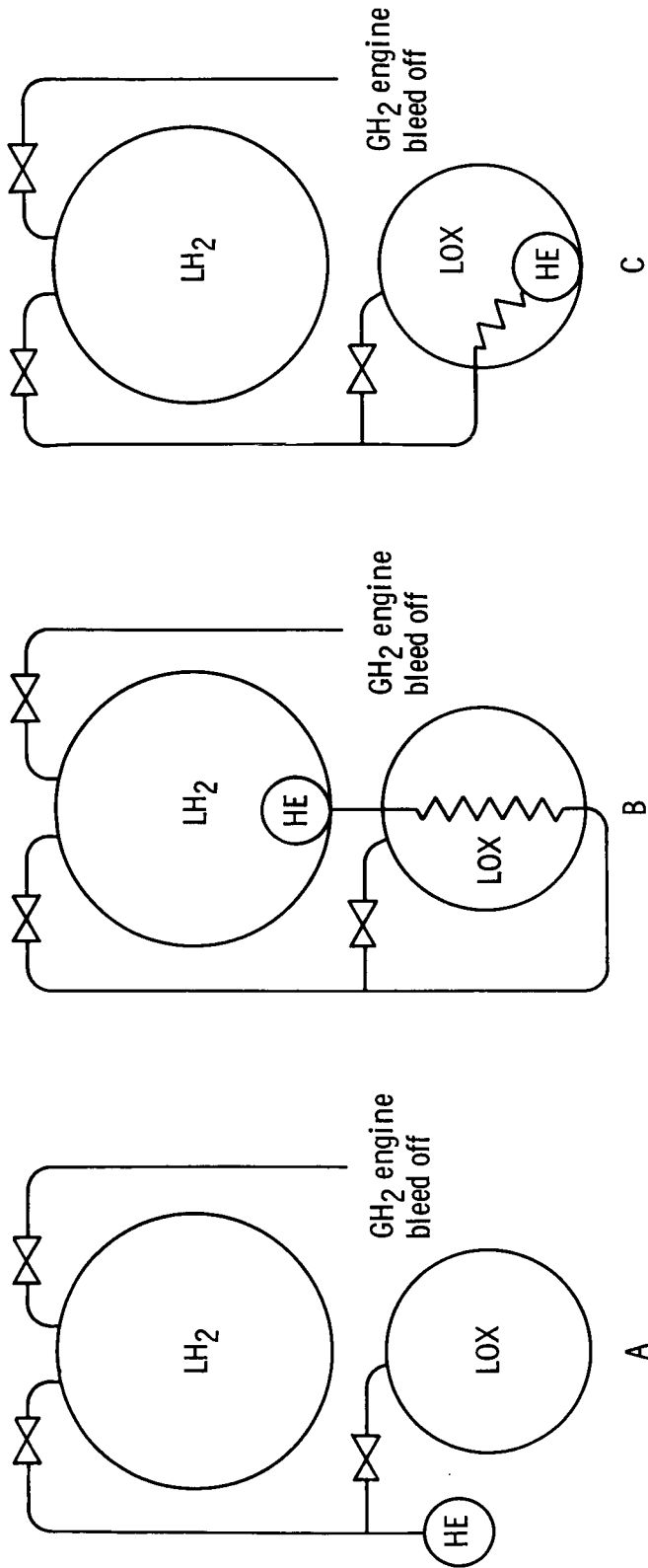


Figure 28. - Typical kick stage pressurization system concepts.

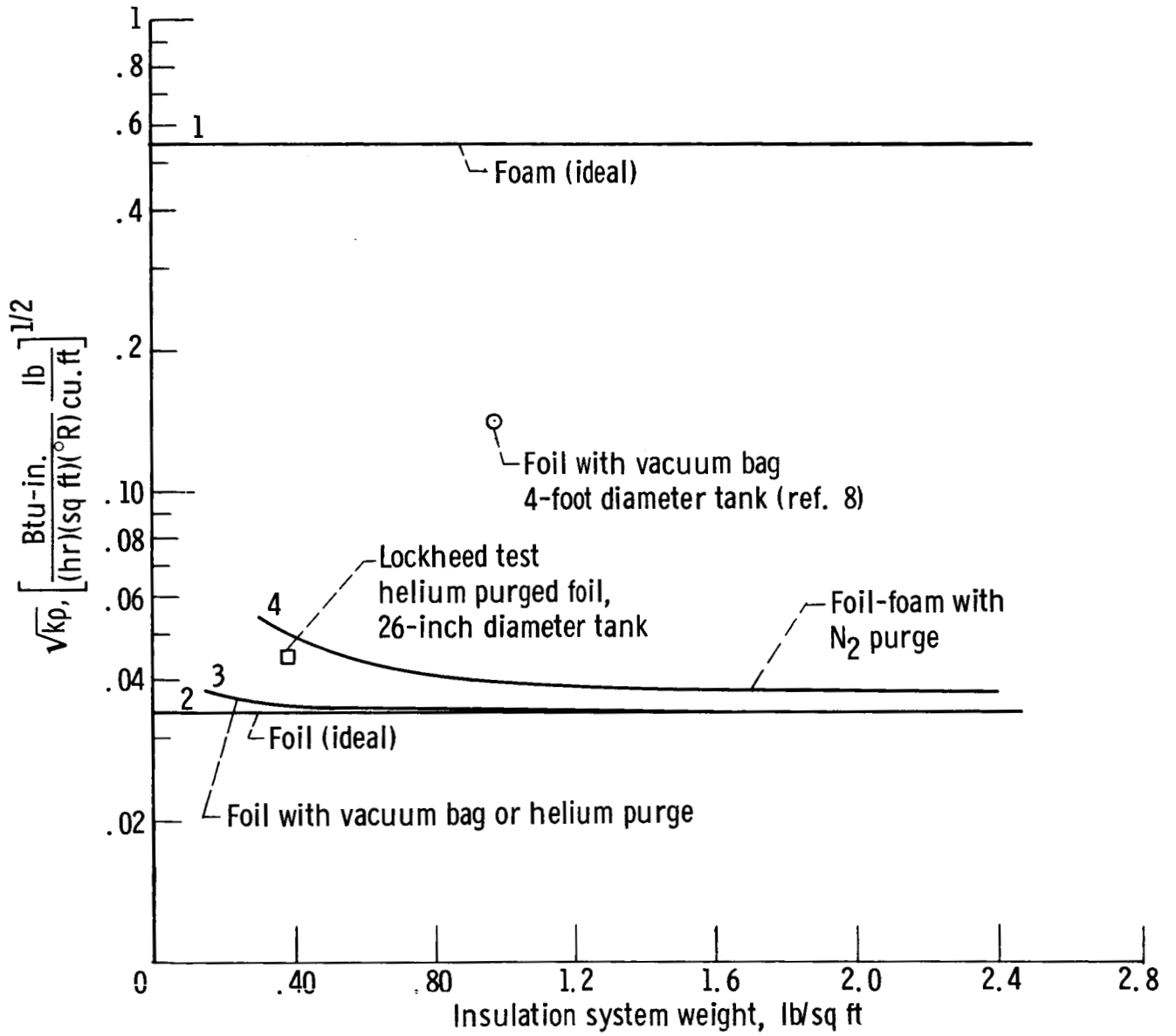


Figure 29. - Effect of various insulation systems on insulation comparison parameter.

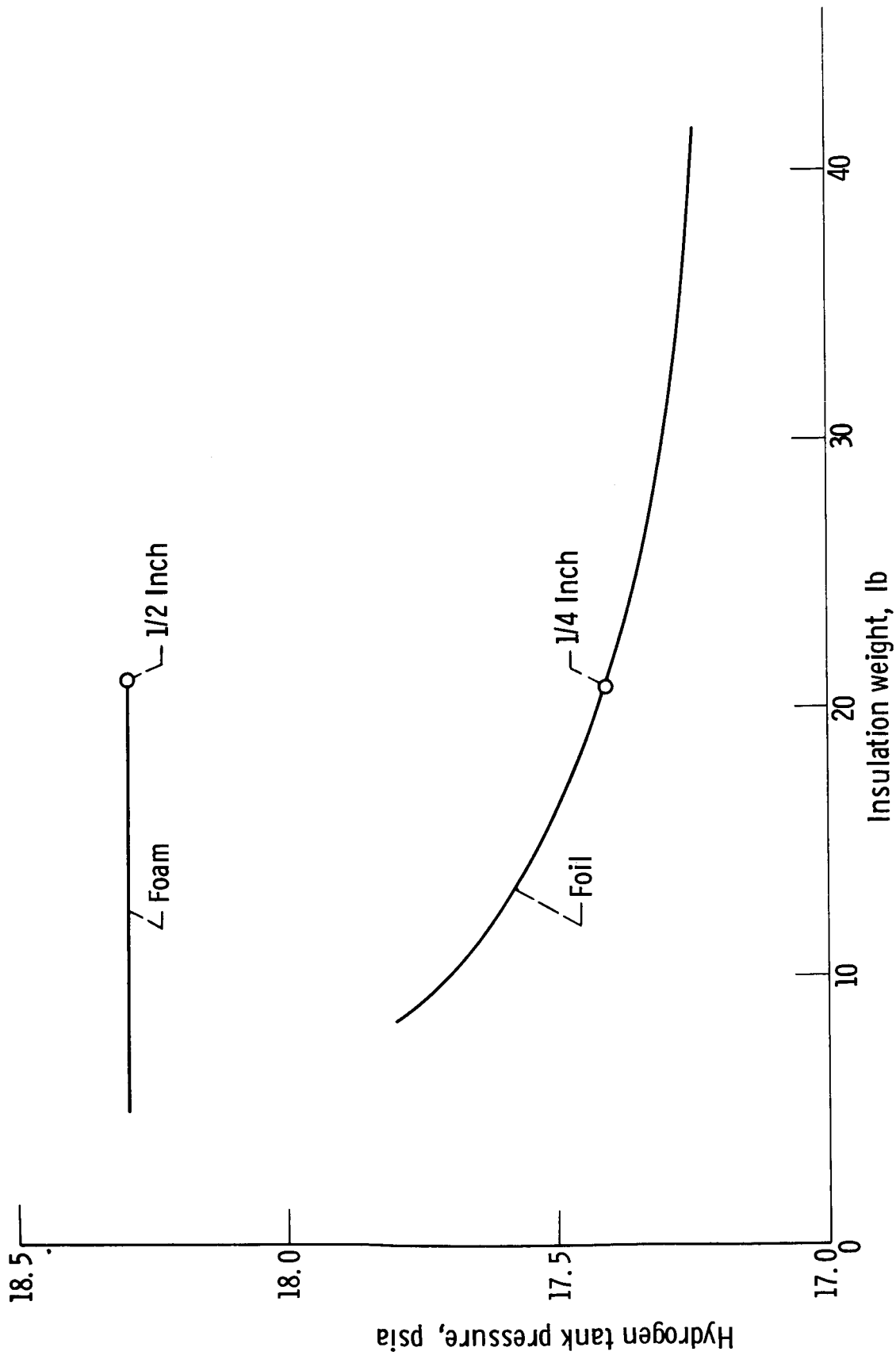
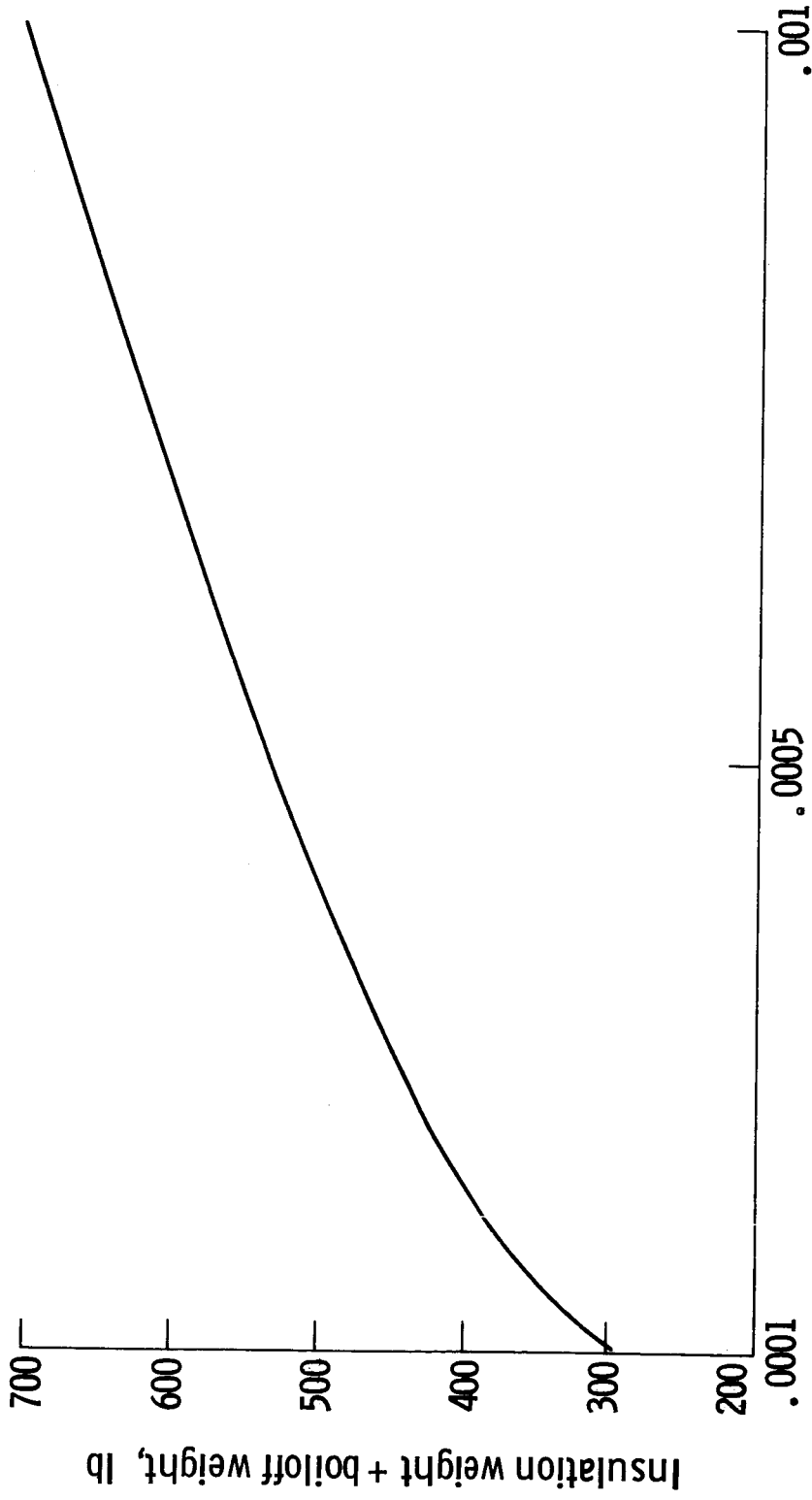


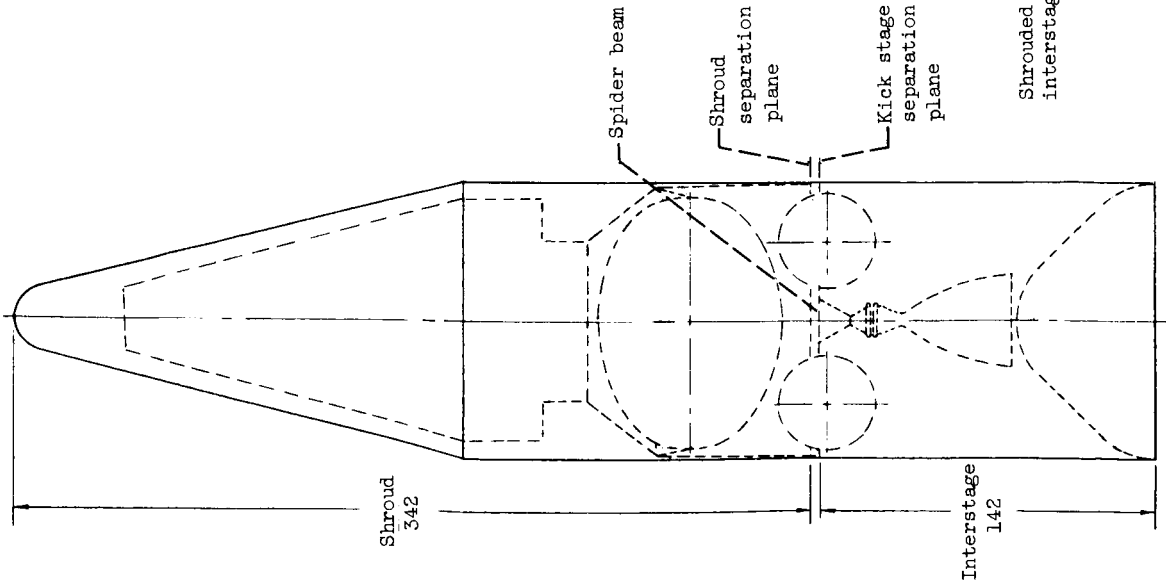
Figure 30. - Effect of insulation and insulation weight on hydrogen tank pressure for six-hour transfer to synchronous orbit.



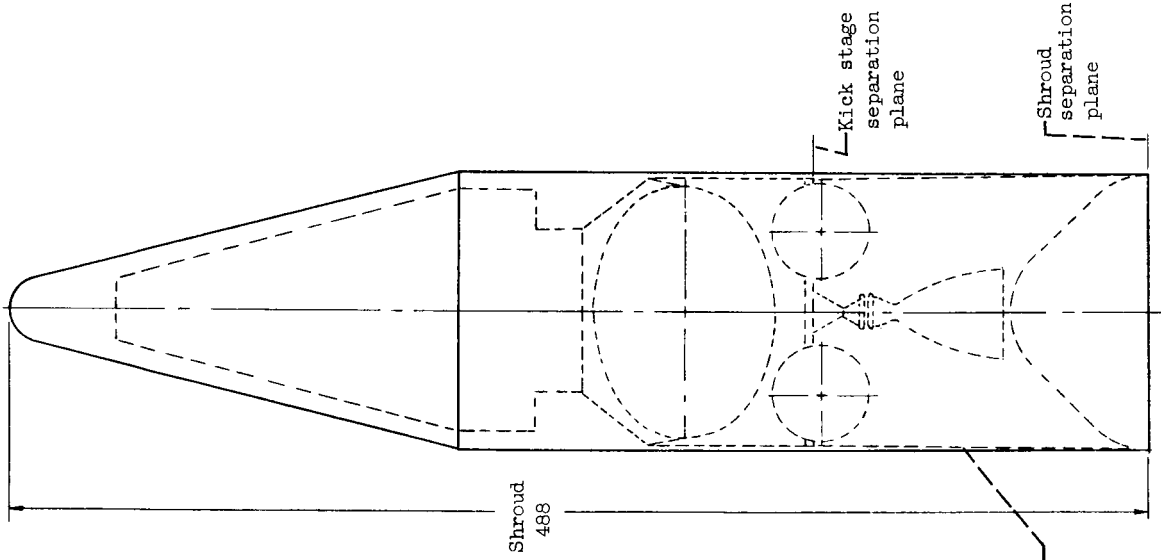
Apparent thermal conductivity, Btu-in. / (hr)(sq ft)(°R)

Figure 31. - Effect of multifoil performance on magnitude of hydrogen tank insulation plus boiloff weight for H-O stage on Mars mission. Coast time, 220 days.

Configuration "A"  
Short shroud



Configuration "B"  
Long shroud



Configuration "C"  
Non shrouded kick stage

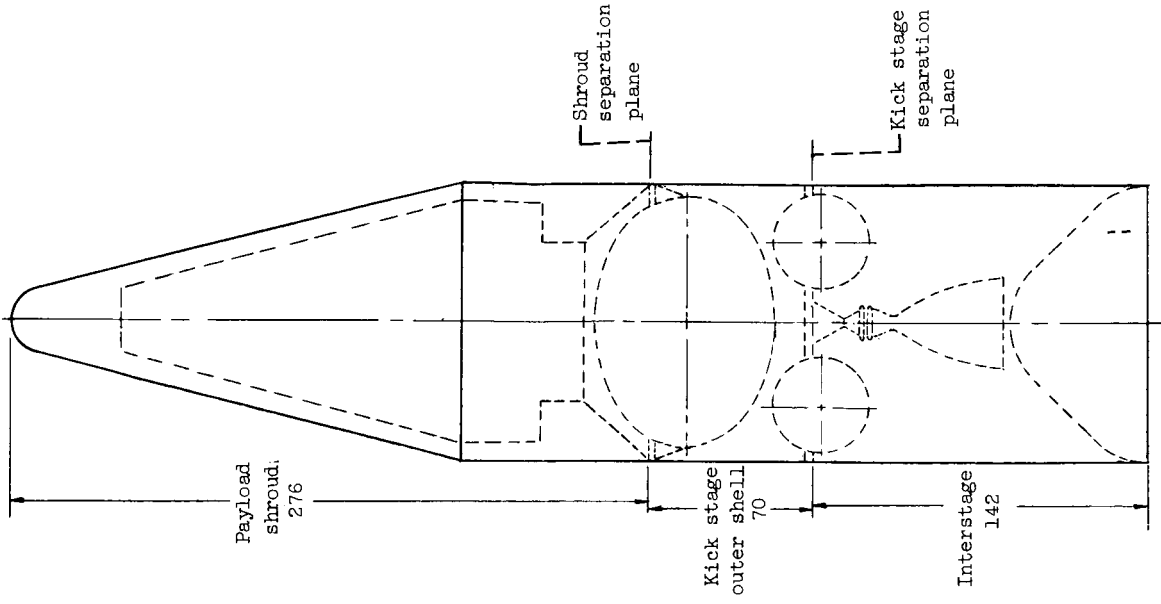


Fig. 32. - Comparison of kick stage shroud concepts.

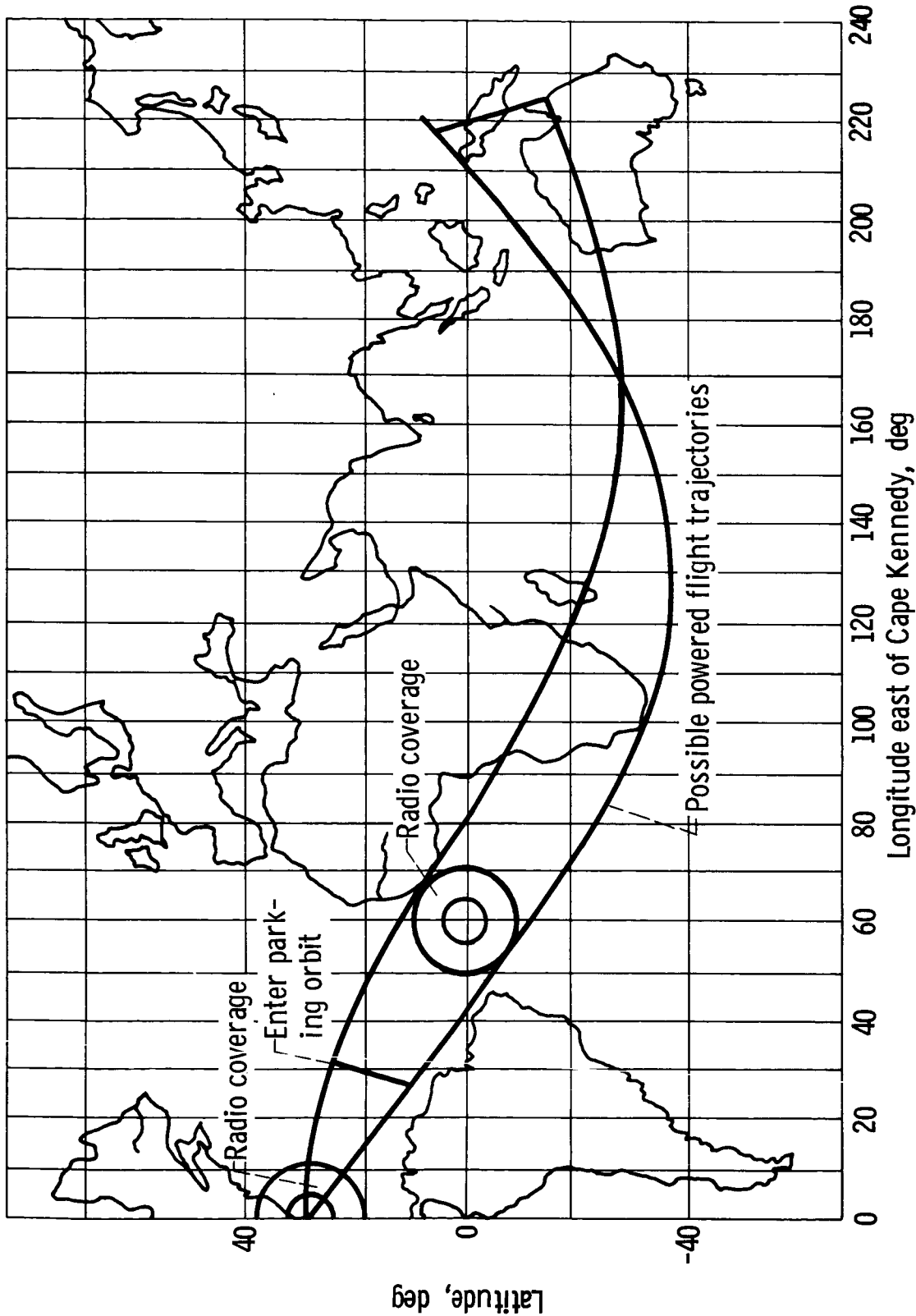


Figure 33. - Boost trajectories for solar probe mission.

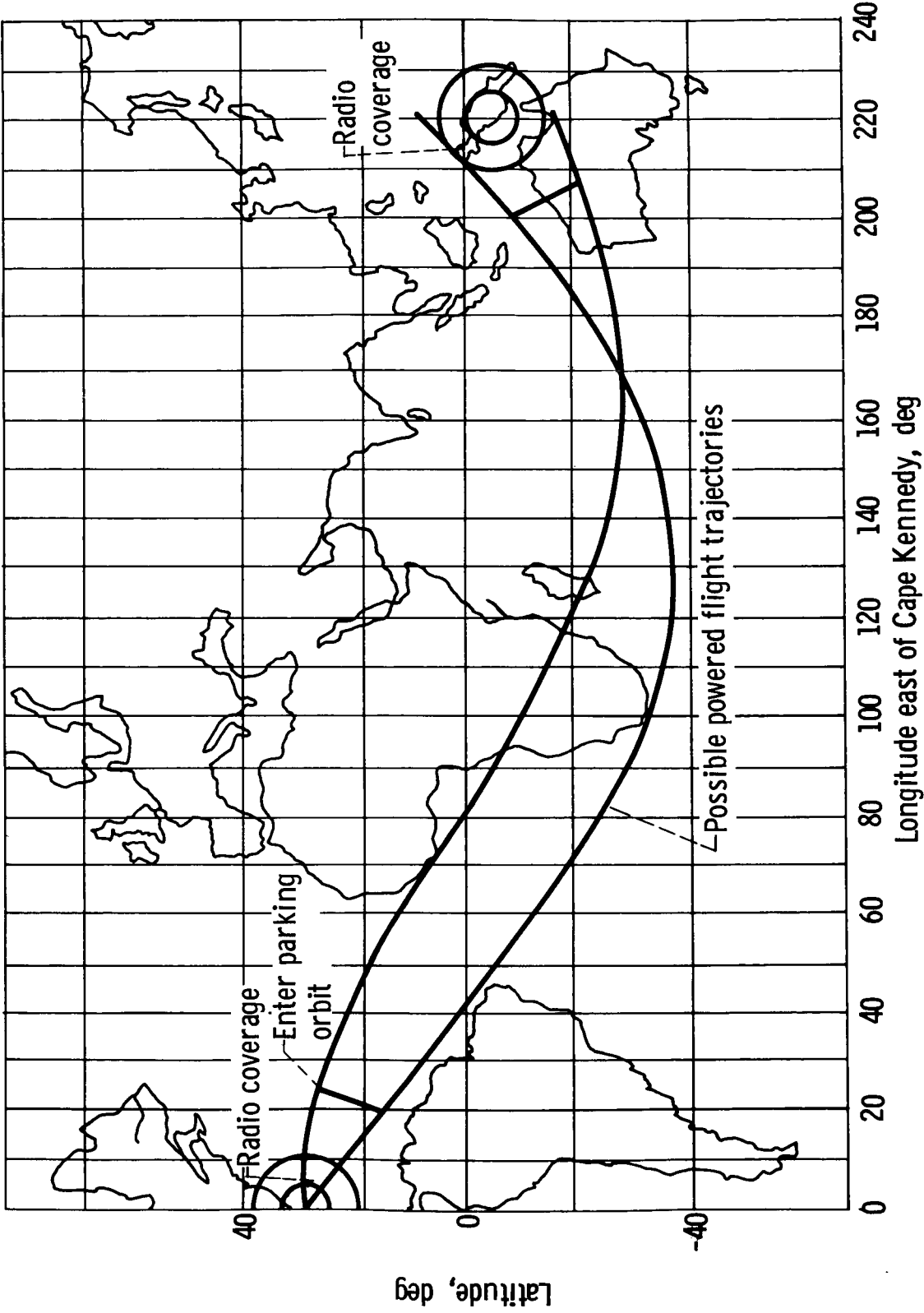


Figure 34. - Boost trajectories for lunar missions.

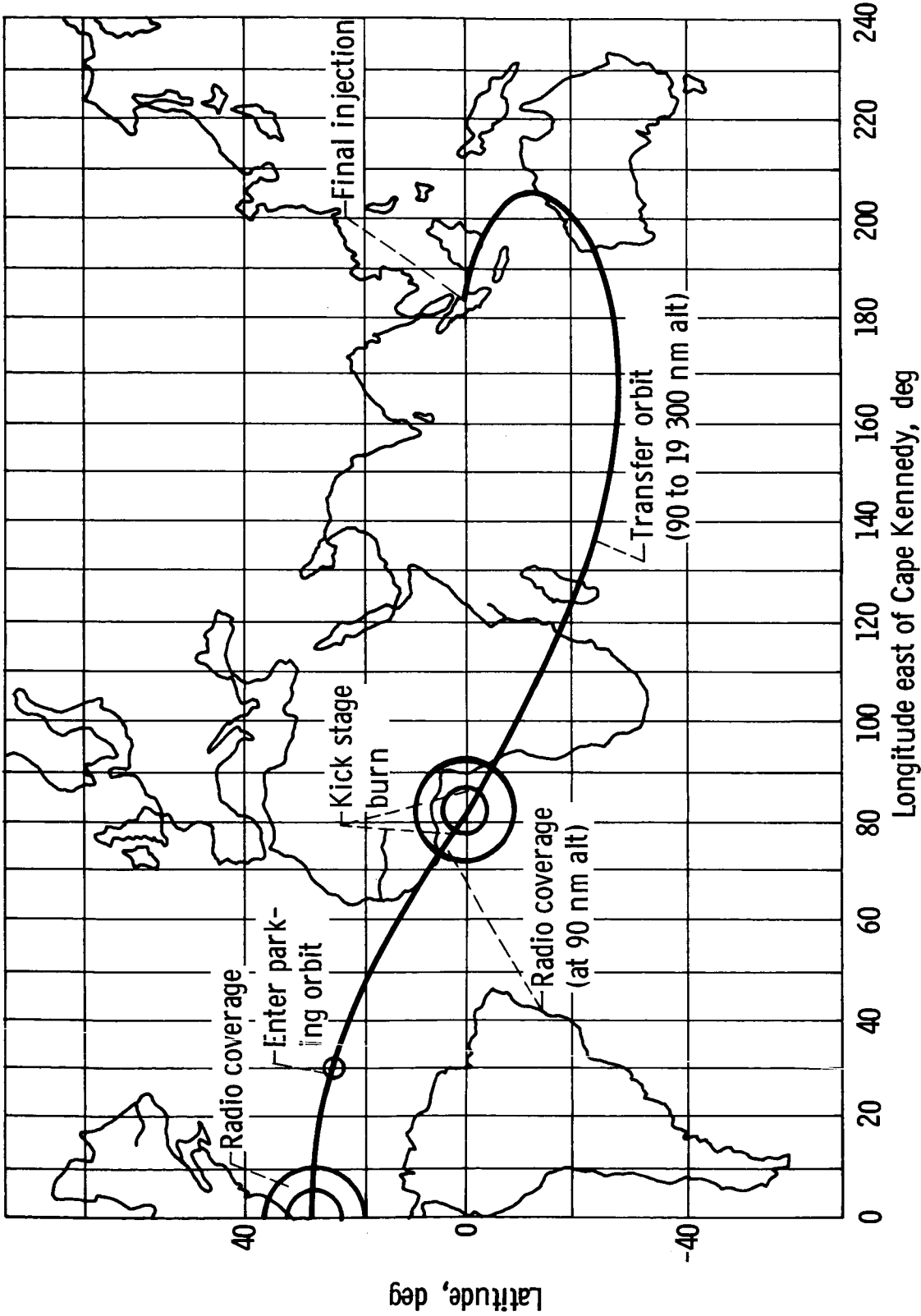


Figure 35. - Boost trajectory for synchronous orbit mission.

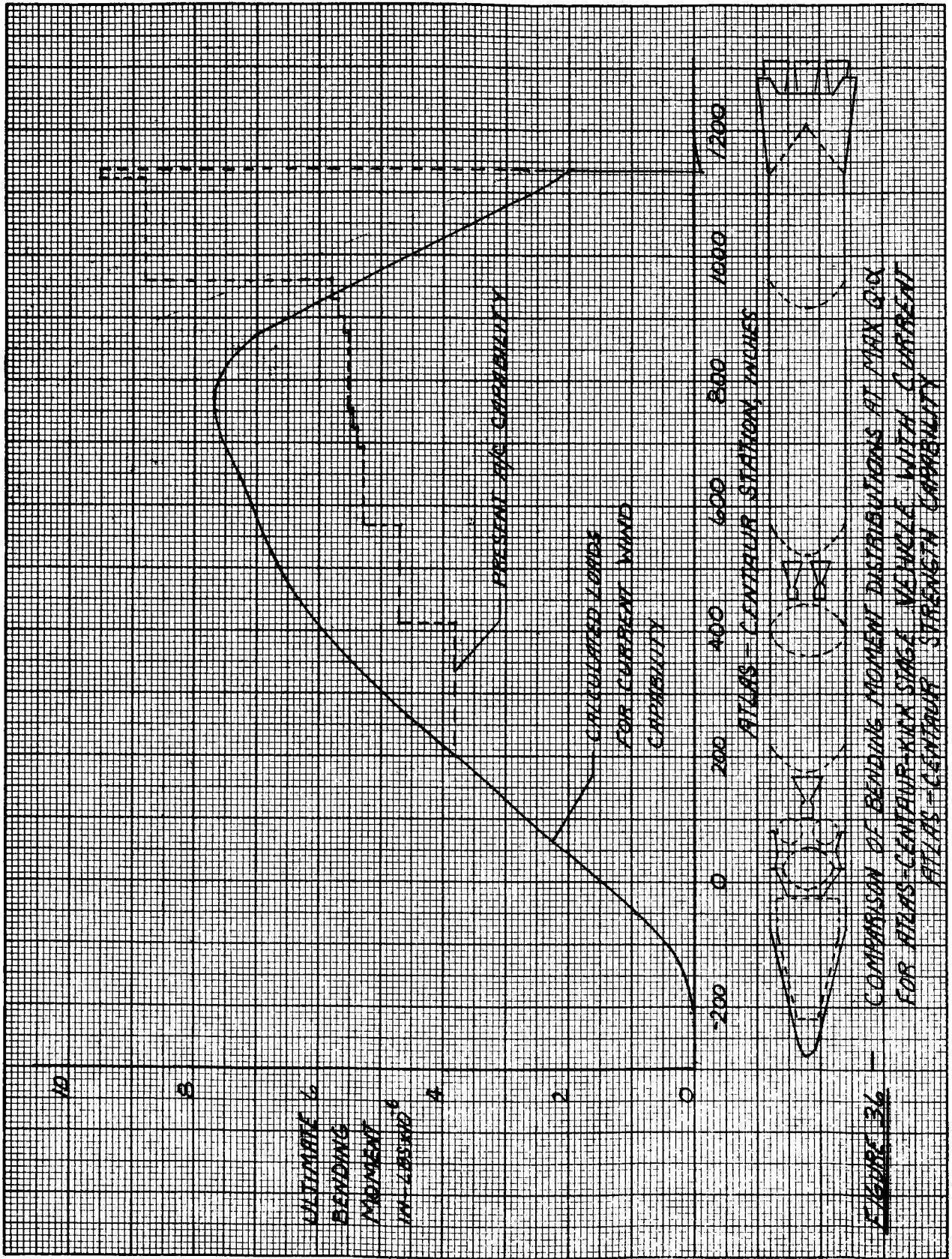


FIGURE 36

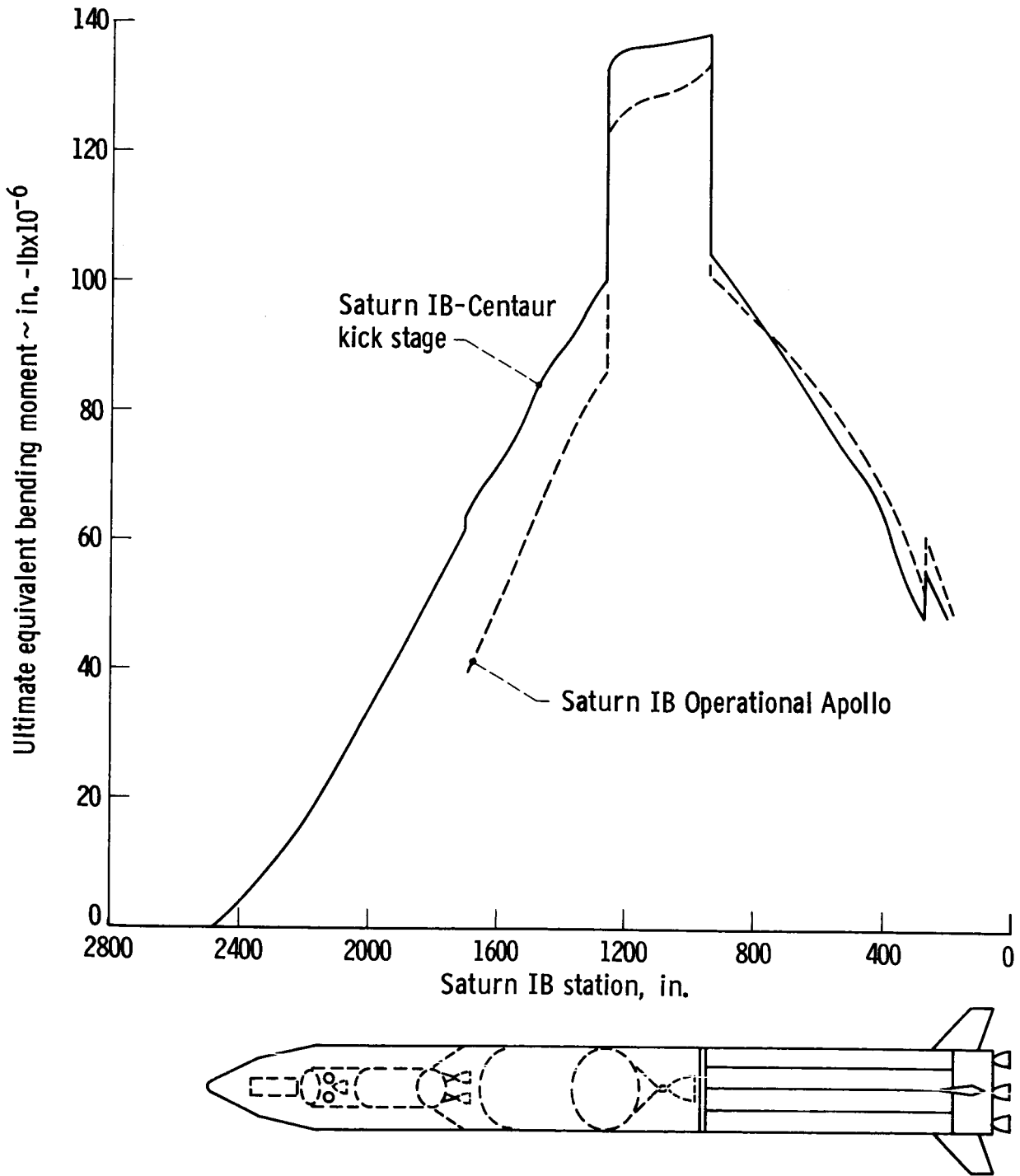


Figure 37. - Comparison of equivalent bending moment distribution for Saturn IB-Centaur kick stage with Saturn IB-Apollo.

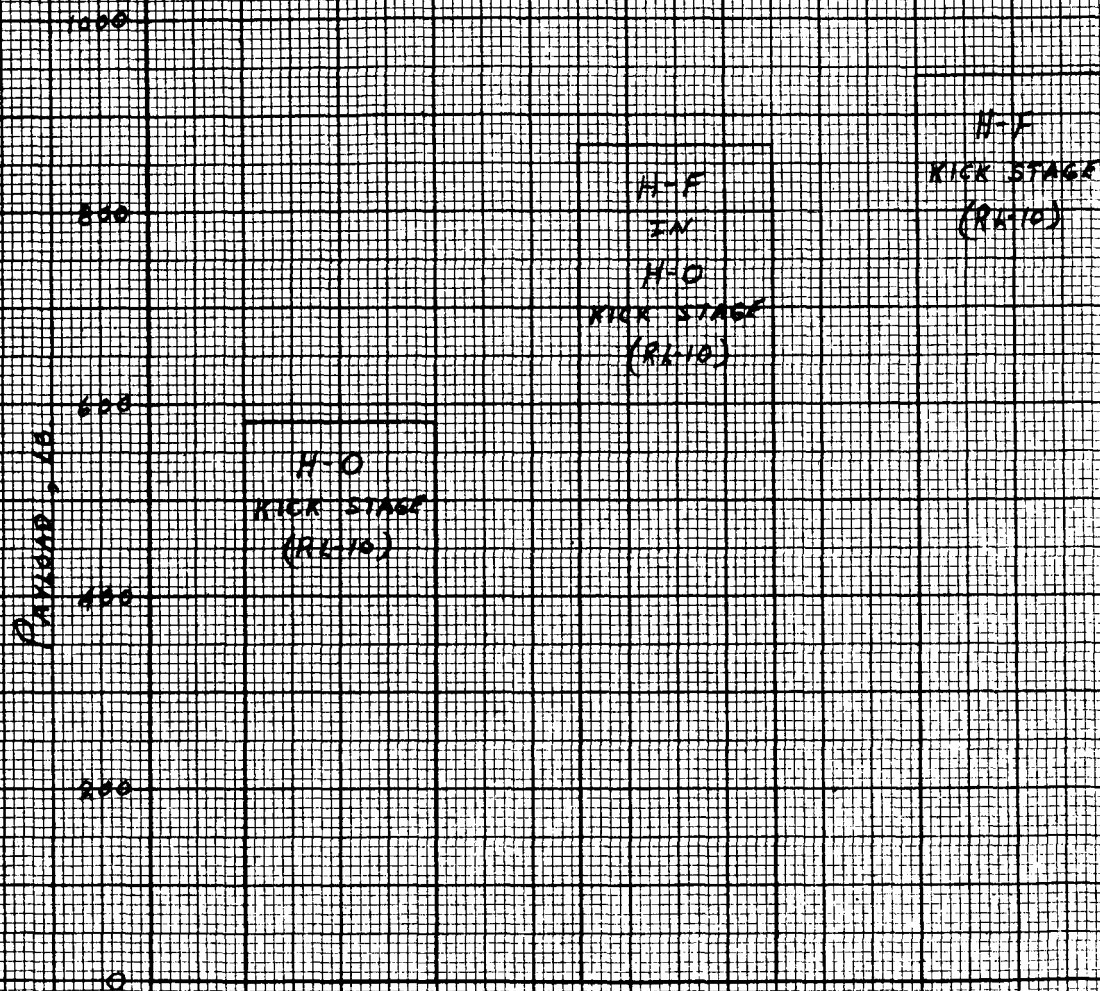


FIGURE 3B - PAYLOAD CAPABILITY OF VARIOUS KICK STAGES FOR A SOLAR PROBE MISSION, ATLAS-CENTAUR LAUNCH VEHICLE; PERIHELION DISTANCE 0.33 A.U.

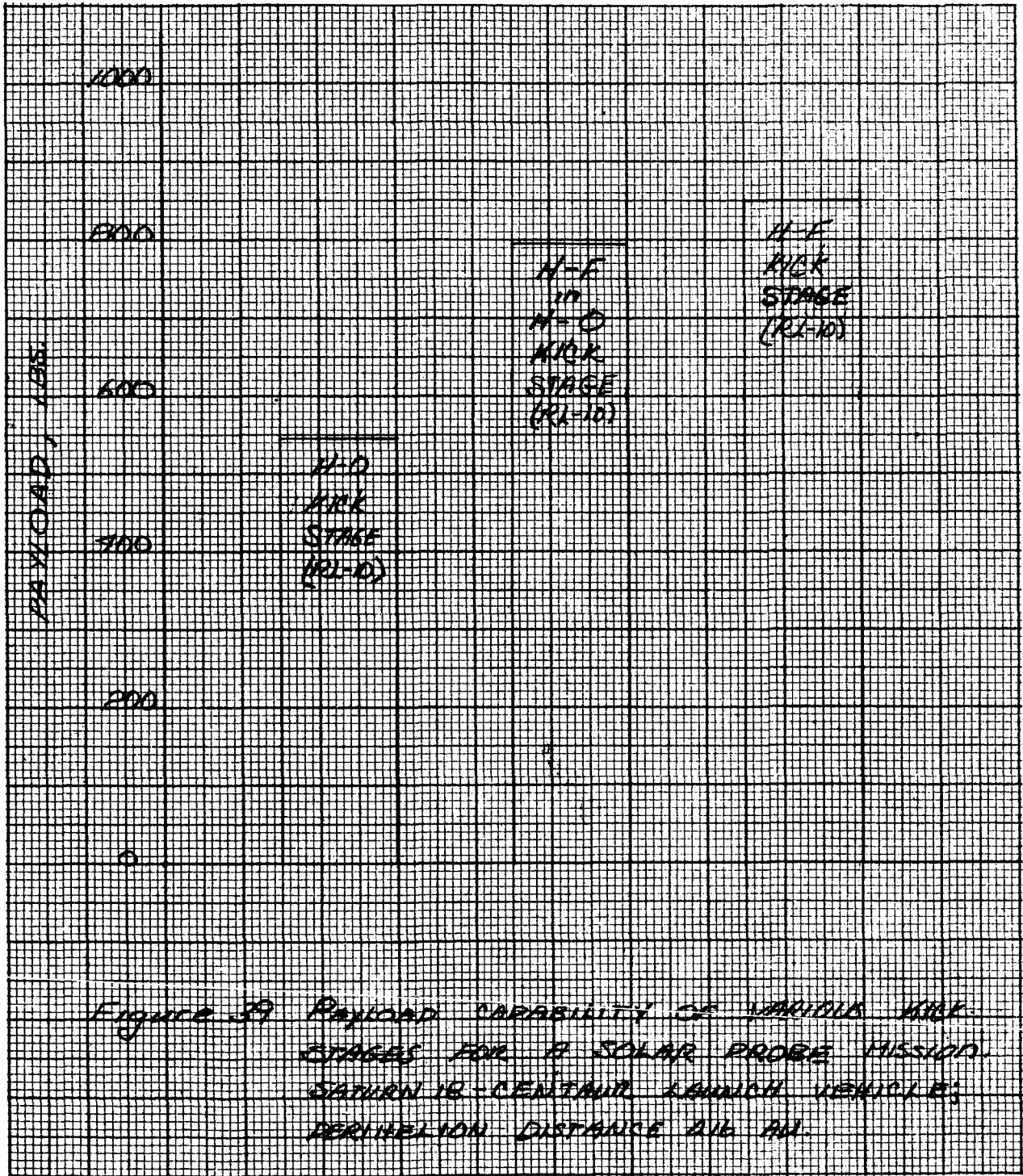


Figure 39 Payload capability of various kick stages for a solar probe mission. Saturn IB-Centaur launch vehicle; perihelion distance 0.16 AU.

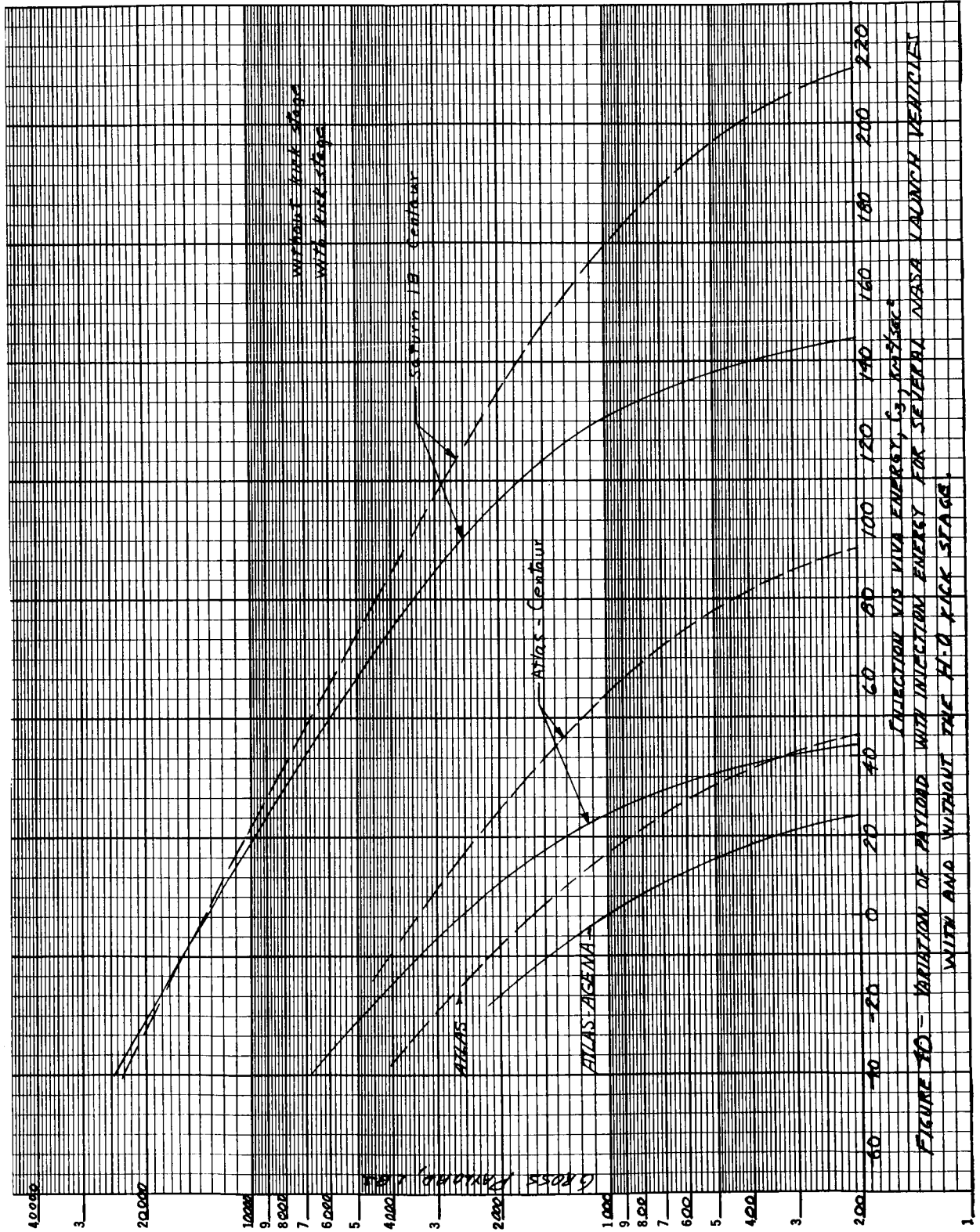


FIGURE 10 - VARIATION OF PAYLOAD WITH AND WITHOUT THE H.D. KICK STAGE.  
 CONSTRUCTION VIA ENERGY (3) NOT SHOWN  
 NASA LAUNCH VEHICLES

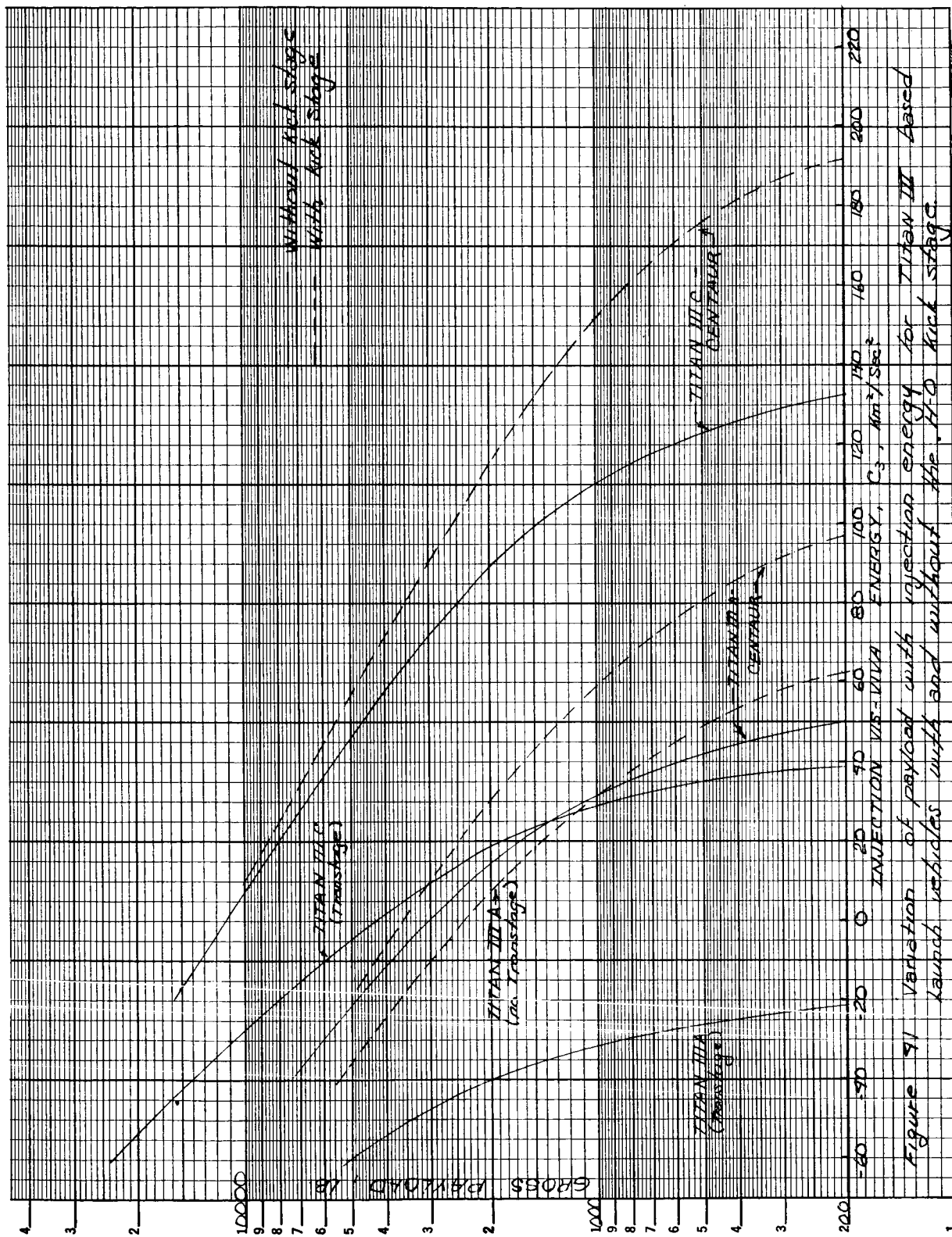


Figure 91 Variation of payload with injection energy for Titan III based launch vehicles with and without the H<sub>2</sub>O kick stage

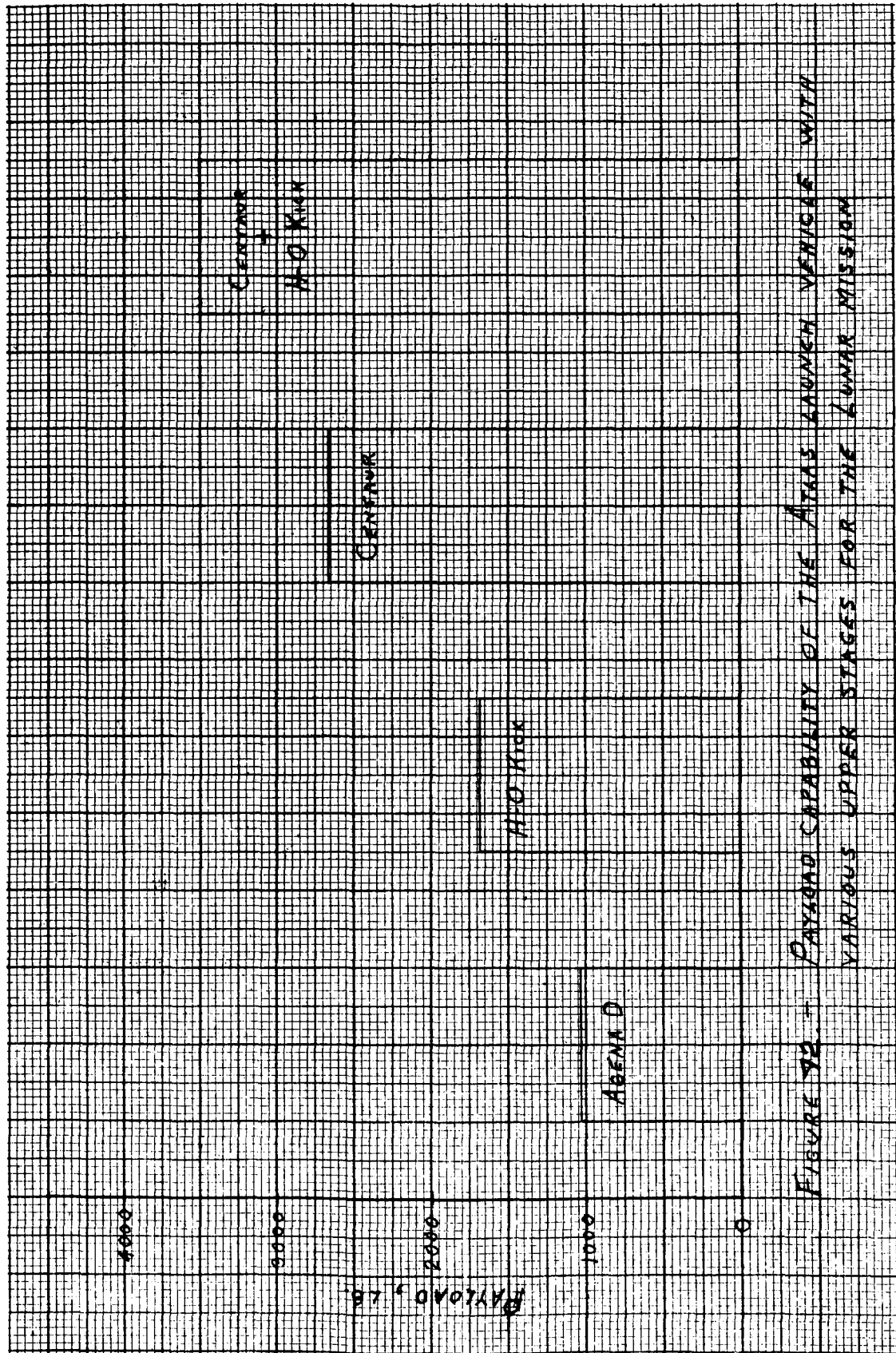


FIGURE 92. PAYLOAD CAPABILITY OF THE ATLAS LAUNCH VEHICLE WITH VARIOUS UPPER STAGES FOR THE LUNAR MISSILE

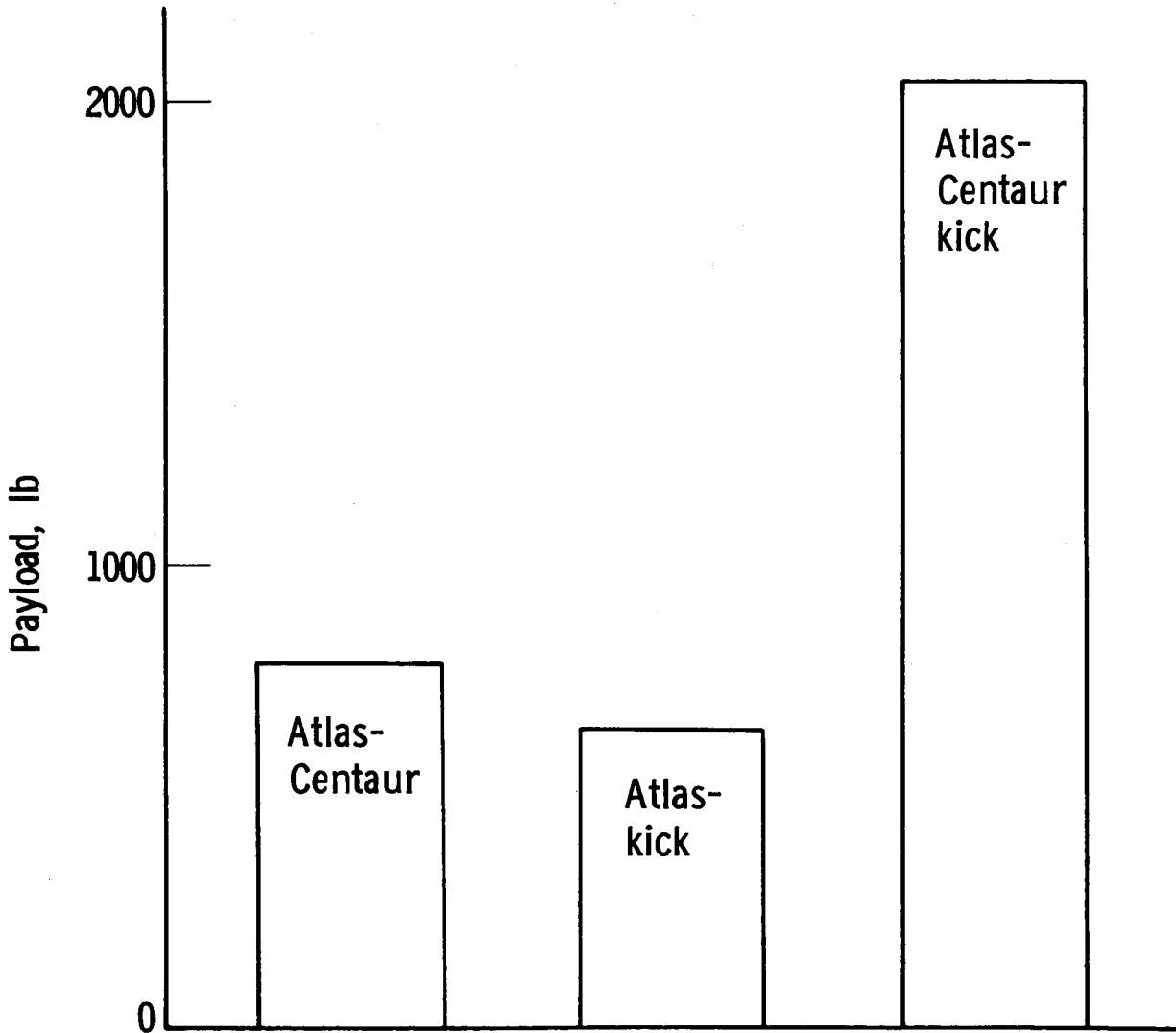


Figure 43. - Payload capability of the Atlas using the Centaur and the H-O kick stage for the 24-hour synchronous orbit mission.

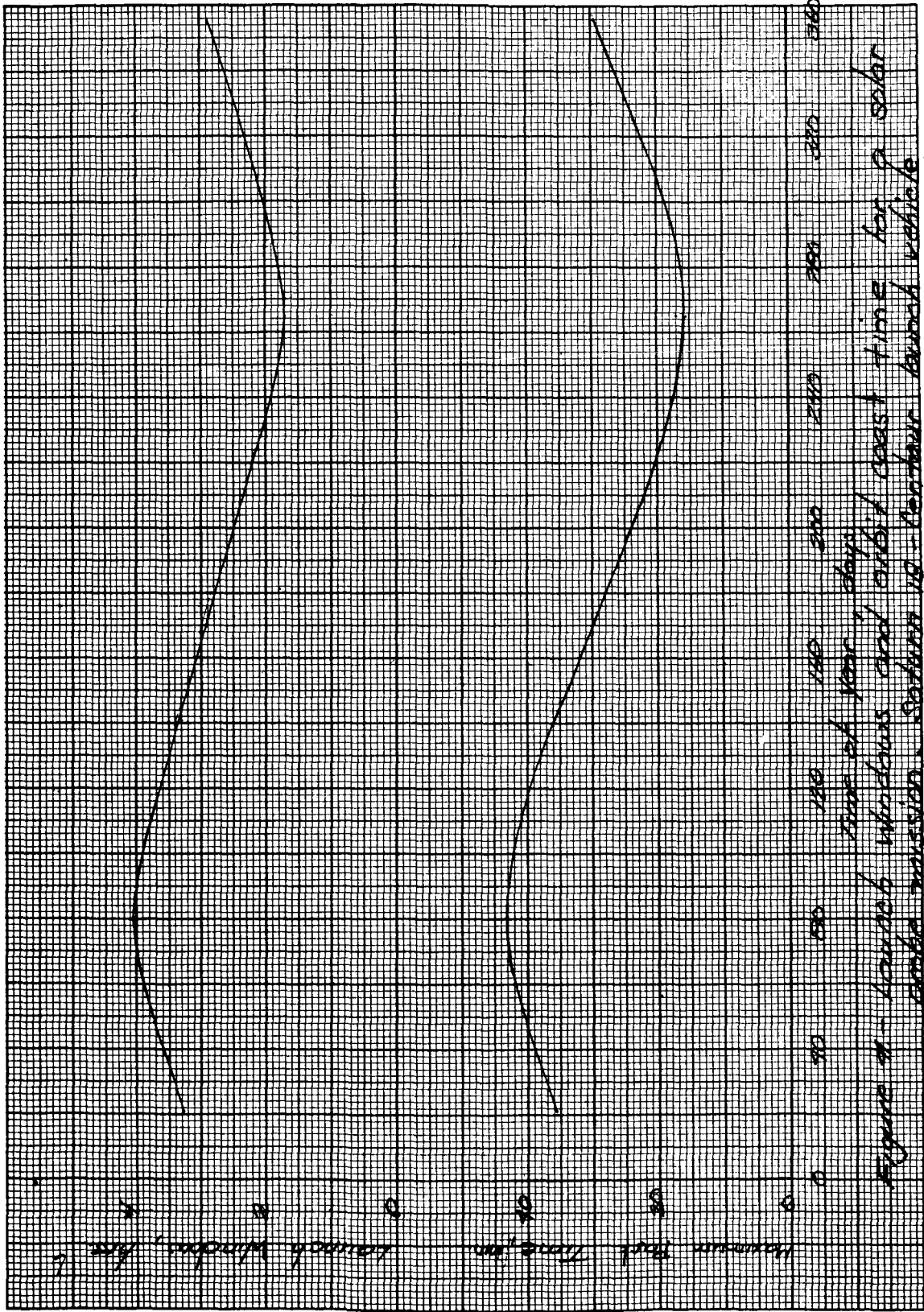


Figure 1 - Launch window for solar probes of key events (used for comparison) - in minutes - 0.5 min = 30 sec. 1 min = 60 sec. 1.5 min = 90 sec. 2 min = 120 sec. 2.5 min = 150 sec. 3 min = 180 sec. 3.5 min = 210 sec. 4 min = 240 sec. 4.5 min = 270 sec. 5 min = 300 sec. 5.5 min = 330 sec. 6 min = 360 sec. 6.5 min = 390 sec. 7 min = 420 sec. 7.5 min = 450 sec. 8 min = 480 sec. 8.5 min = 510 sec. 9 min = 540 sec. 9.5 min = 570 sec. 10 min = 600 sec.

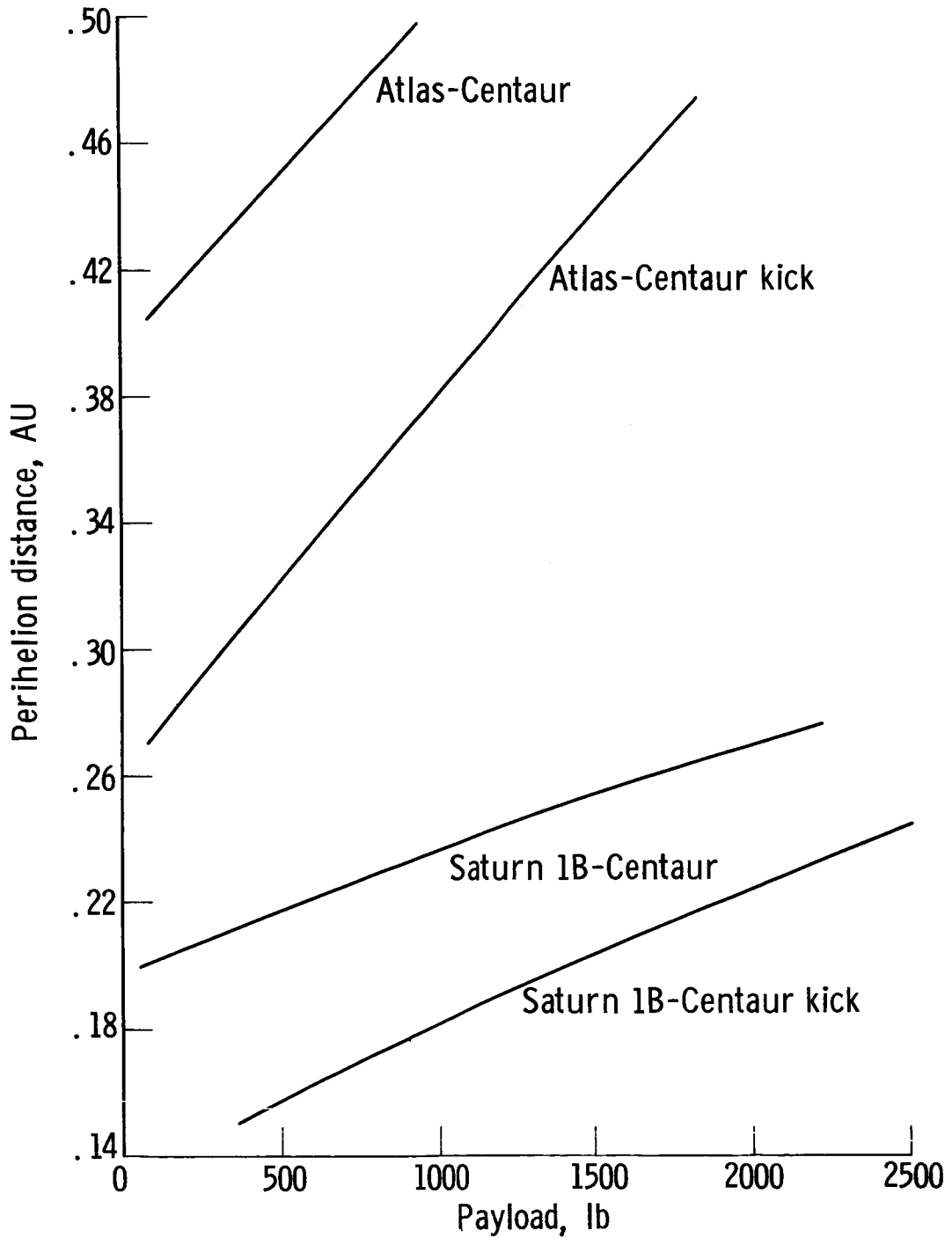


Figure 45. - Payload capability of the Atlas-Centaur and Saturn 1B-Centaur launch vehicles with and without the H-O kick stage. Solar probe mission.

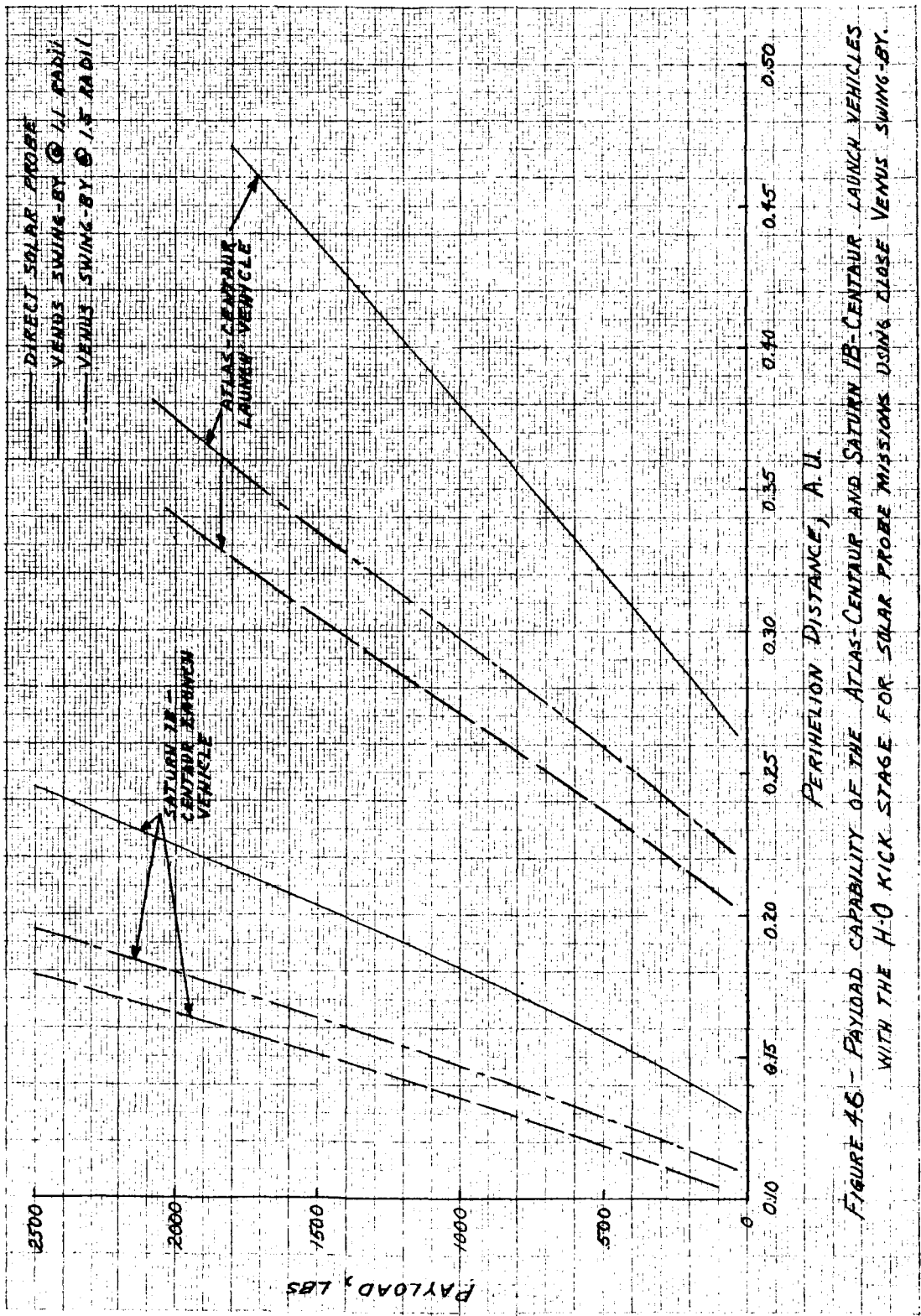


FIGURE 46 - PAYLOAD CAPABILITY OF THE ATLAS-CENTAUR AND SATURN IB-CENTAUR LAUNCH VEHICLES WITH THE H-0 KICK STAGE FOR SOLAR PROBE MISSIONS USING CLOSE VENUS SWING-BY.

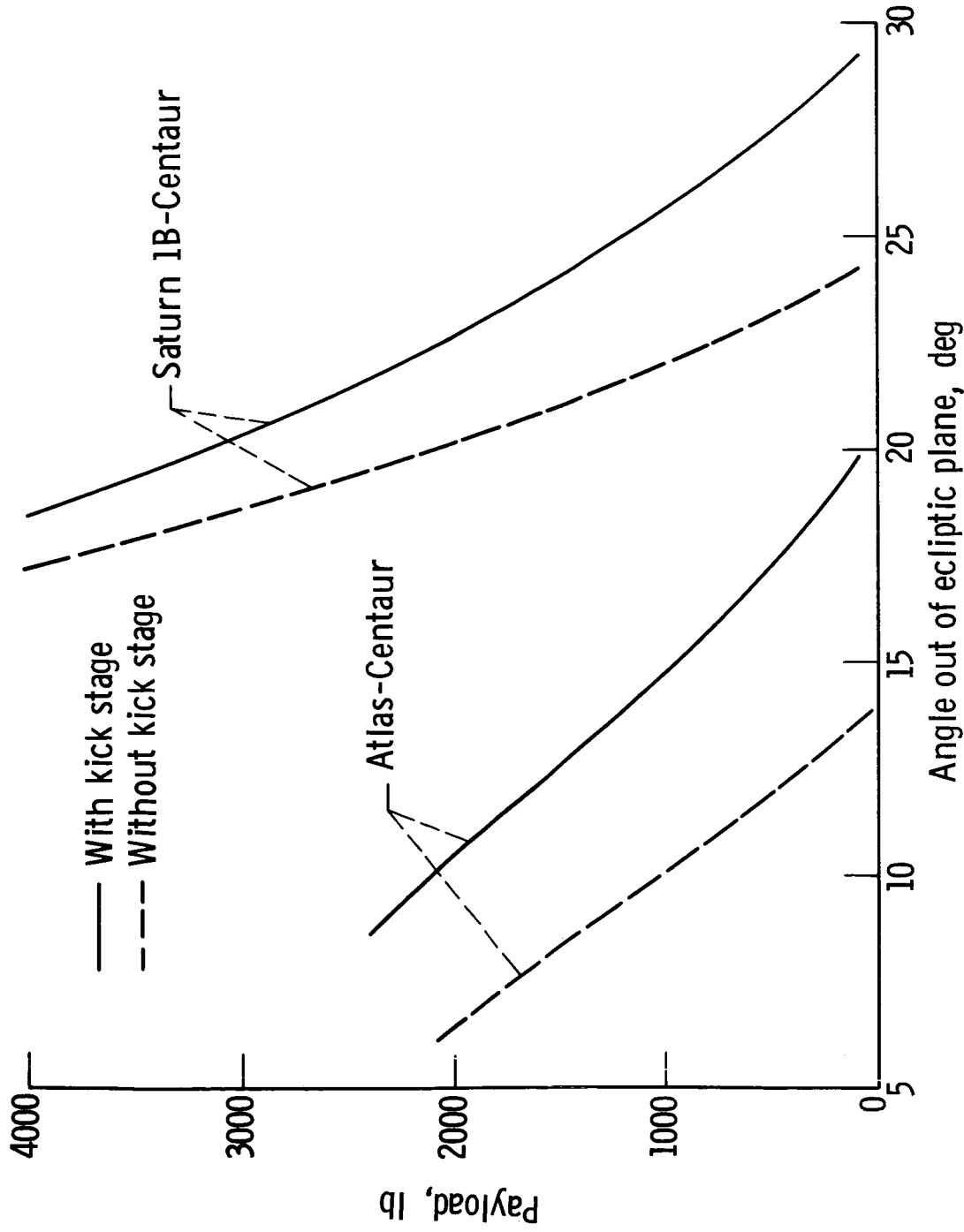


Figure 47. - Payload capability of the Saturn 1B-Centaur and Atlas-Centaur launch vehicles for out of the ecliptic plane missions with and without the H-O kick stage.

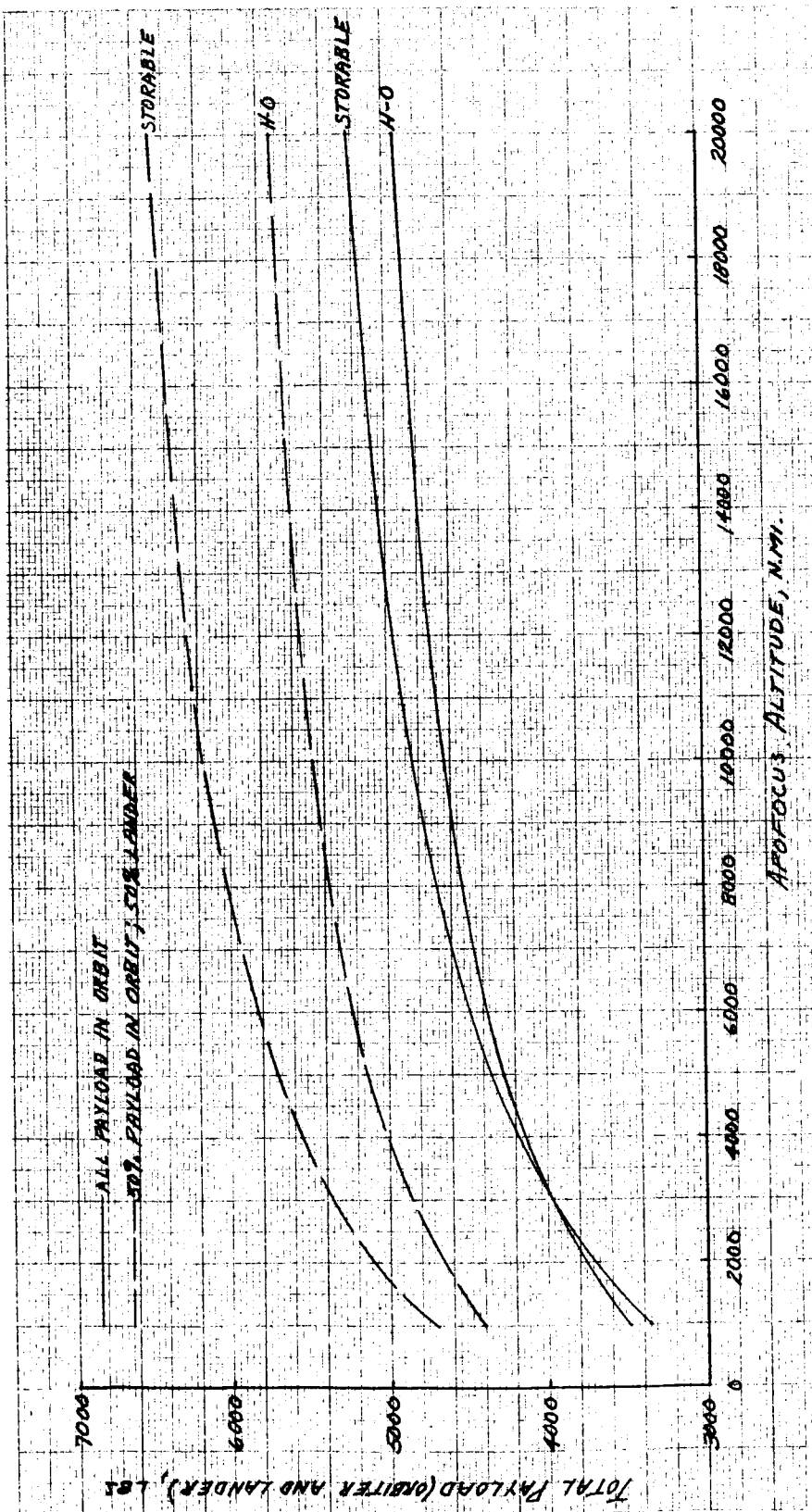


FIGURE 18 - PAYLOAD CAPABILITY OF THE H-O AND STORABLE PROPELLANT KICK STAGES FOR THE MARS ORBIT MISSION. SATURN 1B-CENTRAE LAUNCH VEHICLE.

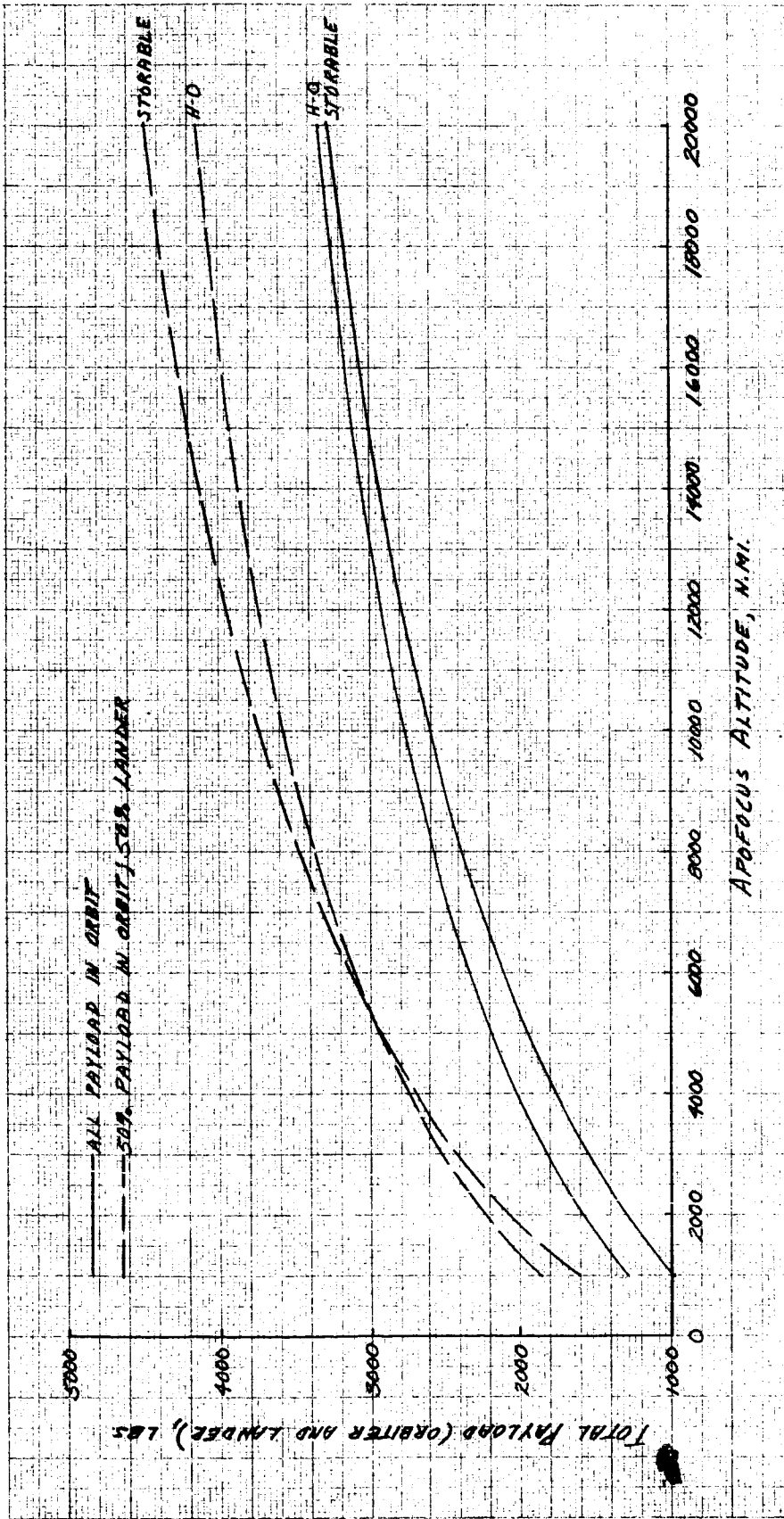


FIGURE 49 - PAYLOAD CAPABILITY OF THE H<sub>2</sub>O AND STORABLE PROPELLANT KICK STAGES FOR THE VENUS ORBIT MISSION. SATURN IB-CENTAUR LAUNCH VEHICLE.

